VŠB - Technical University of Ostrava
Faculty of Electrical Engineering
and Computer Science

SIMULATION AND MODELLING OF WIRELESS POWER IN COOPERATIVE NETWORKS

Ph.D. Thesis

2019 Nguyen Nhat Tan

VŠB - Technical University of Ostrava
Faculty of Electrical Engineering and Computer Science
Department of Telecommunications

SIMULATION AND MODELLING OF WIRELESS POWER IN COOPERATIVE NETWORKS

Ph.D. Thesis

Doctoral Study Branch: 2601V018 Communication Technology

Doctoral Study Programme: P1807 Computer Science, Communication Technology and Applied Mathematics

2019 Nguyen Nhat Tan

VŠB – TECHNICAL UNIVERSITY OF OSTRAVA
FACULTY OF ELECTRICAL ENGINEERING AND COMPUTER SCIENCE
DEPARTMENT OF TELECOMMUNICATIONS

SIMULATION AND MODELLING OF WIRELESS POWER IN COOPERATIVE NETWORKS

Ph.D. Thesis; Delivered in February 2019

Doctoral Study Programme:
P1807 Computer Science, Communication Technology and Applied Mathematics

Doctoral Study Branch:
2601V018 Communication Technology

Ph.D. Student: Nguyen Nhat Tan
VŠB - Technical University of Ostrava
Faculty of Electrical Engineering and Computer Science
Department of Telecommunications
17. listopadu 2172/15, 708 00 Ostrava, Czech Republic
tan.nhat.nguyen.st@vsb.cz

Supervisor: prof. Ing. Miroslav Vozňák, Ph.D.
VŠB - Technical University of Ostrava
Faculty of Electrical Engineering and Computer Science
Department of Telecommunications
17. listopadu 2172/15, 708 00 Ostrava, Czech Republic
miroslav.voznak@vsb.cz

OSTRAVA, 2019

DECLARATION

I hereby declare that I am the sole author of this PhD thesis. This is a true copy of the thesis, including any required final revisions, as accepted by my examiners.

I understand that my thesis may be made electronically available to the public.

In Ostrava, May 2019

.....

Nguyen Nhat Tan

ACKNOWLEDGEMENT

The work presented in this dissertation would not have been possible without my close association with a lot of people who were always there when I needed them the most. I take this opportunity to acknowledge them and extend my sincere gratitude for helping me to make this dissertation a possibility.

The research leading to this dissertation was carried out under the supervision of prof. Dr. Miroslav Vozňák. I would like to thank him for his encouragement and tremendous supports and also I would like to thank him a lot for his help during my stay in Ostrava.

This dissertation has improved substantially thanks to the valuable comments and feedback from Dr. Tran Thanh Phuong, Vice-Dean at Faculty of Electrical and Electronics Engineering, Ton Duc Thang University, Ho Chi Minh City, Vietnam. I'm very grateful to him for the time invested in studying my work.

I would like to thank Pavol, Lukaš, Jaroslav, and Jakub, my Czech classmates, who were always available for helping, assistance, improvement my English, a cup of coffee and the occasional game of soccer.

Finally, I would like to thank my girlfriend Hien for all her love, support, understanding and constant motivation. My parents, Thang and Phuong, deserve special thanks for their continued supports and encouragements. Without such a team behind me, I think that I would not be in this place today. This dissertation is dedicated to them.

ABSTRAKT

Rychlý vývoj bezdrátových elektronických systémů s nízkou spotřebou energie vedl k nespočetnému množství výzkumných aktivit v souvislosti s proveditelností dálkového či bezdrátového napájení těchto systémů. Z tohoto důvodu se bezdrátový přenos napájení (Wireless Power Transmission; WPT), také nazývaný jako bezdrátové získávání energie (wireless energy harvesting), stal předmětem zájmu na mnoho let. Jedná se o proces, kdy je energie z externích zdrojů získána, zachycena a uchována pro potřeby malých bezdrátových autonomních zařízení, kdy následně dochází k jejímu použití pro další přenos informací z tohoto zařízení.

V bezdrátových přenosových sítích mohou být některé uzly použity jako přenosové, které napomáhají efektivně přenášet informace z jednoho či více zdrojů do jednoho či více cílů. Tento proces vyžaduje mnoho energie, a to především kvůli potřebě přenosových uzlů uchovávat energii pro jejich vlastní přenos, který bude dříve či později vyžadován. Proto je nepostradatelné uplatnit v přenosových sítích získávání energie. Dostupná energie je v daném časovém okamžiku v podstatě náhodná, což činí hlavní výzvu v návrhu získávání energie v přenosových sítích. Toto je důvodem, proč musí dojít k navržení optimálních přenosových protokolů pro využití dostupné energie a tím tak úspěšně zlepšit efektivitu sítě.

Výše uvedená problematika vedla v této disertační práci ke studii strategie používání technologie získávání energie v souvislosti s bezdrátovými přenosovými sítěmi. Konkrétně se zaměřuji na studii efektivity přenosových sítí umožňujících získávání energie, kdy jsou uplatňovány různé strategie získávání energie nebo protokoly za použití různých přenosových modelů. Na druhé straně je též zkoumán vliv nežádoucích podmínek, jako jsou například nekorektní informace o stavu kanálu a hardwarové nedokonalosti. Pro účely testování a ověření matematické analýzy je nastavena a provedena Monte Carlo simulace pro každý výsledek analýzy.

KLÍČOVÁ SLOVA

Získávání energie, výběr přenosového uzlu, hardwarové nedokonalosti, nedokonalé CSI, pravděpodobnost výpadku, propustnost.

ABSTRACT

The rapid development of low power wireless electronic systems has led to countless research activities in connection with the feasibility of a remote or wireless powering of those systems. Therefore, wireless power transmission (WPT), also called wireless energy harvesting, has become a focal point of interest for many years. This is the process by which energy is derived from external sources, captured, and stored for small, wireless autonomous devices, then is used for other information transmissions from that device.

In wireless relay networks, certain nodes can be used as relay nodes to help forward the information from one or multiple sources to one or multiple destinations efficiently. This is a process that requires much energy, especially because the relay nodes need to keep energy for their own transmission demand sooner or later. Hence, applying energy harvesting in relay networks is indispensable. The main challenge in the design of energy harvesting relay networks is that the available energy at any time instance is essentially random. Hence, optimal transmission protocols to exploit available energy must be designed so that the performance of the network can be improved in a successful way.

Motivated by the above issue, in this dissertation, I aim to study the strategy of using energy harvesting technologies in the context of wireless relay networks. Specifically, I focus on studying the performance of energy harvesting enabled relaying networks by applying different energy harvesting strategies or protocols in various models of relaying. On the other hand, the effect of different undesired condition, such as channel estimation error and hardware impairment, on the performance of the proposed energy harvesting schemes for relay networks is also investigated. In order to test and verify the mathematical analysis, a Monte Carlo simulation is set up and run for each analysis result.

KEYWORDS
Energy harvesting, relay selection, hardware impairment, imperfect CSI, outage probability, throughput.

TABLE OF CONTENTS

LIST OF FIGURES

LIST OF TABLES

LIST OF ABBREVIATIONS

AF	Amplify-and-Forward
DF	Decode-and-Forward
AWGN	Additive White Gaussian Noise
RF	Radio Frequency
WPT	Wireless Power Transfer
SWIPT	Simultaneous Wireless Power and Information Transfer
WPCN	Wireless Powered Communication Network
EM	Electromagnetic
LPF	Low-Pass Filter
RE	Rate-Energy
ID	Information Decoding
EH	Energy Harvesting
WIT	Wireless Information Transfer
WET	Wireless Energy Transfer
H-APs	Hybrid Access Points
DL	Downlink
UL	Uplink
ICs	Integrated Circuits
HD	Half-Duplex
FD	Full-Duplex
CSI	Channel State Information
HI	Hardware Impairment
SER	Symbol Error Rate
FDRN	Full-Duplex Relay Network
TSR	Time-Switching Relaying
PSR	Power-Splitting Relaying
CR	Cognitive radio
PUs	Primary Users
SUs	Secondary users
QoS	Quality of Service
ST	Secondary Transmitters

PT	Primary Transmitter
SR	Secondary Receiver
PR	Primary Receiver
OP	Outage Probability
PDF	Probability Density Function
CDF	Cumulative Distribution Function
SNR	Signal-to-Noise-Ratio
SINR	Signal-to-Interference-and-Noise-Ratio
GSS	Golden Section Search

1 INTRODUCTION

1.1 Motivations and goals

In a wireless network, the source and destination may not communicate to each other directly because the distance between the source and destination is greater than the transmission range of both of them, hence the need for the intermediate node(s) to relay. Relaying is an effective way to combat the performance degradation caused by fading, shadowing, and path loss [1], [2]. In relay networks, the relay nodes help to boost the information exchange between source nodes and destination nodes, by forwarding (with or without decoding) the information-bearing radio frequency signals from sources to destinations.

Conventionally, wireless devices are powered by batteries, which have a limited operational lifetime, and have to be replaced or recharged periodically to maintain the network connectivity. In practice, this could be costly, inconvenient, and even infeasible. In particular, because of the important role of relays, the energy problem becomes vital in wireless relay networks. So far, there have been numerous attempts to improve the efficiency of energy using at the relay nodes, for example in [3], [4].

Recently, energy harvesting wireless networks are expected to introduce several transformative changes in wireless networking [5]. While conventional wireless devices are powered by batteries, for energy harvesting wireless devices, the energy can be continuously and stably supplied by available RF sources over the air [6]. Advanced relay networks suffer from energy saving problem, because of relaying activities as well as user mobility. So, a prospective approach is to apply energy harvesting technologies to relay networks.

In my dissertation, I consider amplify-and-forward (AF) and decode-and-forward (DF) protocols in both full-duplex and half-duplex relay networks using energy harvesting, where a battery-free relay node harvests energy from the received radio frequency (RF) signals from a source node and uses the harvested energy to forward the source information to destination node [tan01-15]. Two energy harvesting relaying protocols are studied, namely, the time-switching relaying (TSR) and power splitting relaying protocol (PSR).

Regarding the uncertainty of systems, I introduce the imperfect channel state information and hardware impairment condition, and investigate the impact of these conditions on the system performance, compared with the perfect condition [tan04-15]. The hardware impairment is assumed at both source and relay nodes [tan04, tan06, tan10, tan13, tan15].

In addition, I propose an energy-harvesting-based spectrum access model in a cognitive radio network including multiple relay nodes and figure out how to choose the best relay to transmit the information to the destination node [tan01, tan10]. Another model is introduced in our analysis, in which relay node can harvest the energy from an access point and then transmit both the information and energy harvested to a user node, then help forward the message from user to the access point. This is called a bidirectional relaying network, and I plan to provide a detailed performance analysis of this system [tan11, 12].

For all cases, I deliver rigorous analysis on the outage probability and average throughput of the considered system. Based on the outage probability and throughput expressions, the optimal time

switching and/or power splitting factor is obtained via the numerical search method. Last but not least, to verify the analysis results as mentioned above, a Monte Carlo simulation is conducted for each case.

1.2 Dissertation structure

This dissertation is organized as follows. After this introduction section, chapter 2 provides background. Chapter 3 introduces state of the art. Chapter 4 specifies the aims of the research. Chapter 5 outlines different system models in various conditions and describes the problems that the dissertation aims to solve. Chapter 6 presents some of my own preliminary works and expected results of energy harvesting in imperfect CSI condition. The performance of energy harvesting with hardware impairment is analyzed in Chapter 7. Finally, Chapter 8 summarizes the achieved results based on some articles that have been published and explains the contributions of the proposed dissertation to this field.

2 BACKGROUND

In this chapter, some related conceptions and technologies are introduced for a better understanding of my work. Firstly, the concepts of wireless power transfer (WPT), simultaneous wireless power and information transfer (SWIPT) and wireless powered communication networks (WPCN) are presented. After that, the system modelling of energy harvesting in half-duplex and full-duplex relay networks is provided as fundamental knowledge to understand my research works that are going to be delivered later in this dissertation.

2.1 Fundamentals of wireless energy harvesting

2.1.1 Wireless Power Transfer

The idea of energy harvesting dates back to the experiment of Nicola Tesla more than a century ago when he attempted to deliver electromagnetic (EM) energy to a distant location without using wires. Since then, there have been studies to implement the transmission of electrical power from an energy source to electrical loads without wire connections, a technique that is called wireless power transfer. In general, WPT technologies can be realized based on three different mechanisms, i.e., inductive coupling, magnetic resonant coupling, and electromagnetic (EM) radiation [37]. The first two types utilize the non-radiative near-field EM properties provided by an antenna for short-range high-power transfer. The two near-field technologies enjoy high-energy transmission efficiency. However, operation distances are small. In contrast, WPT based on EM radiation exploits the far-field radiative properties of electromagnetic (EM) waves, by which the EM field along with the RF signals is propagated through space where the energy can be harvested by remote devices by capturing the RF signals. In general, the RF-enabled WPT can support larger operation distances, from a few meters to tens of meters, depending on different receiver sensitivities. Moreover, transferring energy to multiple devices becomes easily owing to the broadcasting property of wireless channels. In this dissertation, I exploit this technique for wireless energy harvesting.

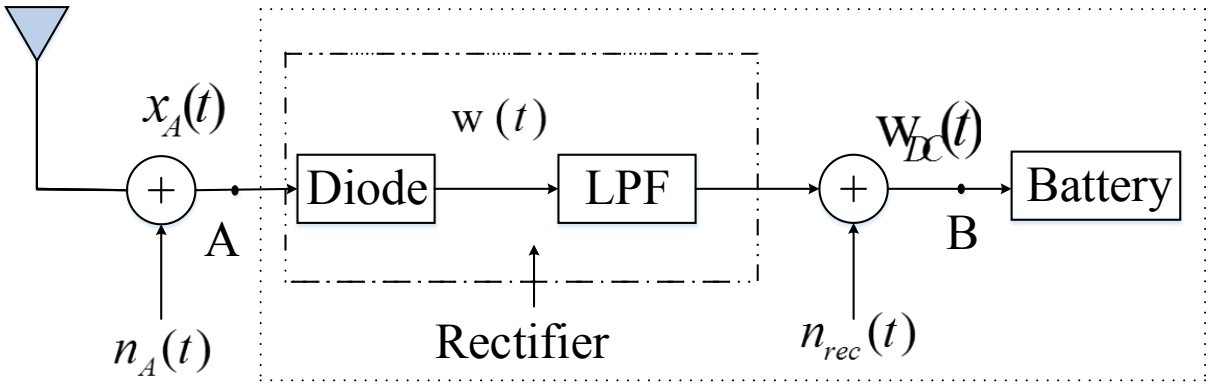

Figure 2.1. Energy harvesting receiver

Figure 2.1 illustrates the architecture of an RF-based energy harvesting receiver, which contains a rectifying circuit, consisting of a diode and a passive low-pass filter (LPF), which is able to convert received RF signals to DC signals to charge the built-in battery, which stores the energy. According to the energy conservation law, the harvested energy E_h can be expressed as

$$E_h = \eta P_r T = \frac{\eta P_t G T}{d^\alpha} \tag{2.1}$$

where $\eta \in (0,1)$ denotes the overall energy conversion efficiency at the receiver. P_t is the transmit power and d is the distance between the energy transmitter and its receiver, α denotes the path loss factor and G represents the combined gain of the transmit and receive antennas as well as the channel.

2.1.2 Simultaneous wireless power and information transfer (SWIPT)

Because RF signals can convey both energy and information simultaneously, an RF-based energy harvesting technique, called simultaneous wireless information and power transfer (SWIPT), is becoming a more and more promising research topic, which attracts increasing attention [38]. SWIPT is able to save spectrum via transmitting energy and information jointly with the same waveform or signals. However, SWIPT involves a rate-energy trade-off at both the transmitter and receiver to balance the information decoding (ID) and energy harvesting (EH) performance.

a. Ideal receiver

The idea of SWIPT was first introduced in 2008 in the seminal paper of Varshney [9], in which authors proposed an ideal receiver design that is able to simultaneously observe the information and extract power from the same received signal. He defined a rate-energy (R-E) function to characterize the performance trade-off. It is shown by [9] that for a point-to-point AWGN channel with amplitude-constrained input, there exists a non-trivial optimal input distribution for the trade-off between harvested energy and the achievable rate. Grover and Sahai extend the work in [9] to frequency-selective channels with AWGN [10].

b. Practical receiver

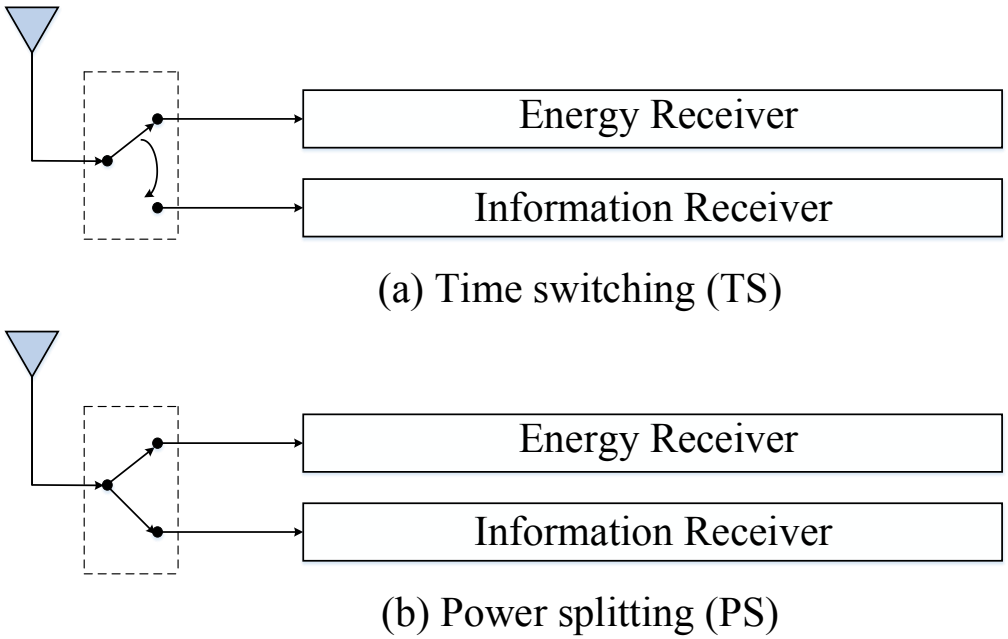

Figure 2.2. Two practical receiver architectures for SWIPT

One critical assumption in [9] and [10] is that the receiver is able to decode information and harvest energy from the same signal with the same circuit. Later, it was pointed out that [11] such an assumption

cannot be realized in practical systems. In [11], Zhang and Ho proposed a separated information and energy receiver for SWIPT based on two realizable receiver architectures design: time switching (TS) and power splitting (PS). These two architectures are displayed in Figure 2.2. For the TS scheme, at any time the received signal is only connected either to the information receiver or to the energy receiver. Hence, EH and ID are performed orthogonally in time. For the PS scheme, the received signal is split into two streams by a power divider with a fixed power ratio, which is used for EH and ID, respectively.

2.1.3 Wireless powered communication networks (WPCN)

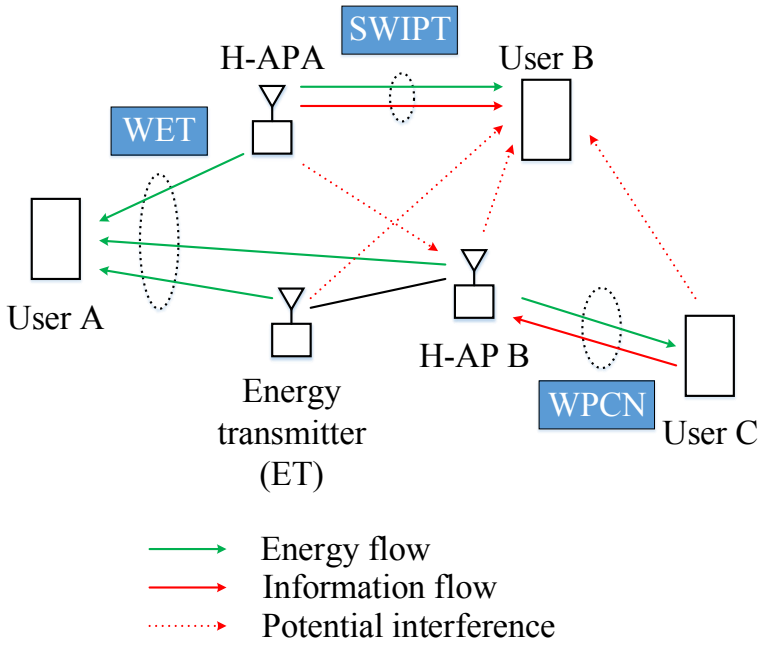

Figure 2.3. A general model of WPCN

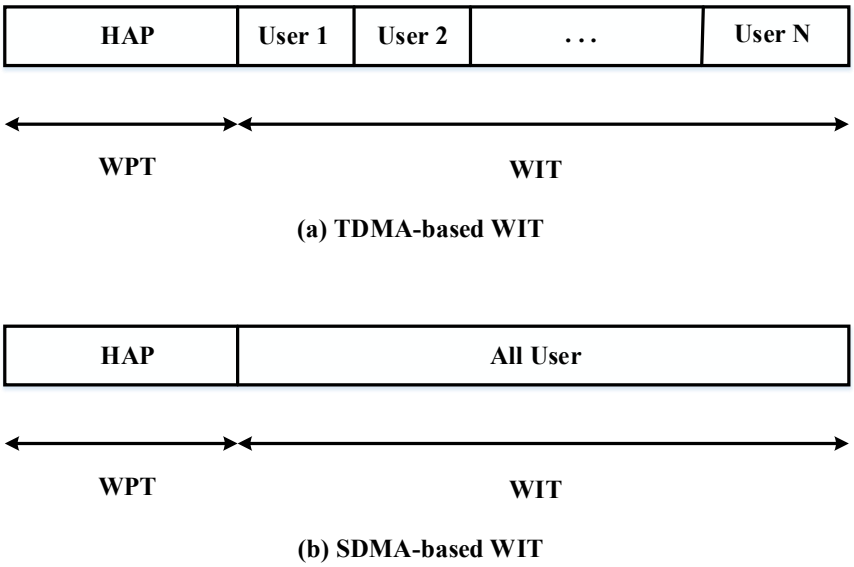

Figure 2.4. Harvest-then-transmit protocol

The idea of wireless energy and information transfer can be exploited for a network with multiple devices [tan02]. Figure 2.3 illustrates the general architecture for WPCN [39]. Hybrid access points (H-

APs) are deployed which are capable of sending wireless power to users via wireless energy transfer (WET) in the downlink (DL) as well as coordinating wireless information transfer (WIT) to/ from users in the DL/ uplink (UL), respectively. In addition, dedicated energy transmitters (ETs) may also be used which only send energy to users via WET in the DL. The transmissions in WPCN consisting of both WET and WIT may interfere with the ID at the H-AP and user receivers.

One of major challenges for WPCN is to jointly design the transmission strategy for DL WET and UL WIT. To overcome this problem, a harvest-then-transmit protocol is proposed in [40], as shown in Figure 2.4. In this protocol, the transmission is divided into 2 phases: WET is performed during the first phase, where all users harvest the energy from the HAP, and WIT is performed during the second phase, where each user transmit their data to HAP, either using TDMA or SDMA method.

2.2 Energy harvesting modelling for half-duplex relay networks

As mentioned above, there are two practical designs for energy harvesting receiver. The performance analysis of these two EH strategies was conducted rigorously by Nasir et al. [12]. In this section and the next section, I describe the fundamental system model for energy harvesting in half-duplex and full-duplex relay networks, which will be used as the milestone to develop our main contribution in this dissertation.

The energy harvesting model for half-duplex relay networks was introduced in [12]. This system model is presented by Figure 2.5, where the source S sends information to the destination D with the help of the relay R. The systems operate in the mode of half-duplex that means the relay nodes in the systems either transmit or receive signals but do not perform both at the same time (or the same time-frequency cell).

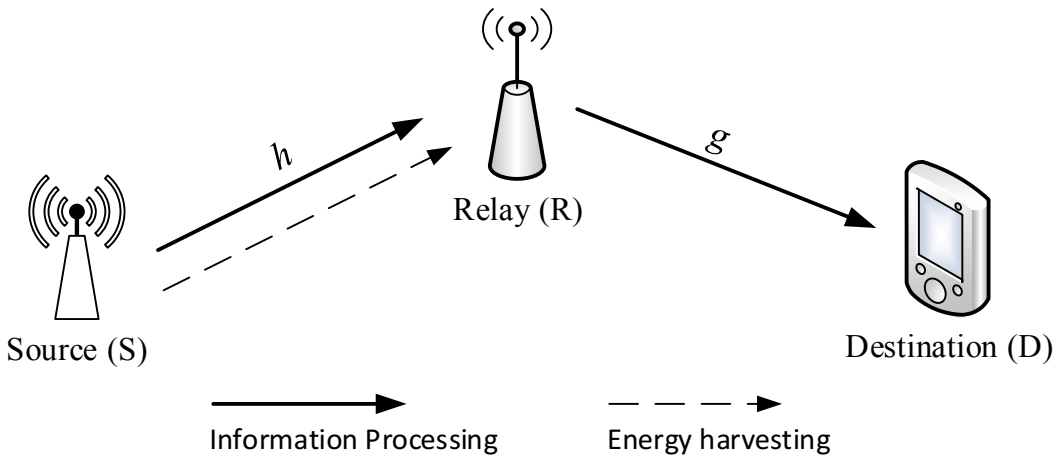

Figure 2.5. Energy harvesting based relay network system for HD

Assume that the direct connection between source and destination is weak, so the relay R is deployed to enhance this connection without having its own data to transmit. Energy harvesting is deployed at the relay node, where it can harvest the energy sent from the source node by the RF signal. To forward the message from the source, the relay is assumed to have no other energy supply but only the energy harvested from the source.

The received signal at the relay node in the second phase can be expressed as

$$y_R = hx_s + n_r, \tag{2.2}$$

where h is the channel coefficient of the source-relay path, x_s is the energy transmitted signal with $E\{x_s^2\} = P_s$, where $E\{.\}$ denotes the expectation operation, n_r is the zero-mean additive white Gaussian noise (AWGN) with variance $\sigma_{n_r}^2$. The received signal at the destination node in the third phase can be expressed as

$$y_d = gx_r + n_d, \tag{2.3}$$

where g is the channel coefficient of the source-relay path, x_r is the energy transmitted signal with $E\{x_r^2\} = P_r$, where $E\{.\}$ denotes the expectation operation, n_d is the zero-mean additive white Gaussian noise (AWGN) with variance $\sigma_{n_d}^2$.

Both channel gains g and h are assumed to be Rayleigh distributed, hence, $|h|^2$ and $|g|^2$ are exponential random variables with mean values $1/\lambda_h, 1/\lambda_g$, respectively.

Two energy harvesting schemes are being considered, namely, time switching relaying (TSR) and power splitting relaying (PSR) protocol.

2.2.1 Time switching relaying (TSR)

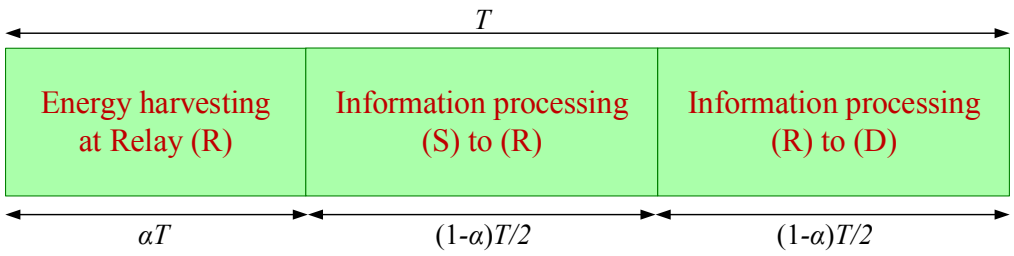

Figure 2.6 TSR protocol for half-duplex energy harvesting

The TSR protocol is presented in Figure 2.6. Here, the total symbol duration T is divided into two intervals with the lengths of α and $1-\alpha$, respectively, where $0 < \alpha < 1$. The first interval corresponds to the energy harvesting phase and the second one corresponds to the information transmission phase. The later interval is then divided into two subintervals with equal length. In the first subinterval, the relay node receives the signal from the source. The received message is either decoded or amplified in the first interval, and then, is forwarded to the destination during the second subinterval.

The transmitted power from the relay is a result of the energy harvesting process from the source in the first phase, so we have the following relationship:

$$P_r = \frac{E_h}{(1-\alpha)T/2} = \frac{2\eta P_s |h|^2 \alpha}{(1-\alpha)} \tag{2.4}$$

where $0 < \eta < 1$ is the energy conversion efficiency which depends on the rectification process and the energy harvesting circuitry [37].

During the second phase, the information is forwarded to the destination. The analysis now then divided into two modes: amplify-and-forward (AF) and decode-and-forward (DF).

a. Amplify-and-forward

For AF mode, the received signal at the relay is amplified by a factor

$$\beta_{TSR} = \frac{x_r}{y_R} = \sqrt{\frac{P_r}{P_s |h|^2 + \sigma_{n_r}^2}} \tag{2.5}$$

From (2.3) and combine with (2.4), (2.5), the received signal can be rewritten as

$$y_d = g x_r + n_d = g\beta y_R + n_d = g\beta \left[h x_s + n_r \right] + n_d = \underbrace{g\beta h x_s}_{signal} + \underbrace{g\beta n_r + n_d}_{noise} \tag{2.6}$$

The signal-to-noise-ratios (SNR) at the destination node can be calculated as

$$SNR_{AF-HD}^{TSR} = \frac{\mathrm{E}\left\{ |signal|^2 \right\}}{\mathrm{E}\left\{ |noise|^2 \right\}} = \frac{|g|^2 \beta^2 |h|^2 P_s}{|g|^2 \beta^2 \sigma_{n_r}^2 + \sigma_{n_d}^2} \tag{2.7}$$

Replace (2.4), (2.5) into (2.7) and doing some algebra the end to end SNR can be obtained as

$$SNR_{AF-HD}^{TSR} = \frac{2\eta P_s^2 |h|^4 |g|^2 \alpha}{2\eta P_s |h|^2 |g|^2 \sigma_{n_r}^2 \alpha + P_s |h|^2 \sigma_{n_d}^2 (1-\alpha) + \sigma_{n_r}^2 \sigma_{n_d}^2 (1-\alpha)} \tag{2.8}$$

The system falls to outage if the SNRs fall below a threshold γ_0. So, the outage probability is expressed as

$$P_{out} = \Pr\left(SNR_{AF-HD}^{TSR} < \gamma_0 \right) \tag{2.9}$$

The achievable throughput of the system can be calculated as

$$\tau = (1 - P_{out}) R \frac{(1-\alpha)T/2}{T} = \frac{(1-P_{out})R(1-\alpha)}{2} \tag{2.10}$$

b. Decode-and-forward

For DF mode, the message from the source is decoded in the first half of the second phase before being forwarded to the destination during the second half. Using the same approach as above, the SNR at the relay node and destination node can be calculated respectively as

$$SNR_1^{TSR} = \frac{P_s |h|^2}{\sigma_{n_r}^2} \tag{2.11}$$

and

$$SNR_2^{TSR} = \frac{P_r |g|^2}{\sigma_{n_d}^2} = \frac{2\eta P_s |h|^2 |g|^2 \alpha}{(1-\alpha)\sigma_{n_d}^2} \tag{2.12}$$

The outage occurs if and only if one of the two links (source-relay and relay-destination) fails, so the outage probability can be defined [16] as

$$P_{out} = P(\min(SNR_1^{TSR}, SNR_2^{TSR}) < \gamma_0) \tag{2.13}$$

2.2.2 Power splitting relaying (PSR)

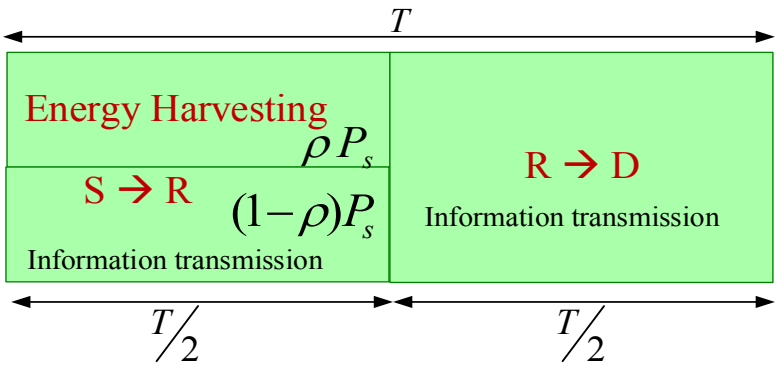

Figure 2.7. PSR protocol for half-duplex energy harvesting

The PSR protocol is presented in Figure 2.7, in which the total symbol duration T is divided into two intervals with the lengths of T/2 and T/2, respectively. The first interval is used for the source to relay information transmission and the remaining interval is used for relay-to-destination information transmission. During the first interval, a fraction of the received signal power ρP_s is used for energy transfer and the remaining power, $(1-\rho)P_s$, is used for information transfer, where $0 < \rho < 1$.

The transmitted power in the first phase is harvested from the source signal with power ρP_s, so we have the following relationship

$$P_r = \frac{E_h}{T/2} = \eta \rho P_s |h|^2 \tag{2.14}$$

a. Amplify-and-forward

The amplify factor in PSR protocol can be given by [12]

$$\beta_{PSR} = \sqrt{\frac{P_r}{(1-\rho)|h|^2 P_s + \sigma_{n_r}^2}} \tag{2.15}$$

Finally, the end-to-end SNR can be obtained:

$$SNR_{AF-HD}^{PSR} = \frac{\eta P_s^2 |h|^4 |g|^2 \rho(1-\rho)}{\eta P_s |h|^2 |g|^2 \sigma_{n_r}^2 \rho + P_s |h|^2 \sigma_{n_d}^2 (1-\rho) + \sigma_{n_r}^2 \sigma_{n_d}^2} \tag{2.16}$$

and the outage probability is defined as $P_{out} = P(SNR_{AF-HD}^{PSR} < \gamma_0)$ as in the previous section. The system throughput is given by

$$\tau = (1 - p_{out})R\frac{T/2}{T} = \frac{(1 - p_{out})R}{2} \tag{2.17}$$

b. Decode-and-forward

The SNR at the relay node in this case is given by

$$SNR_1^{PSR} = \frac{(1-\rho)P_s|h|^2}{\sigma_{n_r}^2} \tag{2.18}$$

From (2.3) and (2.14), the SNR at the destination node can be found as

$$SNR_2^{PSR} = \frac{P_r|g|^2}{\sigma_{n_d}^2} = \frac{\eta\rho P_s|h|^2|g|^2}{\sigma_{n_d}^2} \tag{2.19}$$

Then the outage probability is computed as $P_{out} = P\left(\min(SNR_1^{PSR}, SNR_2^{PSR}) < \gamma_0\right)$ and the throughput is obtained by (2.17).

2.3 Energy harvesting modelling for full-duplex relay networks

The energy harvesting model for full-duplex relay networks was introduced in [16]. The relay operates in full-duplex scheme then they can receive the transmitted signal from the source as well as transmit their own signal to the destination at the same time. This system model is presented by Figure 2.8, where the source S sends information to the destination D with the help of the relay R. Again, I assume that the direct connection between source and destination is weak, so the relay R is deployed to enhance this connection without having its own data to transmit. The relay is equipped with a transmit antenna and a receive antenna, which suffers from residual self-interference due to signal leakage from the transmit antenna to the receive antenna at the relay [41].

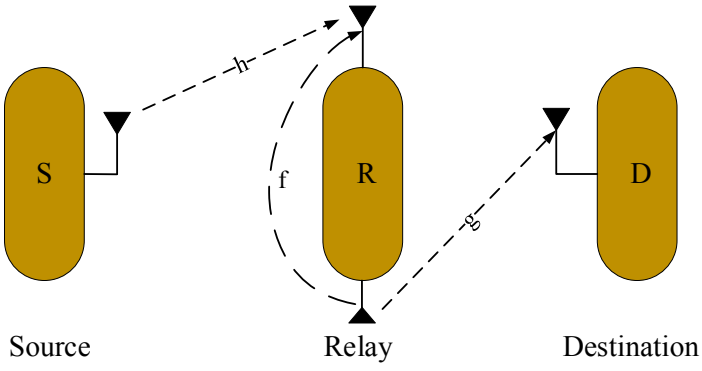

Figure 2.8. Dual-hop full-duplex relay networks model

Again, for separating between information transferring and energy harvesting processes at the relay node, we can adopt one of two protocols, TSR or PSR. Each of these protocols will be presented respectively in the next two subsections.

2.3.1 Time-switching relaying (TSR)

Here, the total symbol duration T is divided into two intervals as illustrated in Figure 2.9. The first interval corresponds to the energy harvesting phase and the second one corresponds to the information transmission phase. During the energy harvesting phase, the second antenna of the relay node is free from transmission duty and can be exploited to harvest energy from the source [15]. During the information transfer phase, the relay receives a message from the source and simultaneously forward another message that it received in the previous transmission block to the destination. Due to the broadcast nature of RF signals, the receiving antenna of the relay also receives the signal transmitted by the relay itself, a phenomenon called the loopback interference. Let h and g denote the channels from the source to the relay and from the relay to the destination, respectively, and let f denote the loopback interference channel at the relay.

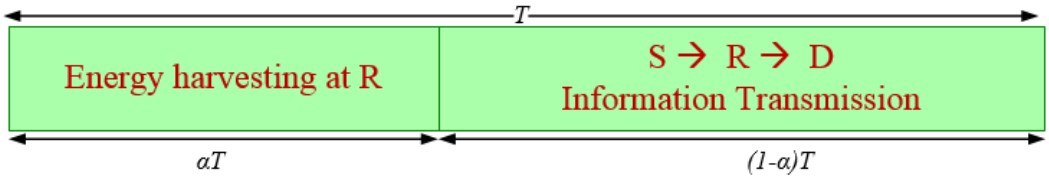

Figure 2.9. TSR protocol for full-duplex energy harvesting

The received signal at the destination node is also given by (2.3) for half-duplex mode. However, because the relay has the loopback interference channel, the received signal at the relay node is now expressed as

$$y_R = hx_s + fx_R + n_r \tag{2.20}$$

where h, g, x_s, n_r, n_d, and x_R are defined similarly as in the half-duplex model. For simplicity, I assume that $\sigma_{n_r}^2 = \sigma_{n_d}^2 = N_0$.

The transmitted power from the relay is a result of the energy harvesting process from the source in the first phase, so we have the following relationship:

$$P_r = \frac{E_h}{(1-\alpha)T} = \frac{\eta P_s |h|^2 \alpha}{(1-\alpha)} = kP_s |h|^2 \tag{2.21}$$

where $k = \dfrac{\eta\alpha}{1-\alpha}$

To continue the analysis, I consider 2 cases as in the previous section: amplify-and-forward and decode-and-forward.

a. Amplify-and-forward:

Following the energy conservation law, the energy used for forwarding message in the second phase must be the same as the energy harvested during the first phase. So, the amplification factor β can be found as

$$\beta_{TSR} = \sqrt{\frac{P_r}{|h|^2 P_s + |f|^2 P_r + N_0}} \tag{2.22}$$

Using a similar approach as for the HD model, the end-to-end SNR can be obtained as

$$SNR_{AF-FD}^{TSR} = \frac{\frac{P_s |h|^2 |g|^2}{|f|^2}}{\frac{N_0 P_s |h|^2}{P_r |f|^2} + P_r |g|^2 + N_0}$$

The outage probability and the achievable throughput are defined as

$$P_{out} = P\left(SNR_{AF-FD}^{TSR} < \gamma_0\right) \tag{2.23}$$

$$\tau = (1 - P_{out}^{AF}) R \frac{(1-\alpha)T}{T} = (1 - P_{out}^{AF}) R (1-\alpha) \tag{2.24}$$

b. Decode-and-forward

For DF mode, to construct the outage probability, both the SNRs at destination and relay nodes should be derived.

So, from (2.20) and (2.21), using the fact that $N_0 << P_s$, we get

$$SNR_1^{TSR} = \frac{P_s |h|^2}{P_r |f|^2 + N_0} = \frac{P_s |h|^2}{k P_s |h|^2 |f|^2 + N_0} \approx \frac{1}{k |f|^2} \tag{2.25}$$

From (2.3) and (2.21), the SNR at the destination can be found as

$$SNR_2^{TSR} = \frac{k P_s |h|^2 |g|^2}{N_0} \tag{2.26}$$

Again the outage probability of the system can be written as $P_{out} = P\left(\min(SNR_1^{TSR}, SNR_2^{TSR}) < \gamma_0\right)$ and the system throughput is the same as (2.24).

2.3.2 Power splitting relaying (PSR)

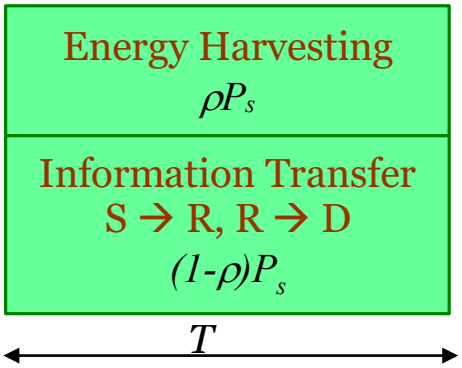

Figure 2.10. PSR protocol for full-duplex energy harvesting

Figure 2.10 illustrates the PSR energy harvesting protocol for full-duplex relaying. During the entire transmission block T, the energy harvesting and information transmission will be carried out concurrently. At the relay node, the received signal will go through a power divider. The first output, with the power of ρP_s, is used for energy harvesting from the source S. The second output, which has the power of $(1-\rho)P_s$, is used for information transmission from S →R. At the same time, the relay node also forwards the message that it received in the previous block to the destination (using the other antenna). The energy harvested from the source is stored and used for forwarding the message to the destination during the next transmission block.

Similar to (2.20), the received signal at the relay node can be expressed as

$$y_R = \sqrt{1-\rho}hx_s + fx_R + n_r \tag{2.27}$$

The transmitted power from the relay is calculated as

$$P_r = \frac{E_h}{T} = \frac{\eta\rho P_s |h|^2 T}{T} = \eta\rho P_s |h|^2 \tag{2.28}$$

Now, the analysis continues with two different cases:

a. Amplify and forward:

In this case, the amplifying factor can be obtained by

$$\beta_{PSR} = \sqrt{\frac{P_r}{(1-\rho)|h|^2 P_s + |f|^2 P_r + N_0}} \tag{2.29}$$

The end-to-end SNR can be found by the same approach as in half-duplex mode:

$$SNR_{AF-FD}^{PSR} = \frac{\frac{(1-\rho)P_s|h|^2|g|^2}{|f|^2}}{\frac{N_0(1-\rho)P_s|h|^2}{P_r|f|^2} + P_r|g|^2 + N_0} \tag{2.30}$$

From this, I can derive the outage probability and the achievable throughput expression by using the following definitions: $P_{out} = P\left(SNR_{AF-FD}^{PSR} < \gamma_0\right)$ (outage probability) and $\tau = (1-P_{out}^{AF})R$ (throughput).

b. Decode and forward:

Similar to TSR protocol, from (2.27) and (2.28), we get

$$SNR_1^{PSR} = \frac{(1-\rho)P_s|h|^2}{P_r|f|^2 + N_0} = \frac{(1-\rho)P_s|h|^2}{\eta\rho P_s|h|^2|f|^2 + N_0} \approx \frac{1}{\psi|f|^2} \tag{2.31}$$

where $\psi = \frac{\eta\rho}{1-\rho}$.

From (2.3) and (2.28), the SNR at the destination can be found as

$$SNR_2^{PSR} = \frac{\eta\rho P_s|h|^2|g|^2}{N_0} \tag{2.32}$$

Again, the outage probability of the system is defined as $P_{out} = P\left(\min(SNR_1^{PSR}, SNR_2^{PSR}) < \gamma_0\right)$ and the system throughput is $\tau = (1-P_{out}^{AF})R$.

2.4 Summary of the results

To complete this background review section, I summarize the key results of the analysis that has been reviewed presented above. The notations which are used in this subsection are listed in Table 2.1, and the key results from [12] and [16] are summarized in Table 2.2. It is sufficient that only the outage probability expressions are presented in this summary because the achievable throughput expressions can follow immediately.

Table 2.1. Notation for sections 2.2 and 2.3

Symbol	Name
η	Energy harvesting efficiency
$1/\lambda_h$	Mean of $\|h\|^2$
$1/\lambda_g$	Mean of $\|g\|^2$
$1/\lambda_r$	Mean of $\|f\|^2$

$K_1(.)$	First-order modified Bessel function of the second kind [38]
γ_0	SNR threshold
R	Source rate
Q	P_s/N_0

Table 2.2. Previous results in energy harvesting for single-relay half-duplex and full-duplex networks

Model	Protocol		Outage Probability
Half-duplex	TSR	AF	$P_{out} = 1 - \lambda_h \int_{\frac{\gamma_0\alpha}{Q}}^{\infty} e^{-\left(\frac{\gamma_0\alpha}{Q}\lambda_h + \frac{\gamma_0(1-\alpha)\lambda_g(Qz+1)}{2\eta Qz(Qz-\gamma_0\alpha)}\right)} dz$ $\approx 1 - e^{-\frac{\gamma_0\alpha\lambda_h}{Q}} \sqrt{\frac{4\gamma_0(1-\alpha)\lambda_h\lambda_g}{2\eta Q}} K_1\left(\sqrt{\frac{4\gamma_0(1-\alpha)\lambda_h\lambda_g}{2\eta Q}}\right)$
		DF	$P_{out} = 1 - e^{-\frac{\lambda_h\gamma_0}{Q} - \frac{(1-\alpha)\lambda_g}{2\alpha\eta}} - \lambda_g \int_0^{\frac{(1-\alpha)}{2\alpha\eta}} e^{-\frac{\gamma_0\lambda_h(1-\alpha)}{2\alpha\eta Qx}} e^{-\lambda_g x} dx$
	PSR	AF	$P_{out} = 1 - \lambda_h \int_{\frac{\gamma_0}{(1-\rho)Q}}^{\infty} e^{-\left(z\lambda_h + \frac{[Q\gamma_0(1-\rho)z+\gamma_0]\lambda_g}{\eta Q\rho z[Q(1-\rho)z-\gamma_0]}\right)} dz$ $\approx 1 - e^{-\frac{\gamma_0\lambda_h}{(1-\rho)Q}} \sqrt{\frac{4\gamma_0\lambda_h\lambda_g}{\eta\rho Q}} K_1\left(\sqrt{\frac{4\gamma_0\lambda_h\lambda_g}{\eta\rho Q}}\right)$
		DF	$P_{out} = 1 - e^{-\frac{\gamma_0\lambda_h}{(1-\rho)Q} - \frac{(1-\rho)\lambda_g}{\eta\rho}} - \lambda_g \int_0^{\frac{(1-\rho)}{\eta\rho}} e^{-\frac{\gamma_0\lambda_h}{\eta\rho Qx}} e^{-x\lambda_g} dx$
Full-duplex	TSR	AF	$P_{out} = 1 - \lambda_r \int_0^{\frac{1}{k\gamma_0}} \sqrt{\frac{\lambda_h\lambda_g\left(\frac{\gamma}{k} + \gamma_0 x\right)}{Q(1-k\gamma_0 x)}} K_1\left(\sqrt{\frac{\lambda_h\lambda_g\left(\frac{\gamma_0}{k} + \gamma_0 x\right)}{Q(1-k\gamma_0 x)}}\right) e^{-x\lambda_r} dx$ where $k = \frac{\eta\alpha}{1-\alpha}$
		DF	$P_{out} = 1 - 2\sqrt{\frac{\lambda_h\lambda_g\gamma_0}{kQ}}\left(1 - e^{-\frac{\lambda_r}{k\gamma_0}}\right) K_1\left(2\sqrt{\frac{\lambda_h\lambda_g\gamma_0}{kQ}}\right)$

			where $k = \dfrac{\eta\alpha}{1-\alpha}$
	PSR	AF	$P_{out} = 1 - \lambda_r \int_0^{\frac{1}{\psi\gamma_0}} \sqrt{\dfrac{\lambda_h\lambda_g\left(\frac{\gamma_0}{\psi}+\gamma_0 x\right)}{[(1-\rho)Q-\gamma_0\eta\rho Q x]}} K_1\left(\sqrt{\dfrac{\lambda_h\lambda_g\left(\frac{\gamma_0}{\psi}+\gamma_0 x\right)}{[(1-\rho)Q-\gamma_0\eta\rho Q x]}}\right) e^{-x\lambda_r} dx$ where $\psi = \dfrac{\eta\rho}{1-\rho}$.
		DF	$P_{out} = 1 - 2\sqrt{\dfrac{\lambda_h\lambda_g\gamma_0}{\eta\rho Q}}\left(1 - e^{-\frac{\lambda_r}{\psi\gamma_0}}\right) K_1\left(2\sqrt{\dfrac{\lambda_h\lambda_g\gamma_0}{\eta\rho Q}}\right)$ where $\psi = \dfrac{\eta\rho}{1-\rho}$.

3 STATE-OF-THE-ART

The idea of wireless power transmission is not new at all; it was first considered more than a century ago by Nikola Tesla [7]. His experiment was not successful though, because of the lack of certain radio-wave technologies at that time. However, since a few years ago, there have been four major technological factors that have been driving the research progress of various wireless power transmission and technologies for about two decades, namely high-density power devices, low-power integrated circuits (ICs), high-efficiency rectennas, and innovative circuit architectures. That opens the door for the field of RF energy transmission again this time with more feasibility.

One of the pioneering works in the field of energy harvesting communications was the study of the information theoretic capacity of a point-to-point energy harvesting communication system in [5]. Other authors have developed several research ideas on microwave-enable wireless energy transfer (WET), where energy is continuously and stabile supplied over the air [8]. More advancingly, the WET technologies to power the devices efficiently open up the potential to build a fully wireless powered communication network (WPCN), in which wireless devices communicate using only the power harvested by means of WET [8]. Moreover, a more natural idea is to apply WET technologies to relay networks.

Simultaneous wireless information and power transfer (SWIPT) is a kind of communications where relay nodes can be powered by energy harvested from the source radio frequency (RF) signals. This interesting idea has been presented firstly in the pioneering works by Varshney [9] and Grover [10]. Later, time-switching and power-splitting have been introduced in [11] as two practical architectures for SWIPT in relay networks. The drawback of that paper is that the authors only shown a performance bound that in general cannot be achieved by practical receivers. Since then, RF energy harvesting and information transfer via relays have also drawn significant attention.

The throughput performance of amplify-and-forward (AF) and decode-and-forward (DF) relaying systems for both time-switching (TSR) and power-splitting (PSR) protocols were studied rigorously in [12] and [13]. In [14], a network with multiple source-destination pairs communicated with each other via EH relays is considered, in which harvested energy is distributed properly among the relays to obtain better performance.

In [15], the author focus on the strategies to select the energy-harvested relays which are randomly located in the network. Nevertheless, all the above works are limited on half-duplex (HD) relaying mechanism only and do not mention the case that the channel state information (CSI) is not perfect.

The application of wireless information and power transfer to full-duplex relaying systems was first introduced in [16]. In that paper, the authors focused on a source-relay-destination dual-hop scenario where the relay is powered via RF energy harvesting and derived throughput performance analysis of the system. More interestingly, Zeng [17] proposed a new protocol for energy harvesting with full-duplex relaying, where part of the energy (loop energy) that is used for information transmission by the relay can be harvested and reused in addition to the dedicated energy sent by the source. Again, all of the above analysis was based on the assumption that the channel state information (CSI) is perfectly available at the relay and the destinations.

Energy harvesting, as well as relaying strategy, is applied in wireless sensor networks as well. In [18], the authors consider a new wireless powered communication system, where a user communicates with an access point (AP) assisted by a bidirectional relay. The user and the relay both powered by the RF energy from the AP. The role of the relay is to forwarding the energy from the AP to the user, as well as forwarding information from the user to the AP. However, the authors in [18] only considered the case that channel gains are known constants.

On the other hand, there have also been several results on performance analysis of relay networks with imperfect CSI but no energy harvesting is employed in these models. For example, the exact integral and approximate closed-form expression for the outage probability of two-way full-duplex relaying networks with residual loop interference and imperfect CSI has been derived in [19], but only conventional energy supplying has been used.

Indeed, Li et al. [20] did take account of the imperfect CSI condition in two-way AF relay systems with EH. Nonetheless, they only derived the maximum achievable sum rate, not the exact ergodic capacity of the system, and their results were limited at the half-duplex model. As of our knowledge, no work has considered the impact of channel estimation error on the performance of full-duplex relaying networks that apply the RF energy harvesting idea.

On another aspect, all these works studying EH in relay networks use a common assumption of perfect transceiver hardware at all nodes. However, in practice, the transceiver hardware is imperfect due to phase noise, I/Q imbalance and amplifier nonlinearities [21]. In [22], the authors have shown that hardware impairments (HI) limit the performance of dual-hop relaying systems, in terms of the capacity, throughput and symbol error rate (SER). The joint impact of HI and co-channel interference on the performance of relay networks was also mentioned in [23]. Therefore, the investigation of EH strategies in the existence of HI should be addressed seriously.

The cognitive radio network is another potential field to apply the energy harvesting idea. Cognitive radio (CR) concept was first introduced by Mitola [24] to overcome the spectrum scarcity problem in the emergence of wireless services. The basic idea of the CR technique is that licensed users (primary users (PUs)) can share licensed bands to unlicensed users (secondary users (SUs), with lower priority) to exploit the availability of resources [25]. In the conventional CR method [26], SUs must detect the presence/absence of PUs. Recently, two spectrum sharing methods have been proposed in which SUs can use licensed bands without detecting PUs' operations. In the first method, named underlay CR [27,28], PUs and SUs can use the licensed bands at the same time, provided that the co-channel interference from SUs must be upper bounded by a certain threshold. The second method is named overlay CR [29–31], in which SUs can use licensed bands but they must help PUs enhance the quality of service (QoS). In particular, SUs can play a role as relays for the primary network and via this assistance, they can find opportunities to access the licensed bands. Besides these operations, CR secondary users also consume energy for spectrum sensing process and for mobility. Therefore, it is very imperative that energy efficiency must be considered for secondary users in CR networks.

In [32], the secondary transmitter (ST) is deployed with a rechargeable battery which can harvest energy from the environment. The authors in [33] proposed optimal spectrum access for EH-based CR networks, where the ST at the beginning of each time slot needs to determine whether to remain idle so as to conserve energy, or to execute spectrum sensing to acquire knowledge of the current spectrum occupancy state.

Published works [34, 35] evaluated the performances of both primary and secondary networks in overlay CR environment, where a single EH-based ST uses the AF or DF technique to forward the combined signals to both primary receiver (PR) and secondary receiver (SR). The authors in [36] proposed a cooperative spectrum access protocol in which the SU can harvest the energy from the primary signals and then assists the primary data transmission using the Alamouti technique.

4 AIMS OF DISSERTATION

This section lists the specific goals and a rough plan for each part of the research proposed.

4.1 Aim 1: provide the basic analysis of outage probability and average throughput of various energy harvesting relay network models.

Applications of renewable energy in the next generation wireless networks will bring huge benefits for continuing operation in mobile equipment. Energy harvesting from the RF signal sources is a promising approach to prolong the lifetime of energy-constrained wireless networks such as cellular networks or wireless sensor networks. Therefore, the first goal of this project is to thoroughly investigate different EH schemes that can be applied to various relay networks, including full-duplex, half-duplex relaying networks and the bidirectional relaying networks in [18]. I will apply both times switching and power splitting EH schemes, as well as both AF and DF, relaying strategies to all the models mentioned above. Our specific goal is to derive the closed-form expression of the outage probability and the average throughput. The analytical results should provide theoretical insights into the effect of various system parameters, such as time switching factor, source transmission rate, and transmitting-power-to-noise ratio on system performance for both AF and DF relaying protocols. For certain scenarios, either the optimal time switching or power splitting ratio can be determined to maximize the information throughput from the sources to the destinations. All of these analyses are then confirmed by Monte-Carlo simulation.

4.2 Aim 2: provide the mathematical analysis and simulation results to evaluate the effect of channel state information error on the performance of energy-harvesting-based relay networks

The second goal of this dissertation is to focus on the throughput performance of wireless information and power transfer schemes in the condition of imperfect CSI at both relay and destination, a topic that there has not been considered in previous works as of the authors' knowledge. Using the similar setup as [16], I consider an AF and DF full-duplex relay network (FDRN) using simultaneous wireless information and power transfer, where a battery-free relay node harvests energy from the received RF signals from a source node and uses the harvested energy to forward the source information to the destination node. The time-switching relaying protocol is studied, with the assumption that the CSI at the relay node is imperfect. I deliver a rigorous analysis of the outage probability of the proposed system. Based on the outage probability expressions, the optimal time switching factor is obtained via the numerical search method. The effect of channel estimation error on the performance of this network is investigated carefully by mathematical analysis and numerical simulation. It is expected that for the imperfect CSI case, the proposed scheme still can provide acceptable outage performance given that the channel estimation error is bounded in a permissible interval.

4.3 Aim 3: provide the mathematical analysis and simulation results to evaluate the effect of hardware impairment on the performance of energy-harvesting-based relay networks

The next goal is to consider the effect of hardware impairment on the performance of EH-based relaying in cooperative and cognitive radio systems.

In the cooperative networks, I take account of the impact of hardware impairments at both source and relay nodes in the analysis of outage probability and throughput performance of wireless information

and power transfer with half-duplex relaying. Regarding the relaying and energy harvesting protocols, I focus on DF and AF relaying and time-switching energy harvesting protocol. The effect of hardware impairments on system performance systems is evaluated both by mathematical analysis and simulation. The impact of other parameters such as power supply and time switching factor on system performance under hardware impairments is also investigated.

In the cognitive radio networks, I study the impact of hardware impairments on the outage performance of the primary and secondary networks. Moreover, I also propose a new cooperative spectrum sharing relaying protocols, where the best EH-based secondary transmitters (ST) is chosen to assist the data transmission between the nodes primary transmitter (PT) and primary receiver (PR). For performance evaluation, I will derive exact and lower-bound expressions of outage probability (OP) over Rayleigh fading channel. Again, Monte-Carlo simulations are performed to verify the theoretical results. I aim to show that the outage performance of both networks can be enhanced by increasing the number of ST-SR pairs. Moreover, the fraction of time used for EH and positions of the secondary users should have a significant impact on the system performance.

5 PERFORMANCE ANALYSIS OF ENERGY HARVESTING PROTOCOL FOR VARIOUS RELAY NETWORK MODELS

In this section, I will clarify the first aim that is mentioned in Chapter 4. The main idea is to provide the basic analysis of outage probability and average throughput of various relay network models. The two typical relay network models, two-hop half-duplex and two-hop full-duplex relay networks, have been considered in the last chapter. The performance analysis for hybrid TSR–PSR alternate energy harvesting relay network or adaptive energy harvesting relaying protocol for two-way half- duplex over Rician fading channels is also conducted in [tan03, tan07]. In this chapter, I present the performance analysis of energy harvesting for an alternative model of relaying, in which a bidirectional relay supports the communication between an access point and a mobile user [tan11, tan12].

5.1 Introduction

In last decade, wireless sensor networks have been more and more attracted by the research community, due to their ability to carry out different kinds of tasks, from traffic monitoring, agriculture monitoring, to smart home and health-care applications. For these networks, network lifetime is a critical aspect to the success of the system. By some previous research, battery lifetime is the bottleneck in determining the lifetime of the whole system. In [42], three wireless powered sensor network models for the infrastructure monitoring application have been proposed, and their performances have been investigated. Another wireless powered sensor network model was presented in [43], in which a number of sensor nodes send common information to a far apart information access point via distributed beam-forming, by using the wireless energy transferred from a set of nearby multi-antenna energy transmitters.

Both of the works in [42] and [43] only introduce normal sensor networks without the helping of relay nodes. Furthermore, the RF energy transmitters in those works are independent of the information transfer process. This would increase the cost of implementation of these models in practice. In [18], the authors have tried to overcome this drawback by considering a new WPC system, where a wireless user communicates with an access point (AP) assisted by a bidirectional relay. The user and the relay both powered by the RF energy from the AP. Here, the role of the relay is to forward the energy from the AP to the user, as well as to forward information from the user to the AP. However, the authors in [18] only considered the case that channel gains are constant, and estimate the maximum achievable throughput of the system. Because of this limitation, there is a large difficulty to apply this result to practical sensor networks. In addition, the work in [18] only considers amplify-and-forward as the relaying strategy.

Continuing to the work of [18], in this chapter we provide a rigorous analysis of the same wireless powered sensor network model. We apply a Rayleigh distribution model for the channel gains between nodes, including the AP, relay node and the wireless user. For information transfer, both amplify-and-forward (AF) and decode-and-forward (DF) relaying protocols are investigated. Regarding the energy harvesting protocol, we focus on time switching (TS) strategy at the relay. The outage probability and the average throughput of the system are derived mathematically. The optimal time switching factor to maximize the system throughput is obtained via numerical algorithm. To verify the analysis mentioned above, Monte-Carlo simulations are also conducted and the results are reported in this chapter, too.

5.2 System model

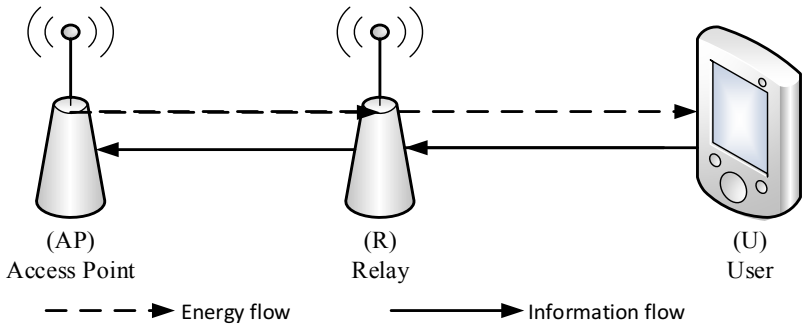

Figure 5.1. The bidirectional relaying network system

By extending the work of the authors in [18], I consider a wireless powered system as illustrated in Figure 5.1, where a mobile user is intended to send information to the AP with the assistance of a relay R. I studied the outage performance and system throughput of bidirectional wireless information and power transfer system with a helping relay. The relay helps forward wireless power from the access point (AP) to the user and also the information from the user to the AP in the reverse direction.

I assume that both the user and relay R have no other energy supply but solely the energy harvested from the AP. Furthermore, it is assumed that the direct connection between the AP and the user is so weak, hence, the only available communication path, as well as power transfer path, is via the relay R. The relay serves the dual roles of both energy relaying from the AP to the user and information forwarding from the user to the AP [18]. To initialize the communication process, a sufficient amount of initial energy is stored in the battery to conduct the first transmission block before energy harvesting, as in [44]. After that, the energy consumed by the user/relay is kept lower than or at most equal to the harvested energy amount during each block, thus no further manual battery replacement/recharging is needed. All nodes are assumed to operate in half-duplex mode, and either amplify-and-forward (AF) or decode-and-forward (DF) relaying strategy can be used at the relay for information transfer. Regarding the channel model, I consider the case that perfect channel state information (CSI) is available at the relay and the AP. Let h and g denote the channels from the AP to the relay and from the user to the relay, respectively. In addition, we assume for simplicity that these channels are reciprocal. Different from work in [18], all channels here experience Rayleigh fading and keep constant during each transmission block so that they can be considered as slow fading. As a result, $|h|^2$ and $|g|^2$ are exponential random variables with parameters $1/\lambda_h$ and $1/\lambda_g$ as table 2.1

5.3 Time Switching Relaying (TSR)

5.3.1 Amplify and forward protocol

For energy harvesting, we employ the time switching relaying (TSR) protocol, which is more convenient to implement in practice. As shown in Fig .5.2, the total symbol duration T is divided into three intervals with the lengths of αT , $(1-\alpha)T/2$ and $(1-\alpha)T/2$, respectively, where $0<\alpha<1$ denotes the time-switching ratio. The first interval corresponds to the energy harvesting phase at the relay R, in which the AP wirelessly sends its energy to R with power P_{ap}. Then, the total energy harvested at R during each

block is given by $E_r = \eta P_{ap} |h|^2 \alpha T$. The second phase of duration $(1-\alpha)T/2$ corresponds to the information transmitted from the user to the relay. In the third phase of the transmission block, R forwards an amplified or decoded signal to the AP and also forwards energy to the user. We assume that the circuit power consumption is negligible as compared to the radiation power, which is reasonable for low-power devices such as sensor nodes.

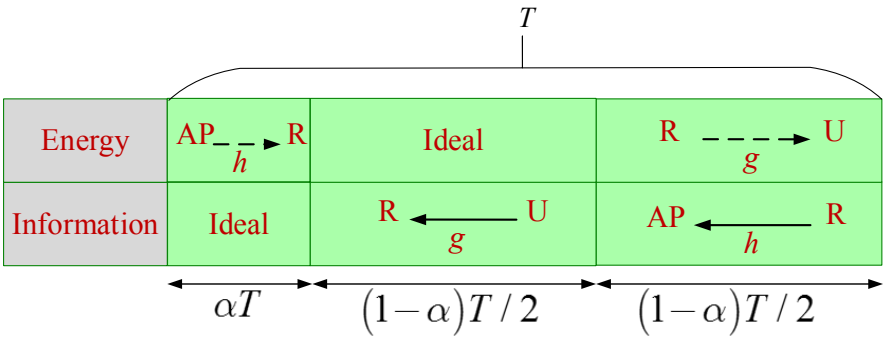

Figure 5.2. Time switching based protocol in the bidirectional relaying network

Let x_u denote the transmitted signal from the user during the second phase and Pu denote the power of this signal. The received signal at R during this phase is expressed as

$$y_r = \sqrt{P_u} g x_u + n_r \tag{5.1}$$

where $n_r \sim N(0,N0)$ denotes the Gaussian distributed noise at the relay R. During the third phase of the transmission, the relay amplifies the received signal from the mobile user and forwards it to both the AP and the user. While the AP receives this signal for the purpose of getting the information message, the user receives the same signal for energy harvesting purpose. The received signal at the AP during this phase is written as:

$$y_d = \sqrt{P_r} h x_r + n_d \tag{5.2}$$

where x_r is the signal transmitted by the relay, which has the power of Pr, and n_d is the zero-mean Gaussian noise at the AP with variance N_0. Because the transmit power of the relay comes from the energy supplied by the AP in the first phase, I must have [18]

$$P_r = \frac{E_r}{(1-\alpha)T/2} = \frac{2\alpha\eta P_{ap}|h|^2}{1-\alpha} = k\eta P_{ap}|h|^2 \tag{5.3}$$

where $k = \dfrac{2\alpha}{1-\alpha}$.

The signal transmitted by the relay is an amplified version of y_r:

$$x_r = \sqrt{\beta} y_r \tag{5.4}$$

According to energy conservation law, the energy consumed by the relay cannot exceed its available energy, which yields [18]

$$\beta = \frac{1}{P_u |g|^2 + N_0} \tag{5.5}$$

Now, I can substitute (5.1), (5.4), and (5.5) into (5.2) and get:

$$y_d = \sqrt{P_r} h \sqrt{\beta} (\sqrt{P_u} g x_u + n_r) + n_d = \underbrace{\sqrt{P_r} h \sqrt{\beta} \sqrt{P_u} g x_u}_{signal} + \underbrace{\sqrt{P_r} h \sqrt{\beta} n_r + n_d}_{noise} \tag{5.6}$$

From (5.6), the SNR at the AP can be computed by:

$$SNR = \frac{P_r \beta P_u |h|^2 |g|^2}{P_r \beta |h|^2 N_0 + N_0} = \frac{P_u |h|^2 |g|^2}{N_0 \left(|h|^2 + \frac{P_u |g|^2 + N_0}{k \eta P_{ap} |h|^2} \right)} \tag{5.7}$$

Let's move on to determine Pu. I know that the received signal at the mobile user during the third transmission phase is $y_u = g x_r = g \sqrt{\beta} y_r$. Hence, the energy harvested during this phase can be determined by:

$$E_u = \eta |g|^2 \beta \mathrm{E}\left\{ |y_r|^2 \right\} (1-\alpha) T / 2 = \eta |g|^2 E_r = \eta^2 P_{ap} |h|^2 |g|^2 \alpha T \tag{5.8}$$

So, the transmit power of the mobile user during the second phase is expressed as

$$P_u = \frac{E_u}{(1-\alpha) T / 2} = k \eta^2 P_{ap} |h|^2 |g|^2 \tag{5.9}$$

By substituting (5.9) into (5.7) and doing some algebra, I obtain the overall SNR for AF protocol:

$$SNR_{AF} = \frac{k \eta^2 P_{ap} |h|^4 |g|^4}{|h|^2 N_0 + \eta N_0 |g|^4 + \frac{N_0^2}{k \eta P_{ap} |h|^2}} \tag{5.10}$$

Assume that the source transmits at a constant rate R, then $\gamma_0 = 2^{2R} - 1$ is the lower threshold for SNR. Here, the outage probability P_{out} and the average throughput of the system can be evaluated by [45]

$$P_{out}^{AF} = \Pr\left(SNR < \gamma_0 \right) \tag{5.11}$$

$$R_{AF} = (1 - P_{out}^{AF}) R \frac{(1-\alpha)}{2} \tag{5.12}$$

Theorem 5.1: provides the exact integral forms for the outage probability and throughput of the proposed system with AF protocol.

$$P_{out}^{AF} = 1 - \lambda_h \int_{\sqrt{\frac{\gamma_0}{\delta}}}^{\infty} e^{-\lambda_h x - \lambda_g \sqrt{\frac{\gamma_0 \delta x^2 + \gamma_0}{\eta \delta^2 x^3 - \eta \gamma_0 \delta x}}} dx \tag{5.13}$$

$$R_{AF} = \frac{R\lambda_h (1-\alpha)}{2} \int_{\sqrt{\frac{\gamma_0}{\delta}}}^{\infty} e^{-\lambda_h x - \lambda_g \sqrt{\frac{\gamma_0 \delta x^2 + \gamma_0}{\eta \delta^2 x^3 - \eta \gamma_0 \delta x}}} dx \tag{5.14}$$

where $\delta = k\eta \frac{P_{ap}}{N_0}$.

Proof.

Let's denote $X = |h|^2, Y = |g|^2$. Note that X and Y are exponential random variables with the parameters $1/\lambda_h$ and $1/\lambda_g$, respectively. The end-to-end SNR of the system can be rewritten as

$$SNR_{AF} = \frac{\eta \delta X^2 Y^2}{X + \eta Y^2 + \frac{1}{\delta X}} = \frac{\eta \delta^2 X^3 Y^2}{\delta X^2 + \eta \delta X Y^2 + 1} \tag{5.15}$$

By substituting (5.15) to (5.11), I obtain:

$$\begin{aligned} P_{out}^{AF} &= \Pr\left(\frac{X^3 Y^2}{\delta X^2 + \eta \delta X Y^2 + 1} < \frac{\gamma_0}{\eta \delta^2} \right) = \Pr\left\{ Y^2 \left(X^3 - \frac{\gamma_0 X}{\delta} \right) < \left(\frac{\gamma_0 X^2}{\eta \delta} + \frac{\gamma_0}{\eta \delta^2} \right) \right\} \\ &= \Pr\left(X^3 < \frac{\gamma_0 X}{\delta} \right) + \Pr\left\{ Y^2 < \frac{\frac{\gamma_0 X^2}{\eta \delta} + \frac{\gamma_0}{\eta \delta^2}}{X\left(X^2 - \frac{\gamma_0}{\delta} \right)} \text{ and } X^3 \geq \frac{\gamma_0 X}{\delta} \right\} \end{aligned} \tag{5.16}$$

The first term of (5.16) can be determined easily as

$$\Pr\left(X^3 < \frac{\gamma_0 X}{\delta} \right) = \Pr\left(X < \sqrt{\frac{\gamma_0}{\delta}} \right) = 1 - e^{-\lambda_h \sqrt{\frac{\gamma_0}{\delta}}} \tag{5.17}$$

I proceed to evaluate the second term of (5.16). Let I denote this term, then I can write:

$$I = \Pr\left\{ Y < \sqrt{\frac{\gamma_0(\delta X^2+1)}{\eta\delta X(\delta X^2-\gamma_0)}} \; and \; X \geq \sqrt{\frac{\gamma_0}{\delta}} \right\} = \int_{\sqrt{\frac{\gamma_0}{\delta}}}^{\infty} f_X(x)dx \int_0^{g(x)} f_Y(y)dy$$
$$= \int_{\sqrt{\frac{\gamma_0}{\delta}}}^{\infty} \lambda_h e^{-\lambda_h x}\left(1-e^{-\lambda_g g(x)}\right)dx = e^{-\lambda_h\sqrt{\frac{\gamma_0}{\delta}}} - \int_{\sqrt{\frac{\gamma_0}{\delta}}}^{\infty} \lambda_h e^{-\lambda_h x-\lambda_g g(x)}dx \quad (5.18)$$

where $g(x) = \sqrt{\frac{\gamma_0(\delta x^2+1)}{\eta\delta x(\delta x^2-\gamma_0)}}$; $f_X(x) = \lambda_h e^{-\lambda_h x}$ and $f_Y(y) = \lambda_g e^{-\lambda_g y}$ are the probability density function (PDF), respectively; $F_X(x) = \int_0^x f_X(x)dx = 1-e^{-\lambda_h x}$ and $F_Y(y) = \int_0^y f_Y(y)dy = 1-e^{-\lambda_h y}$ are the cumulative distribution function (CDF), respectively which are defined in [12].

Now, (5.13) can be obtained by substituting (5.17) and (5.18) into (5.16). Then, I substitute (5.13) into (5.12) to get (5.14).

Theorem 5.2: closed-form approximations of the outage probability and throughput in terms of Meijer function are derived for high source-power-to-noise ratio regime.

At high P_{ap}/N_0 regime, the outage probability and average throughput of the proposed system with AF protocol can be respectively approximated to

$$P_{out}^{AF} \approx 1 - \frac{e^{-\lambda_h\sqrt{\frac{\gamma_0}{\delta}}}}{\sqrt{\pi}} \times G_{0,3}^{3,0}\left(\frac{\lambda_g^2\gamma\lambda_h}{4\eta\delta}\middle| 0, \frac{1}{2}, 1\right) \quad (5.19)$$

and

$$R_{AF} \approx \frac{R(1-\alpha)e^{-\lambda_h\sqrt{\frac{\gamma_0}{\delta}}}}{2\sqrt{\pi}} \times G_{0,3}^{3,0}\left(\frac{\lambda_g^2\gamma_0\lambda_h}{4\eta\delta}\middle| 0, \frac{1}{2}, 1\right) \quad (5.20)$$

where $G_{p,q}^{m,n}(.|...)$ is the Meijer function (Sec. 9.3 of [46]).

Proof.

Obviously, $\frac{1}{\delta} \to 0$ as $\frac{P_{ap}}{N_0} \to \infty$. Hence, at high values of $\frac{P_{ap}}{N_0}$, I can use the following approximation:

$$\frac{X+\eta Y^2+\frac{1}{\delta X}}{X+\eta Y^2+\sqrt{\frac{\gamma_0}{\delta}}} \approx 1$$

Now, by multiplying this term to the expression of SNR_{AF} in (5.15), I obtain:

$$SNR_{AF} = \frac{\eta\delta X^2 Y^2}{X + \eta Y^2 + \sqrt{\frac{\gamma_0}{\delta}}} \tag{5.21}$$

Using the same procedure as in Proof 1, I have:

$$\begin{aligned} P_{out}^{AF} &= \Pr\left(\frac{X^2Y^2}{X + \eta Y^2 + \sqrt{\frac{\gamma_0}{\delta}}} < \frac{\gamma_0}{\eta\delta} \right) = \Pr\left\{ Y^2\left(X^2 - \frac{\gamma_0}{\delta} \right) < \frac{\gamma_0}{\eta\delta}\left(X + \sqrt{\frac{\gamma_0}{\delta}} \right) \right\} \\ &= \Pr\left(X^2 < \frac{\gamma_0}{\delta} \right) + \Pr\left\{ Y^2 < \frac{\frac{\gamma_0}{\eta\delta}\left(X + \sqrt{\frac{\gamma_0}{\delta}} \right)}{X^2 - \frac{\gamma_0}{\delta}} \text{ and } X^2 \geq \frac{\gamma_0}{\delta} \right\} \\ &= 1 - e^{-\lambda_h\sqrt{\frac{\gamma_0}{\delta}}} - \Pr\left\{ Y^2 < \frac{\gamma_0}{\eta\delta\left(X - \sqrt{\frac{\gamma_0}{\delta}} \right)} \text{ and } X^2 \geq \frac{\gamma_0}{\delta} \right\} \end{aligned} \tag{5.22}$$

Again, I use the same argument as in the proof of Theorem 1 to rewrite the last term of (5.22) as:

$$I = \Pr\left\{ Y < \sqrt{\frac{\gamma_0}{\eta\delta\left(X - \sqrt{\frac{\gamma_0}{\delta}} \right)}} \text{ and } X \geq \sqrt{\frac{\gamma_0}{\delta}} \right\} = e^{-\lambda_h\sqrt{\frac{\gamma_0}{\delta}}} - \int_{\sqrt{\frac{\gamma_0}{\delta}}}^{\infty} \lambda_h e^{-\lambda_h x - \lambda_g h(x)} dx \tag{5.23}$$

Where $h(x) = \sqrt{\frac{\gamma_0}{\eta\delta\left(x - \sqrt{\frac{\gamma_0}{\delta}} \right)}}$

Then, (5.22) can be rewritten as

$$P_{out}^{AF} = 1 - \int_{\sqrt{\frac{\gamma_0}{\delta}}}^{\infty} \lambda_h e^{-\lambda_h x - \lambda_g \sqrt{\frac{\gamma_0}{\eta\delta\left(x - \sqrt{\frac{\gamma_0}{\delta}} \right)}}} dx \tag{5.24}$$

Finally, by changing variable $u = \lambda_h \left(x - \sqrt{\frac{\gamma_0}{\delta}} \right)$, I obtain:

$$\begin{aligned} P_{out}^{AF} &= 1 - \int_0^{\infty} e^{-u-\lambda_h\sqrt{\frac{\gamma_0}{\delta}}-\lambda_g\sqrt{\frac{\gamma_0\lambda_h}{\eta\delta u}}} du = 1 - e^{-\lambda_h\sqrt{\frac{\gamma_0}{\delta}}} \Gamma\left(1, 0, \lambda_g\sqrt{\frac{\gamma_0\lambda_h}{\eta\delta}}, \frac{1}{2}\right) \\ &= 1 - \frac{e^{-\lambda_h\sqrt{\frac{\gamma_0}{\delta}}}}{\sqrt{\pi}} \times G_{0,3}^{3,0}\left(\frac{\lambda_g^2\gamma_0\lambda_h}{4\eta\delta} \middle| 0, \frac{1}{2}, 1 \right) \end{aligned} \tag{5.25}$$

where $\Gamma(\alpha, x, b, \beta) \triangleq \int_x^{\infty} t^{\alpha-1} e^{-t-bt^{-\beta}} dt$ is the extended incomplete Gamma function, which is defined in [47] and the last equality comes from the Corollary (3.20) of [47]. From (5.25), I can easily get the throughput formula (5.20).

5.3.2 Decode and forward protocol

For DF relaying protocol, the data communication is divided into two separating hops, which do not depend on each other. Hence, the outage occurs if and only if either the source-relay path or the relay destination path fails to satisfy the corresponding SNR constraint. Different from the AF protocol, the message transmitted by the relay during the third transmission phase is the decoded message x_r, instead of x_r, and the transmit power of the relay in this phase is the same as the one given in [48]. Hence, the energy harvested by the mobile user during the same transmission phase is given by (5.8). As a result, the transmit power of the mobile user in the second phase is the same as in [42].

According to the equations (5.1) and (5.2), the SNR values at the relay R and the AP are respectively determined by:

$$SNR_R = \frac{P_u |g|^2}{N_0} = \delta\eta |h|^2 |g|^4 \tag{5.26}$$

and

$$SNR_{AP} = \frac{P_r |h|^2}{N_0} = \delta |h|^4 \tag{5.27}$$

The outage probability of the system can be written as

$$P_{out}^{DF} = \Pr\left(\min\left\{ SNR_R, SNR_{AP} \right\} < \gamma_0 \right) = 1 - \Pr\left(SNR_R \geq \gamma_0, SNR_{AP} \geq \gamma_0 \right) \tag{5.28}$$

Now we can claim the following theorem on the outage probability and the average throughput of the system of interest.

Theorem 5.3.

For the DF protocol, the outage probability and the average throughput of the proposed system can be expressed as

$$P_{out}^{DF} = 1 - \Gamma\left(1, \lambda_h x_0, \lambda_g y_0 \sqrt{x_0 \lambda_h}, \frac{1}{2}\right) \tag{5.29}$$

and

$$R_{DF} = \frac{R(1-\alpha)}{2} \Gamma\left(1, \lambda_h x_0, \lambda_g y_0 \sqrt{x_0 \lambda_h}, \frac{1}{2}\right) \tag{5.30}$$

where

$$x_0 = \sqrt{\frac{\gamma_0 N_0}{k\eta P_{ap}}} \tag{5.31}$$

$$y_0 = \sqrt{\frac{\gamma_0 N_0}{k\eta^2 P_{ap} x_0}} \tag{5.32}$$

Proof. Again, let X denote $|h|^2$ and Y denote $|g|^2$. The SNR values in (5.26) and (5.27) now become

$$SNR_R = \delta\eta |h|^2 |g|^4 = \delta\eta XY^2$$

$$SNR_{AP} = \delta |h|^4 = \delta X^2$$

where $\delta = k\eta \frac{P_{ap}}{N_0}$. Also, from (5.31) and (5.32), I have $x_0 = \sqrt{\frac{\gamma_0}{\delta}}$ *and* $y_0 = \sqrt{\frac{\gamma_0}{\delta\eta x_0}}$.

From (5.28), the outage probability can be rewritten as

$$P_{out}^{DF} = 1 - \Pr\left(\delta\eta XY^2 \geq \gamma_0, \delta X^2 \geq \gamma_0\right) = 1 - \Pr\left(Y \geq \sqrt{\frac{\gamma_0}{\eta\delta X}}, X \geq x_0\right)$$
$$= 1 - \Pr\left(Y \geq y_0\sqrt{\frac{x_0}{X}}, X \geq x_0\right) = 1 - \Pr\left(X \geq x_0, y_0\sqrt{\frac{x_0}{X}} \leq Y < y_0\right) - \Pr\left(X \geq x_0, Y \geq y_0\right) \quad (5.33)$$
$$= 1 - e^{-\lambda_h x_0 - \lambda_g y_0} - \int_{x_0}^{\infty} f_X(x)\left(\int_{y_0\sqrt{\frac{x_0}{x}}}^{y_0} f_Y(y)dy\right)dx$$

Denote the last term in (5.33) as I_1, then I have:

$$I_1 = -\int_{x_0}^{\infty} \lambda_h e^{-\lambda_h x}\left(\int_{y_0\sqrt{\frac{x_0}{x}}}^{y_0} \lambda_g e^{-\lambda_g y} dy\right)dx = -\int_{x_0}^{\infty} \lambda_h e^{-\lambda_h x}\left(e^{-\lambda_g y_0\sqrt{\frac{x_0}{x}}} - e^{-\lambda_g y_0}\right)dx \quad (5.34)$$
$$= -\int_{x_0}^{\infty} \lambda_h e^{-\lambda_h x} e^{-\lambda_g y_0\sqrt{\frac{x_0}{x}}} dx + e^{-\lambda_g y_0 - \lambda_h x_0} = -\int_{\lambda_h x_0}^{\infty} e^{-u} e^{-\lambda_g y_0\sqrt{\frac{\lambda_h x_0}{u}}} du + e^{-\lambda_g y_0 - \lambda_h x_0}$$

By substituting this into (5.33) and using the definition of extended incomplete gamma function (formula (1.9) in [40]), I obtain (5.29). Finally, (5.30) is obtained by including (5.29) in the definitive formula of average throughput.

5.3.3 Optimal Time-switching factor

To find the optimal time-switching factor that gives the best performance in terms of outage probability or average throughput, I solve the equations $\frac{dP_{out}(\alpha)}{d\alpha} = 0 \; and \; \frac{dR(\alpha)}{d\alpha} = 0$, respectively; where $P_{out}(\alpha) \; and \; R(\alpha)$ are outage probability and throughput functions with respect to the time-switching factor. By investigating the outage probability functions with respect to α for both AF and DF, we can easily see that these are non-increasing functions. That means the best outage performance is obtained when we exploit energy harvesting at full-scale. However, we should keep in mind that this outage performance only based on the comparison of power between signal and noise. It ignores other factors of the communication process. In practice, we cannot set α to 1 because it means that no communication data is transferred. Hence, the average throughput should be a more reasonable performance factor to be optimized. By plotting the throughput functions for AF and DF protocols versus α, I learn that these functions are concave functions, which have a unique maximum on the interval [0,1]. The optimal factor α∗ can be found numerically by some iterative methods, for instance, Golden section search method [49].

5.3.4 Numerical Results and Discussion

In this section, I conduct a Monte Carlo simulation to verify the analysis developed in the previous section. For simplicity, in our simulation model, we assume that the source relay and relay-destination distances are both normalized to unit value. Other simulation parameters are listed in Table 5.1.

Symbol	Name	Values
R	Source rate	1.5 bps/Hz
γ_0	SNR threshold	7
η	Energy harvesting efficiency	0.9
$1/\lambda_h$	Mean of $\|h\|^2$	0.5
$1/\lambda_g$	Mean of $\|g\|^2$	0.5
P_{ap}/N_0	Source (AP) Power to Noise Ratio	0-20 dB

Table 5.1. **Simulation parameters**

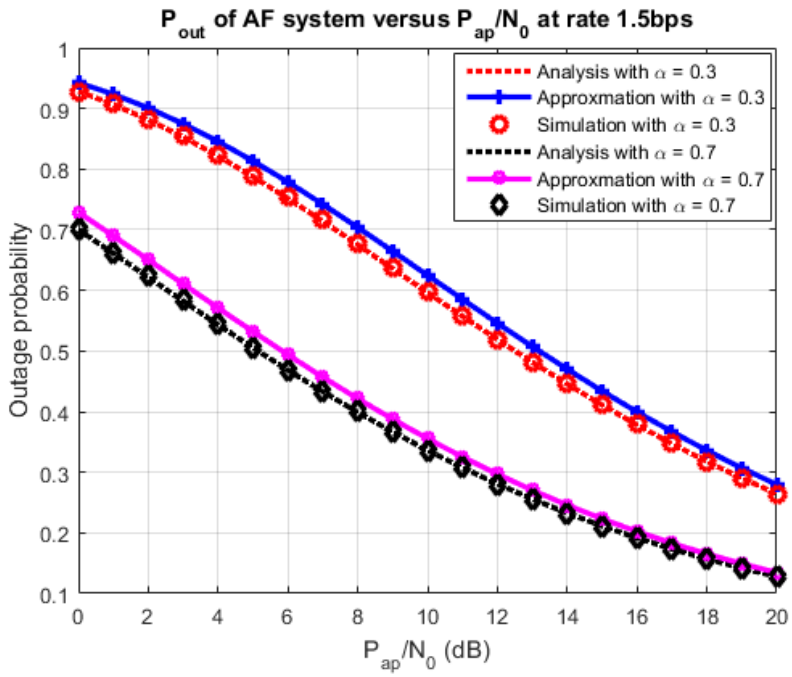

Figure 5.3. Outage probability versus source power to noise ratio for AF protocol

In Figure 5.3 and Figure 5.4, the achievable throughput and outage probability of the system with AF protocol are plotted against P_{ap} / N_0 ratio with the data rate set to be 1.5 bps. The times witching factor α is chosen to be 0.3 and 0.7. It's can be observed that the outage probability is a decreasing function with respect to P_{ap} / N_0, while the throughput grows with P_{ap} / N_0. In addition, the simulation and analysis curves are overlapping. The approximate outage probability and throughput are also plotted in these figures. They are close to the exact curves, especially when P_{ap} / N_0 is large. This confirms the correctness of my analysis in the previous section.

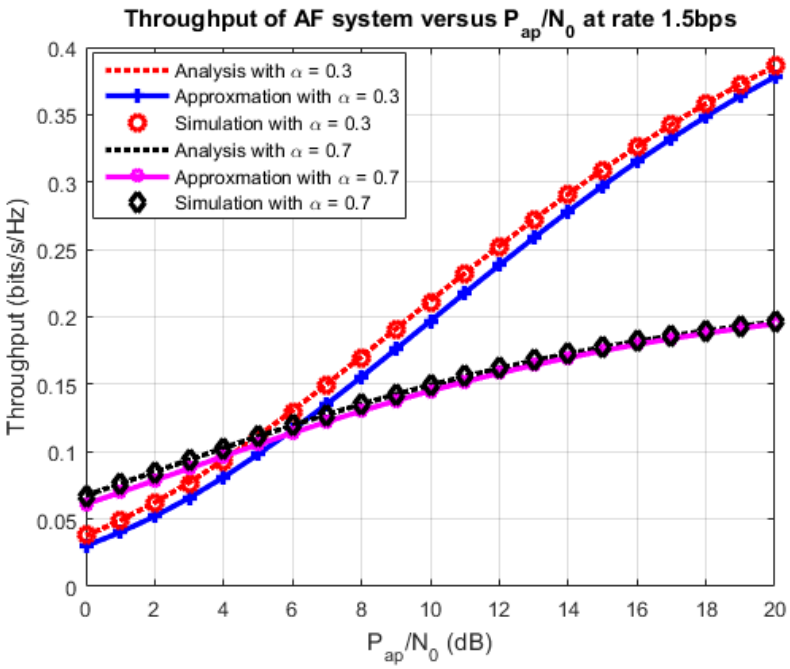

Figure 5.4. Throughput versus source power to noise ratio for AF protocol

The impact of time switching factor on system performance with AF protocol is illustrated in Figure 5.5 and Figure 5.6. In this experiment, P_{ap} / N_0 is set to 5 dB, and the rate can be varied at 1.5 bps, 1 bps, and 0.5 bps. It can be observed that the outage probability is reduced when we increase the value of α. On the other hand, the simulation result shows that there exists a unique time switching factor at which the average throughput is maximized. Indeed, this optimal factor can be found iteratively using numerical methods.

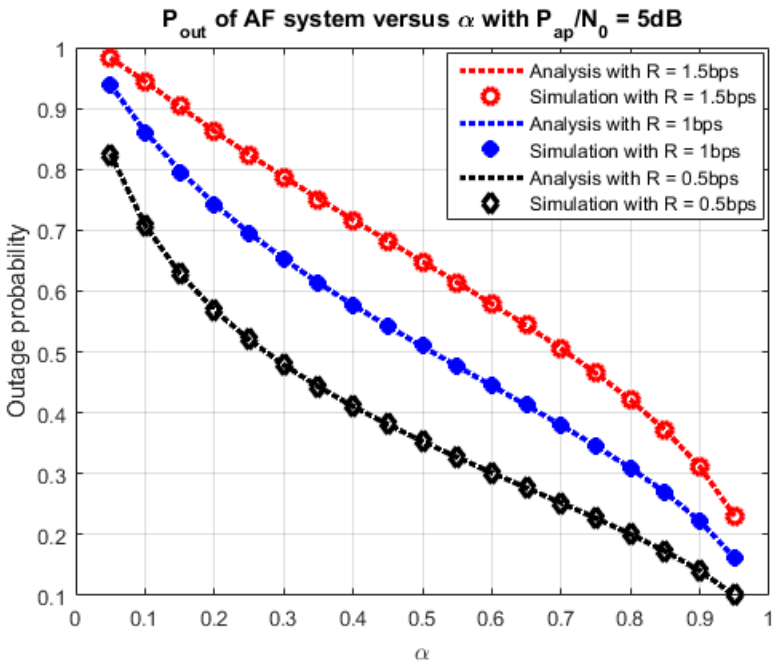

Figure 5.5. Outage probability versus time-switching factor for AF protocol

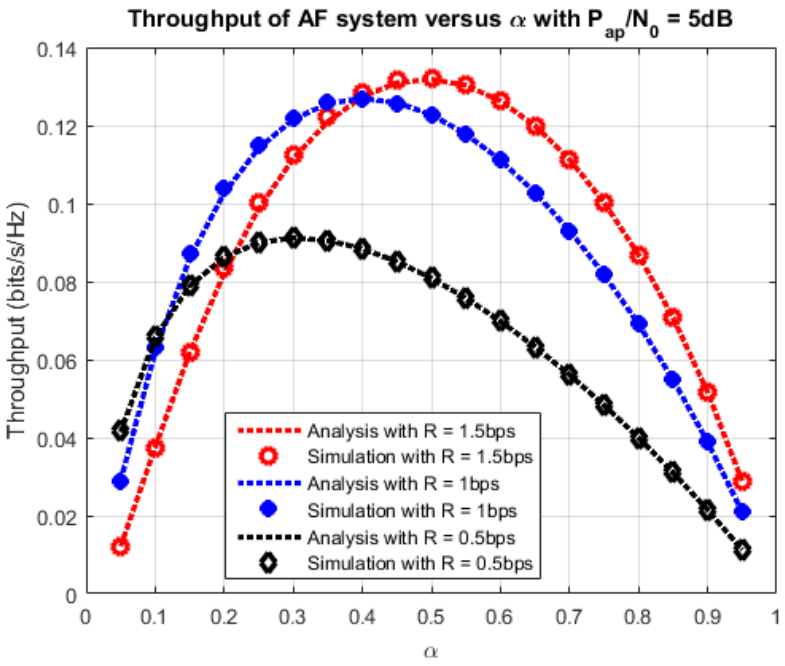

Figure 5.6. Throughput versus time-switching factor for AF protocol

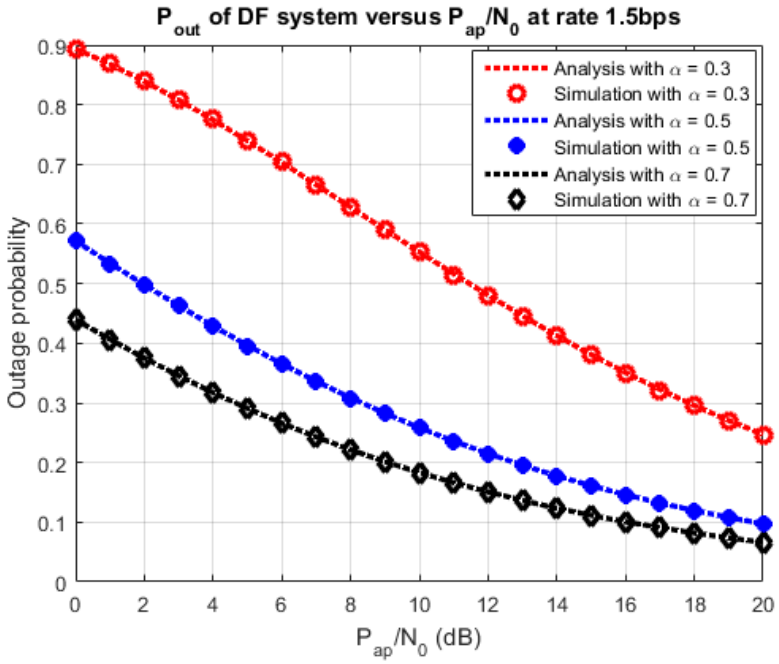

Figure 5.7. Outage probability versus source power to noise ratio for DF protocol

For decode-and-forward protocol, we also have similar results about the impact of various parameters, such as P_{ap} / N_0 and α on the average throughput and the outage probability of the system. Specifically,

Figure 5.7 and Figure 5.8 respectively plot the outage probability and throughput against P_{ap} / N_0 , while Figure 5.9 and Figure 5.10 show the dependence of these performance characteristics on time-switching factor α.

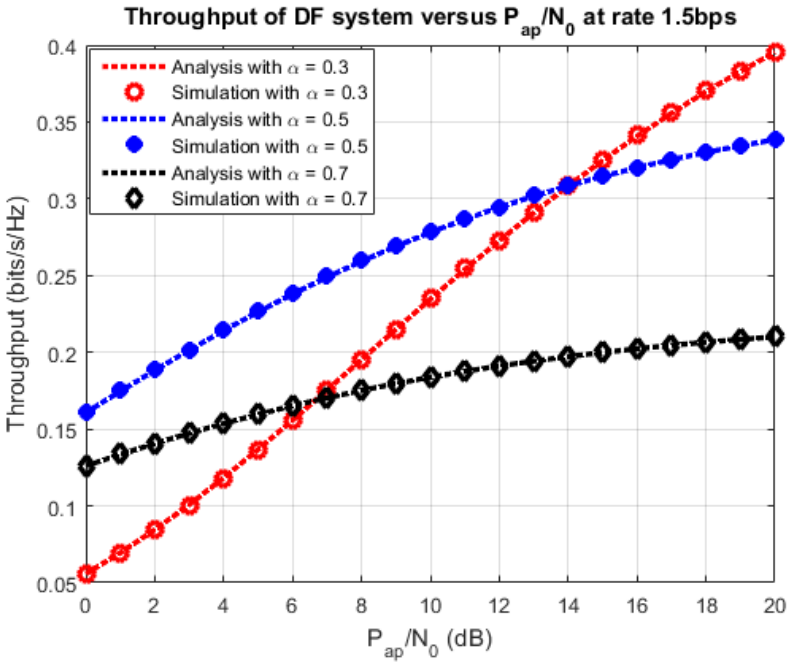

Figure 5.8. Throughput versus source power to noise ratio for DF protocol

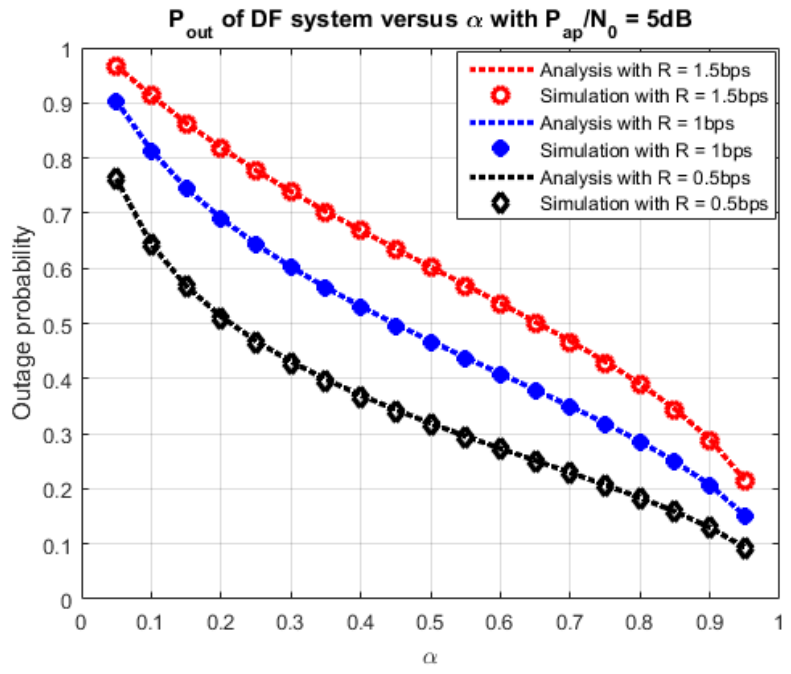

Figure 5.9. Outage probability versus time-switching factor for DF protocol

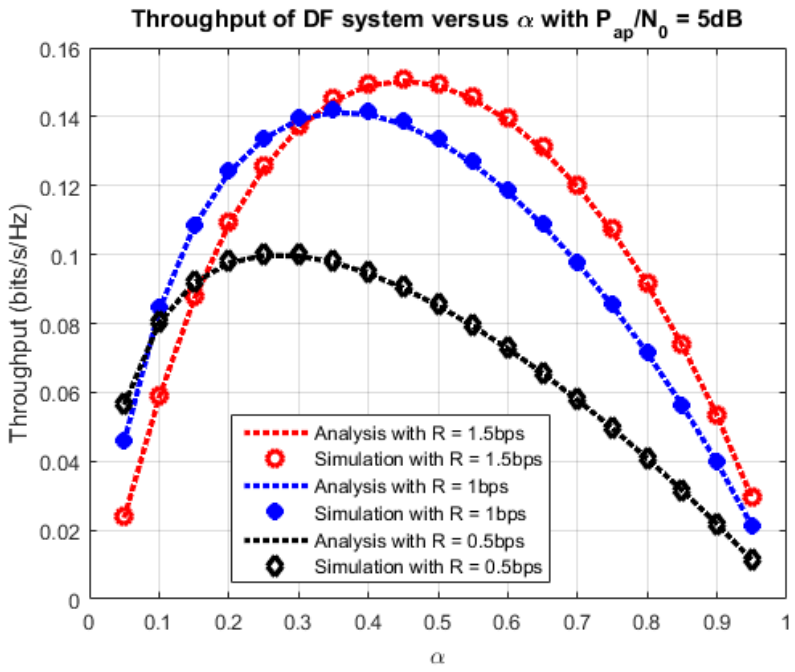

Figure 5.10. Throughput versus time-switching factor for DF protocol

Figure 5.11 and Figure 5.12 compare the performance of two protocols that are considered in this paper. The results show that the DF protocol is slightly better than AF protocol in terms of both outage probability and throughput because the noise at the relay is eliminated in DF protocol, while it's accumulated and amplified in AF protocol.

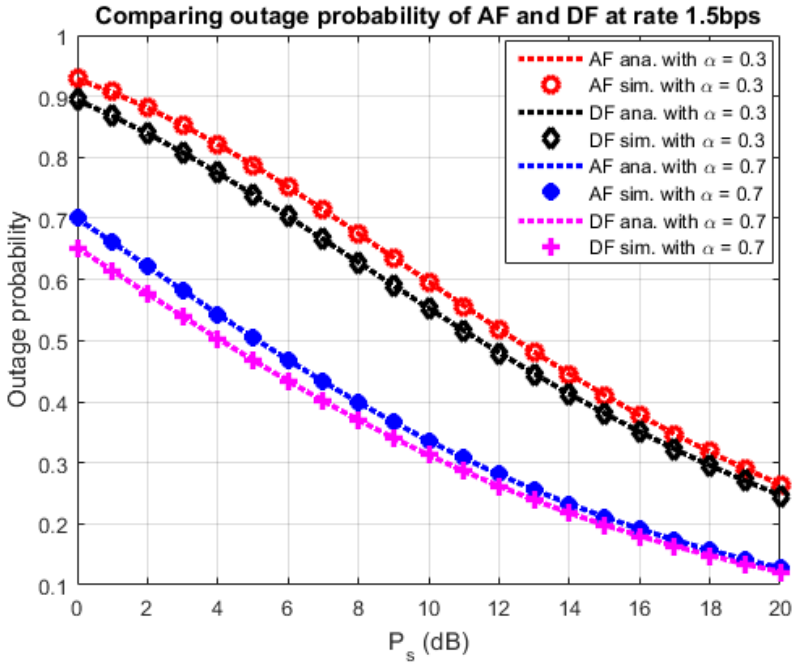

Figure 5.11. Outage probability of AF and DF protocol at rate 1.5 bps

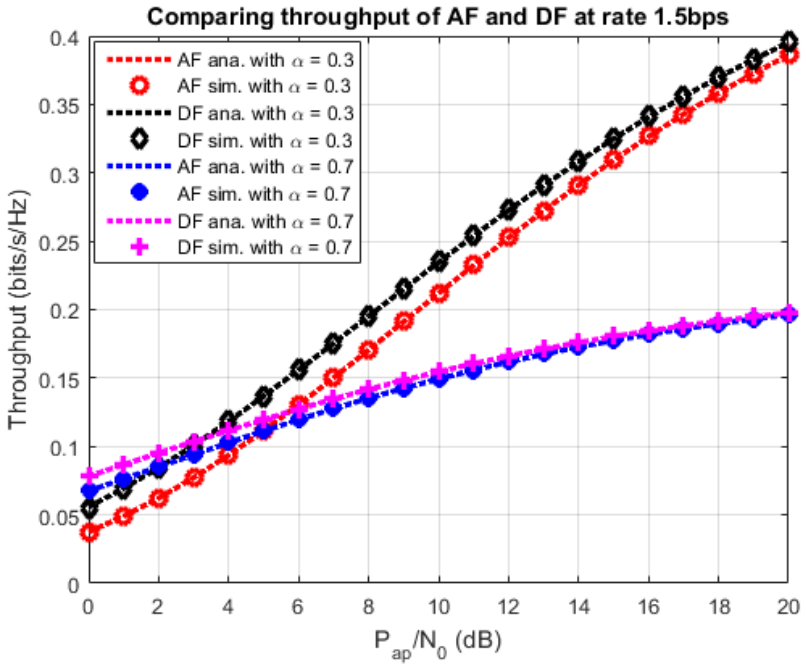

Figure 5.12. The throughput of AF and DF protocol at rate 1.5 bps

Finally, the optimal values of α at different values of source-power-to-noise-ratio for both AF and DF protocols are shown in Figure 5.13. We can see that the α value that optimizes the throughput has a tendency to decrease when P_{ap} / N_0 increases.

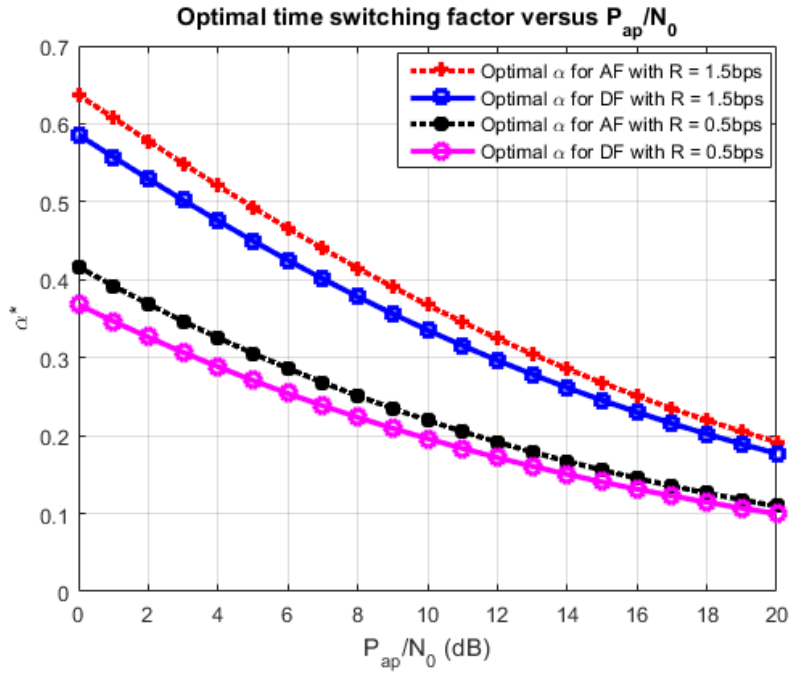

Figure 5.13. Optimal time-switching factor versus P_{ap} / N_0

5.4 Power Splitting Relaying (PSR)

5.4.1 Amplify and forward protocol

In this section, to apply the energy-harvesting idea, I select the power-switching relaying protocol because it can exploit the time resource at the best. The alternative method, namely, time-switching protocol, is more convenient to implement but requires a separate time slot for energy transmission. Hence, the time-switching protocol is not appropriate for applications with high transmission efficiency and will be addressed in another paper. For the power-switching relaying protocol, the symbol duration T is divided into 2 intervals with equal lengths of T/2 as illustrated in Figure 5.14.

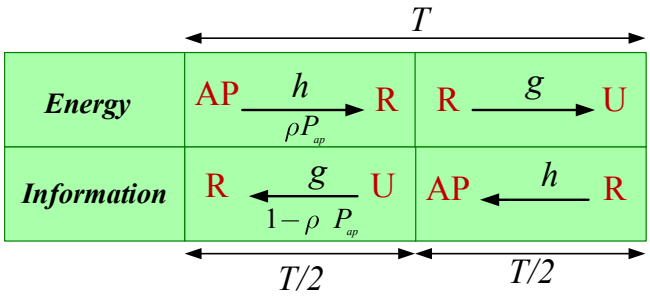

Figure 5.14. Power Splitting based protocol in the bidirectional relaying network

Energy harvesting and information transfer are expected to be performed at the same time but in opposite directions. In the first interval, the relay node receives both the information message transmitted by the mobile user and the RF energy-bearing signal sent from the AP for energy harvesting. Hence, the received signal at the relay R during the energy-harvesting phase is given by:

$$y_r = \sqrt{P_{ap}}hx_{ap} + \sqrt{P_u}gx_u + n_r \tag{5.35}$$

where x_{ap} and x_u denote the transmitted signals from the AP and the mobile user, respectively; Pap and Pu denote the power of these signals, respectively; and nr denotes the antenna noise at the relay R, which is Gaussian distributed with zero mean.

The power of the received signal at the relay in the first phase is split into 2 components: The first one is used for energy harvesting, and the other is used for information relaying in the second phase. Let ρ denote the power splitting ratio for energy harvesting, where $0 < \rho < 1$. During the second interval, the relay node simultaneously forwards energy to the mobile user and information message to the AP. The energy received by the user during this phase will be used for transmitting the user data in the first phase of the next block. Please be noticed that the AP is usually put at a fixed location and is supplied by stable energy sources. So it is not necessary for the AP to harvest the energy wirelessly. The goal of this scheme is to supply the energy to the relay node and the user, which are in mobility and energy supply is their vital issue. Here, I assume that the energy-bearing signal x_{ap} in (5.35) and the channel gain h are perfectly known by the relay. Hence, x_{ap} can be pre-cancelled at the relay before relaying to exploit

more energy for forwarding the desired message [18]. Recall that I assume the circuit power consumption is supplied by the relay and the user themselves, so we only focus on the energy consumption for transmitting and relaying information.

As mentioned above, a portion of received power is kept by the relay, implying that the energy harvested at R during a transmission period is expressed as $E_r = \eta\rho \mathrm{E}\left[\left|y_r\right|^2\right](T/2) \approx \eta\rho P_{ap}\left|h\right|^2 (T/2)$, where $0 < \eta < 1$ is the energy conversion efficiency at the relay node. Here, we have ignored the noise and user signal power for energy harvesting at R due to the fact that P_U is much less than P_{ap} in practice. Furthermore, as we will see later in our model, the energy available at the user is originated from the AP via R after double channel attenuations and a series of other losses.

After pre-cancelling the signal x_{ap}, the remaining part of the received signal at the relay is written as:

$$y_r = \sqrt{1-\rho}\left(\sqrt{P_u} g x_u + n_r\right) + n_r^{'} \tag{5.36}$$

According to the AF protocol, the signal transmitted by R during the second phase is:

$$x_r = \beta\left\{\sqrt{1-\rho}\left(\sqrt{P_u} g x_u + n_r\right) + n_r^{'}\right\} \tag{5.37}$$

where β is the amplification coefficient and $n_r^{'}$ is the additional processing noise as a relay, which is assumed to be Gaussian distributed with zero mean and variance of N_0. It is also assumed that this noise dominates the antenna noise n_r, so that we can ignore n_r from now on. The energy consumed by the relay must be equal to the energy harvested during the first phase according to energy conservation law, which gives us

$$\beta = \sqrt{\frac{\eta\rho P_{ap}\left|h\right|^2}{(1-\rho)P_u\left|g\right|^2 + N_0}} \tag{5.38}$$

The received signal at the AP during the phase now can be written as

$$y_d = h\beta\left(\sqrt{1-\rho}\sqrt{P_u} g x_u + n_r^{'}\right) + n_d = \underbrace{h\beta\sqrt{1-\rho}\sqrt{P_u} g x_u}_{signal} + \underbrace{h\beta n_r^{'} + n_d}_{noise} \tag{5.39}$$

where n_d is the AWGN noise at the AP with zero mean and variance N_0.

While the AP receives the information signal, the mobile user also receives the RF energy sent from the relay. By ignoring the noise energy, which is negligible as compared with the signal energy, the received signal at the mobile user is $y_u = g x_r$; hence, the energy harvested at the mobile user is $E_u = \eta\left|g\right|^2 \mathrm{E}\left\{\left|x_r\right|^2\right\}$

Again, by using the energy conservation law, I obtain:

$$P_u = \frac{E_u}{T/2} = \eta^2 \rho P_{ap} |h|^2 |g|^2 \tag{5.40}$$

From (5.39), the end to end SNR at the AP can be computed by

$$SNR_{AF} = \frac{\beta^2 |h|^2 |g|^2 (1-\rho) P_u}{\beta^2 |h|^2 N_0 + N_0} = \frac{|h|^2 |g|^2 (1-\rho) P_u}{|h|^2 N_0 + N_0 / \beta^2} \tag{5.41}$$

By substituting P_u in (5.40) and β in (5.38) into the above equation, I obtain:

$$SNR_{AF} = \frac{|h|^4 |g|^4 \eta^2 \rho (1-\rho) P_{ap}}{|h|^2 N_0 + N_0 \dfrac{(1-\rho)\eta^2 \rho P_{ap} |h|^2 |g|^4 + N_0}{\eta \rho P_{ap} |h|^2}} \tag{5.42}$$

with the assumption that the data transmission rate of the mobile user is R, then the lowest acceptable value of SNR is still $\gamma_0 = 2^{2R} - 1$. The system outage occurs if $SNR_{AF} < \gamma_0$, and the outage probability, as well as the average throughput of the system, can be calculated by [45].

$$P_{out}^{AF} = \Pr\left(SNR_{AF} < \gamma_0\right) \tag{5.43}$$

$$R_{AF} = \left(1 - P_{out}^{AF}\right) \frac{R}{2} \tag{5.44}$$

Using this approach, I can also obtain the closed-form expressions of the outage probability and system throughput for AF protocol as previous section 5.2.1.

Theorem 5.4 (exact form).

The outage probability and the average throughput of the proposed system with AF relaying protocol is given as

$$P_{out}^{AF} = 1 - \lambda_h \int_{\sqrt{\frac{a_3\gamma_0}{a_1}}}^{\infty} e^{-\lambda_h x - \lambda_g \sqrt{\frac{\gamma_0\left(a_2 x^2 + 1\right)}{a_1 x\left(x^2 - \frac{a_3\gamma_0}{a_1}\right)}}} dx \tag{5.45}$$

$$R_{AF} = \frac{R\lambda_h}{2} \int_{\sqrt{\frac{a_3\gamma_0}{a_1}}}^{\infty} e^{-\lambda_h x - \lambda_g \sqrt{\frac{\gamma_0\left(a_2 x^2 + 1\right)}{a_1 x\left(x^2 - \frac{a_3\gamma_0}{a_1}\right)}}} dx \tag{5.46}$$

where $a_1 = \eta^3 \rho^2 \left(\frac{P_{ap}}{N_0}\right)^2 (1-\rho),\ a_2 = \eta\rho \frac{P_{ap}}{N_0}$, *and* $a_3 = \eta^2 \frac{P_{ap}}{N_0} \rho(1-\rho)$.

Proof.

Again, let me denote $X = |h|^2, Y = |g|^2$. By substituting these variables into (5.42), and then into (5.43), I obtain:

$$\begin{aligned} P_{out}^{AF} &= \Pr\left\{Y^2\left(a_1X^3 - a_3\gamma_0 X\right) < \gamma_0\left(a_2X^2\right)\right\} \\ &= \Pr\left(a_1X^3 - a_3\gamma_0 X < 0\right) + \Pr\left\{\begin{bmatrix} Y^2(a_1X^3 - a_3\gamma_0 X) < \gamma_0(a_2X^2+1) \\ a_1X^3 - a_3\gamma_0 X \geq 0 \end{bmatrix}\right\} \end{aligned} \tag{5.47}$$

The first term of (5.47) can be determined easily as:

$$I = \Pr\left(X < \sqrt{\frac{a_3\gamma_0}{a_1}}\right) = 1 - e^{-\lambda_h\sqrt{\frac{a_3\gamma_0}{a_1}}} \tag{5.48}$$

The second term of (5.47) can be rewritten as

$$\begin{aligned} J &= \Pr\left\{Y < \sqrt{\frac{\gamma_0(a_2X^2+1)}{X(a_1X^2 - a_3\gamma_0)}}\ and\ X \geq \sqrt{\frac{a_3\gamma_0}{a_1}}\right\} \\ &= \int_{\sqrt{\frac{a_3\gamma_0}{a_1}}}^{\infty} f_X(x)dx \int_0^{p(x)} f_Y(y)dy = e^{-\lambda_h\sqrt{\frac{a_3\gamma_0}{a_1}}} - \int_{\sqrt{\frac{a_3\gamma_0}{a_1}}}^{\infty} \lambda_h e^{-\lambda_h x - \lambda_g p(x)}dx \end{aligned} \tag{5.49}$$

where $p(x) = \sqrt{\frac{\gamma_0(a_2x^2+1)}{x(a_1x^2 - a_3\gamma_0)}}$.

Now, equation (5.45) can be obtained by substituting (5.48) and (5.49) into (5.47). Then, equation (5.46) follows immediately.

Theorem 5.5 (closed-form approximation).

$$P_{out}^{AF} \approx 1 - \frac{e^{-\lambda_h\sqrt{\frac{\gamma_0}{\eta\rho\psi}}}}{\sqrt{\pi}} \times G_{0,3}^{3,0}\left(\frac{\lambda_g^2\gamma_0\lambda_h}{4\eta^2\psi\rho(1-\rho)}\middle| 0, \frac{1}{2}, 1\right) \tag{5.50}$$

and

$$R_{AF} \approx \frac{R \times e^{-\lambda_h\sqrt{\frac{\gamma_0}{\eta\rho\psi}}}}{2\sqrt{\pi}} \times G_{0,3}^{3,0}\left(\frac{\lambda_g^2\gamma_0\lambda_h}{4\eta^2\psi\rho(1-\rho)}\middle| 0, \frac{1}{2}, 1\right) \tag{5.51}$$

where $\psi = \frac{P_{ap}}{N_0}$.

Proof.

Equation (5.47) can be rewritten as

$$P_{out}^{AF} = \Pr\left(\frac{\eta^3 \rho^2 (1-\rho) X^2 Y^2}{\eta\rho X + \eta^2 \rho(1-\rho) Y^2 + \frac{1}{\psi X}} < \gamma_0 \right) \tag{5.52}$$

Obviously, $\frac{1}{\psi} \to 0$ as $\frac{P_{ap}}{N_0} \to \infty$. Hence, at high values of $\frac{P_{ap}}{N_0}$, I can use the following approximation:

$$\frac{\eta\rho X + \eta^2 \rho(1-\rho) Y^2 + \frac{1}{\psi X}}{\eta\rho X + \eta^2 \rho(1-\rho) Y^2 + \sqrt{\frac{\gamma_0 \eta\rho}{\psi}}} \approx 1$$

Now, by multiplying this term with SNR_{AF} in (5.52), I get

$$P_{out}^{AF} \approx \Pr\left\{ \frac{\eta^3 \rho^2 (1-\rho) X^2 Y^2}{\eta\rho X + \eta^2 \rho(1-\rho) Y^2 + \sqrt{\frac{\gamma_0 \eta\rho}{\psi}}} < \gamma_0 \right\} \tag{5.53}$$

After doing some algebra, I obtain

$$P_{out}^{AF} = \Pr\left(X^2 < \frac{\gamma_0}{a_2} \right) + \Pr\left\{ Y^2 < \frac{\gamma_0}{a_3\left(X - \sqrt{\frac{\gamma_0}{a_2}} \right)} \text{ and } X^2 \geq \frac{\gamma_0}{a_2} \right\} \tag{5.54}$$

Now, using the same procedure as Proof of Theorem 1, I have

$$P_{out}^{AF} = 1 - e^{-\lambda_h \sqrt{\frac{\gamma_0}{a_2}}} + \int_{\sqrt{\frac{\gamma_0}{a_2}}}^{\infty} f_X(x)dx \int_0^{g(x)} f_Y(y)dy = 1 - \int_{\sqrt{\frac{\gamma_0}{a_2}}}^{\infty} \lambda_h e^{-\lambda_h x - \lambda_g \sqrt{\frac{\gamma_0}{a_3\left(x - \sqrt{\frac{\gamma_0}{a_2}} \right)}}} dx \tag{5.55}$$

where $g(x) = \sqrt{\frac{\gamma_0}{a_3\left(x - \sqrt{\frac{\gamma_0}{a_2}}\right)}}$.

Finally, by changing the variable $t = \lambda_h\left(x - \sqrt{\frac{\gamma_0}{a_2}}\right)$, I obtain:

$$\begin{aligned} P_{out}^{AF} &= 1 - \int_0^{\infty} e^{-t - \lambda_h\sqrt{\frac{\gamma_0}{a_2}} - \lambda_g\sqrt{\frac{\gamma_0\lambda_h}{a_3 t}}}\, dt = 1 - e^{-\lambda_h\sqrt{\frac{\gamma_0}{a_2}}}\,\Gamma\left(1, 0, \lambda_g\sqrt{\frac{\gamma_0\lambda_h}{a_3}}, \frac{1}{2}\right) \\ &= 1 - \frac{e^{-\lambda_h\sqrt{\frac{\gamma_0}{a_2}}}}{\sqrt{\pi}} \times G_{0,3}^{3,0}\left(\frac{\lambda_g^2\gamma_0\lambda_h}{4a_3}\middle| 0, \frac{1}{2}, 1\right) \end{aligned} \tag{5.56}$$

where $\Gamma(\alpha, x, b, \beta) \triangleq \int_x^{\infty} t^{\alpha-1} e^{-t - bt^{-\beta}}\, dt$ is the extended incomplete Gamma function, which is defined in [47] and I use the Corollary (3.20) to get the last equality of (5.56); then from that, the results of Theorem 5.5 should follow.

5.4.2 Decode and forward protocol

For DF relaying strategy, the relay needs to decode the message symbol from the source node before retransmitting it to the destination. As a result, the outage probability can occur if either the channel between source and relay or the channel between relay and destination fails to meet the required constraint. However, by energy conservation law, the transmit power from the relay to the mobile user during the second interval as well as from the mobile user to the relay in the first interval must be the same as in (5.40). Hence, I can derive the formulas of SNR values at the relay R and the AP, respectively, as

$$SNR_R = \frac{(1-\rho)P_u |g|^2}{N_0} = \frac{\eta^2\rho(1-\rho)P_{ap}|h|^2|g|^4}{N_0} \tag{5.57}$$

and

$$SNR_{AP} = \frac{P_r |h|^2}{N_0} = \frac{\eta\rho P_{ap}|h|^4}{N_0} \tag{5.58}$$

Now, the overall outage probability of the system is derived as

$$P_{out}^{DF} = \Pr\left\{\min\left(SNR_R, SNR_{AP}\right) < \gamma_0\right\} = 1 - \Pr\left(SNR_R \geq \gamma_0, SNR_{AP} \geq \gamma_0\right) \tag{5.59}$$

Then, I can state the following theorem for DF protocol.

Theorem 5.6. The outage probability and the average throughput of the proposed system with DF relaying protocol is given as

$$P_{out}^{DF} = 1 - \Gamma\left(1, \lambda_h \sqrt{\frac{\gamma_0}{a_2}}, \lambda_g \sqrt{\frac{\gamma_0 \lambda_h}{a_3}}, \frac{1}{2}\right) \tag{5.60}$$

and

$$R_{DF} = \frac{R}{2} \Gamma\left(1, \lambda_h \sqrt{\frac{\gamma_0}{a_2}}, \lambda_g \sqrt{\frac{\gamma_0 \lambda_h}{a_3}}, \frac{1}{2}\right) \tag{5.61}$$

where $\Gamma(\alpha, x, b, \beta)$ is the extended incomplete gamma function [47].

Proof.

By letting $a_2 = \eta\rho \frac{P_{ap}}{N_0}$ *and* $a_3 = \eta^2 \frac{P_{ap}}{N_0} \rho(1-\rho)$, the SNR values in (5.57) and (5.58) now become

$$SNR_R = a_3 XY^2, SNR_{AP} = a_2 X^2 \tag{5.62}$$

From (5.59), the outage probability can be rewritten as:

$$\begin{aligned} P_{out}^{DF} &= 1 - \Pr\left\{a_3 XY^2 \geq \gamma_0, a_2 X^2 \geq \gamma_0\right\} = 1 - \int_{\sqrt{\frac{\gamma_0}{a_2}}}^{\infty} f_X(x)dx \int_{\sqrt{\frac{\gamma_0}{a_3 x}}}^{\infty} f_Y(y)dy \\ &= 1 - \lambda_h \int_{\sqrt{\frac{\gamma_0}{a_2}}}^{\infty} e^{-\lambda_h x - \lambda_g \sqrt{\frac{\gamma_0}{a_3 x}}} dx = 1 - \Gamma\left(1, \lambda_h \sqrt{\frac{\gamma_0}{a_2}}, \lambda_g \sqrt{\frac{\gamma_0 \lambda_h}{a_3}}, \frac{1}{2}\right) \end{aligned} \tag{5.63}$$

Finally, equation (5.61) is obtained by substituting equation (5.60) into the definitive formula of the average throughput.

5.4.3 Optimal Power-splitting factor

By the definitive formulas of the average throughput and the outage probability, it is obviously seen that once the average throughput is maximized, the outage probability is also minimized. The optimal power-splitting factor that minimizes the outage probability and maximizes the average throughput of the system of interest can be found by solving the equation $\frac{dP_{out}(\rho)}{d\rho} = 0$, where $P_{out}(\rho)$ is the outage probability function with respect to the power-splitting factor. As seen in Figures 5.17 and 5.21, the throughput functions are concave functions with respect to ρ, which have a single maximum on [0,1]. Hence, this optimal factor ρ∗ can be found by the Golden section search method [49] as shown in the following section.

5.4.4 Numerical Results and Discussion

For verification purpose, Monte Carlo simulation has been conducted to investigate the performance factors of the proposed system. In this section, I am also not going to study the impact of the link distances on system performance. Hence, without loss of generality, I can set both the link distances (from the AP to the relay and from the relay to the mobile user) to 1. Table 5.1 have listed all the values of the parameters that are used in my simulation.

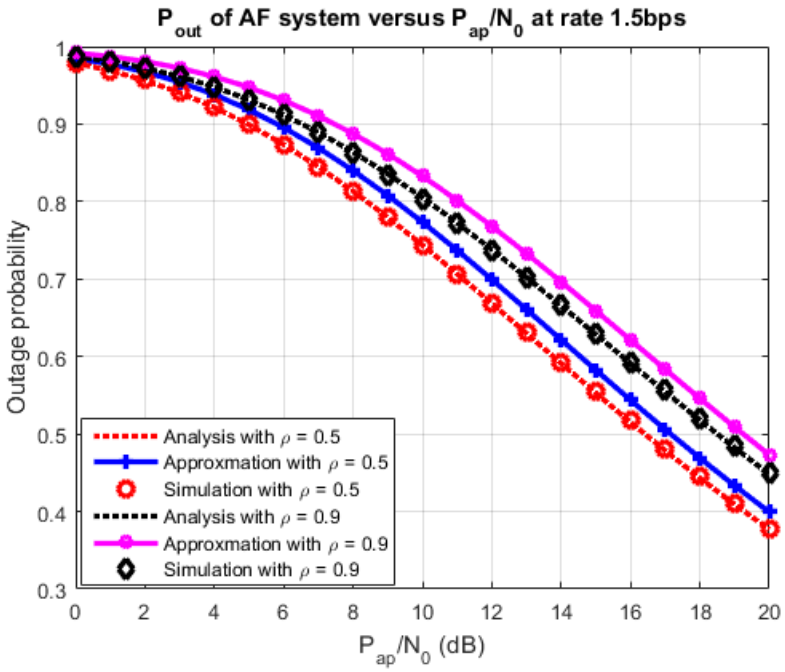

Figure 5.15. Outage probability versus Pap/N_0 for AF protocol

Figures 5.15 and 5.16 illustrate the system throughput and outage probability with AF protocol at various values of Pap/N_0 ratio. Here, the data rate is set to be 1.5 bps/Hz, and the power-splitting factor ρ is set to 0.5 and 0.9. It can be observed that the outage and throughput performance is improved with higher values of Pap/N_0. The simulation curves exactly match the theoretical analysis ones. Furthermore, the approximate outage probability and throughput curves approach closely to the exact curves as Pap/N_0 becomes large. This verifies the theoretical analysis stated in Theorem 5.5.

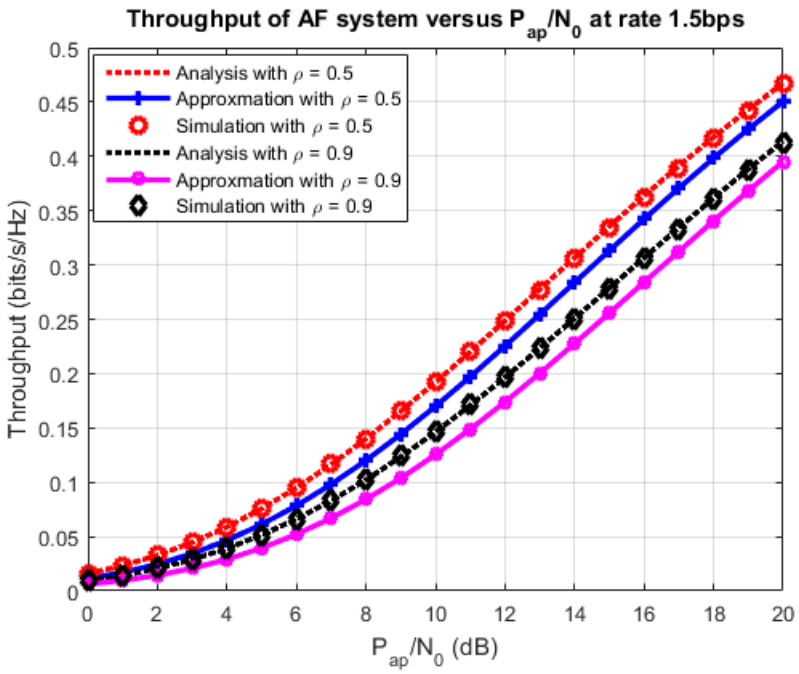

Figure 5.16. Throughput versus Pap/N_0 for AF protocol

Figures 5.17 and 5.18 show the impact of the power-splitting factor on the AF relaying system performance. For this study, Pap/N0 is fixed at 20 dB, while the rate can vary among 1.5, 1, and 0.5 bps. It can be seen that the outage probability is a convex function, while the throughput is a concave function with respect to ρ. Hence, there exists a unique power-splitting factor that maximizes the average throughput. Because of the concavity of the throughput function, this optimal factor can be found numerically by using iterative algorithms such as the golden-section search method.

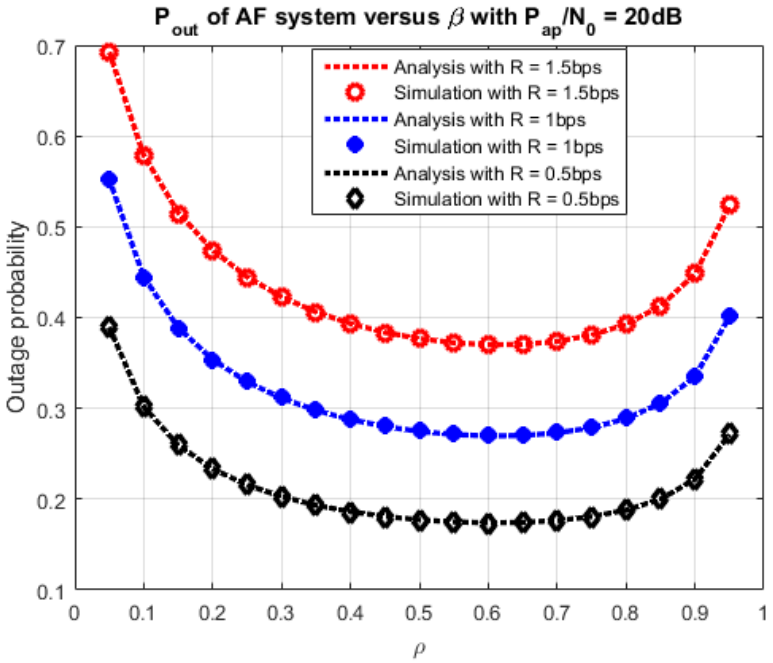

Figure 5.17. Outage probability versus power-splitting factor for AF protocol

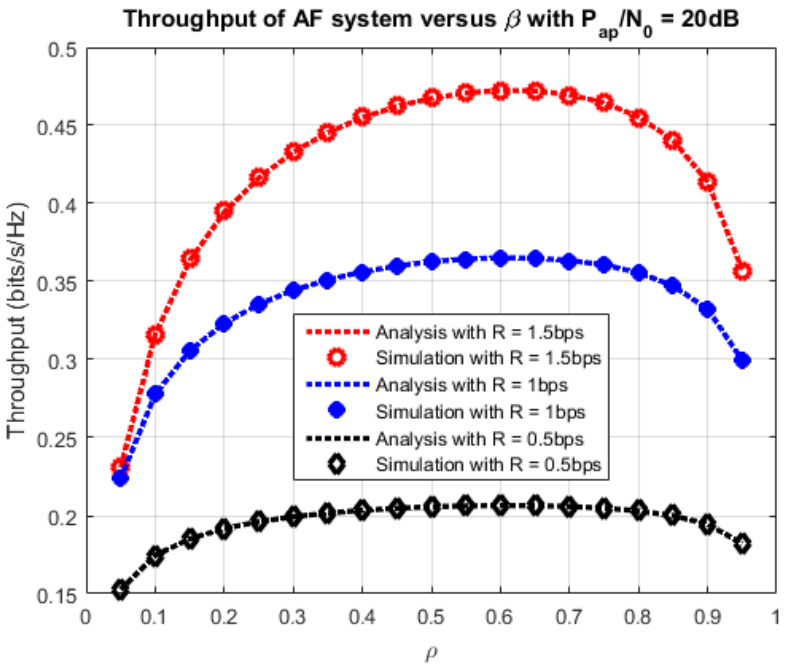

Figure 5.18. Throughput versus power-splitting factor for AF protocol

The impact of Pap/N_0 on the DF relaying system performance is illustrated in Figures 5.19 and 5.20, which is similar to the results with AF protocol. Figures 5.21 and 5.22 also display the dependence of outage probability and throughput on the power splitting factor ρ.

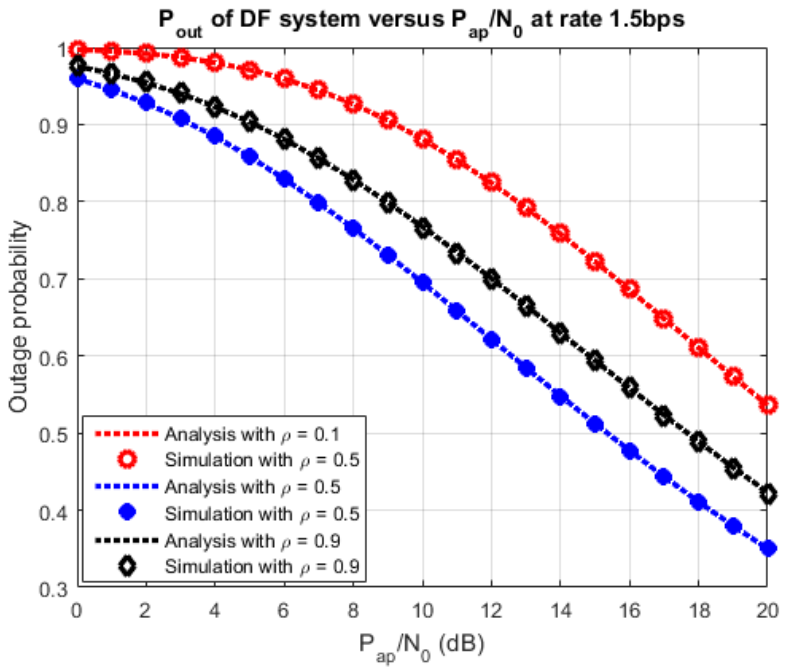

Figure 5.19. Outage probability versus Pap/N_0 for DF protocol

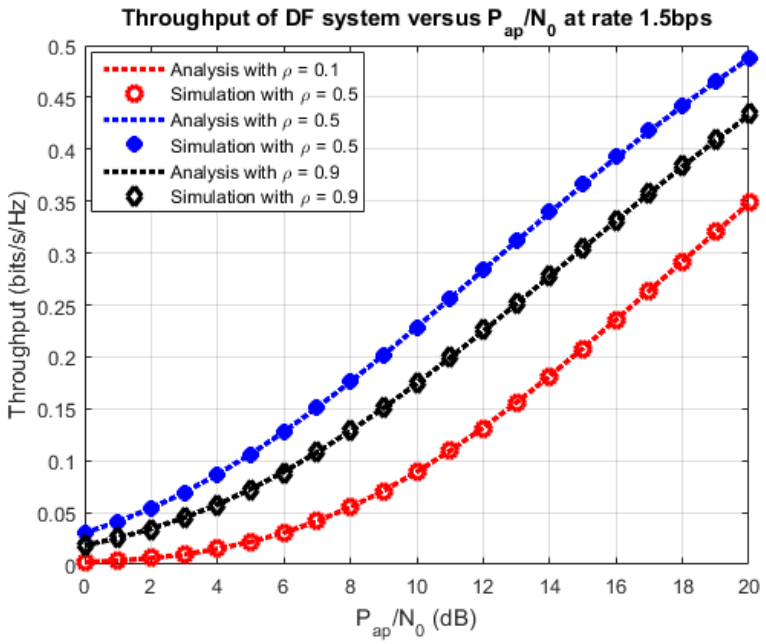

Figure 5.20. Throughput versus Pap/N0 for DF protocol

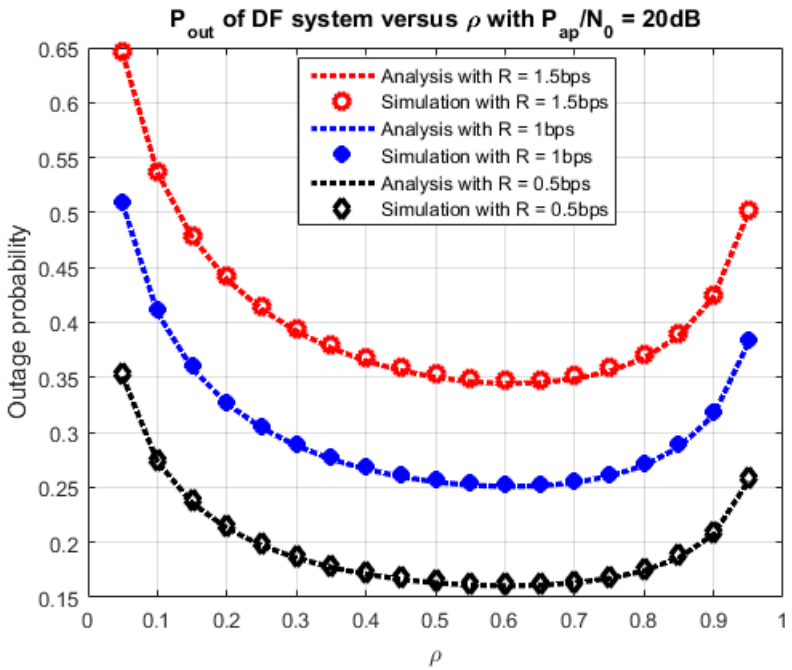

Figure 5.21. Outage probability versus power-splitting factor for DF protocol

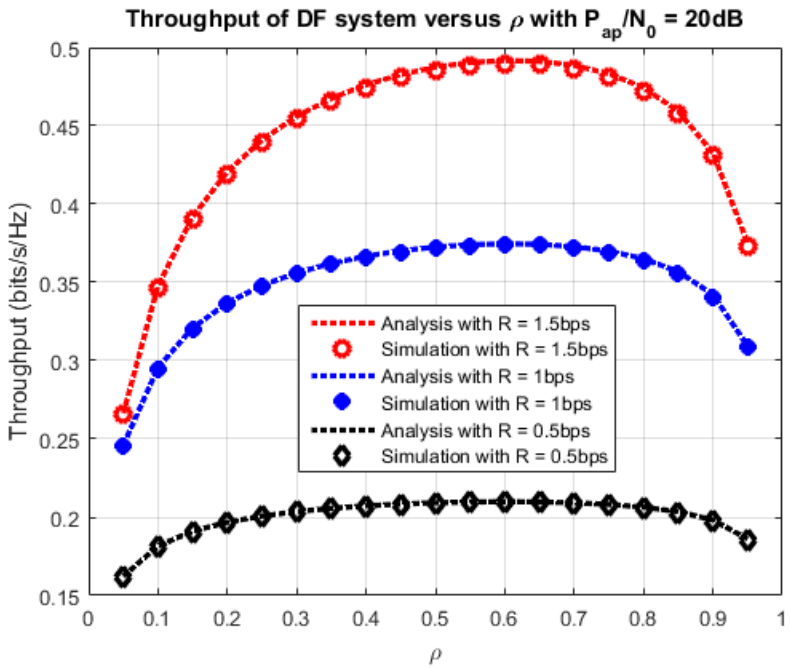

Figure 5.22. Throughput versus power-splitting factor for DF protocol

In Figures 5.23 and 5.24, the performances of two relaying strategies that are considered in the proposed energy-harvesting scheme are compared together. It can be seen that the DF protocol can provide better performance than AF protocol with the same energy-harvesting configuration. This can be explained by the elimination of noise at the relay when using the DF protocol.

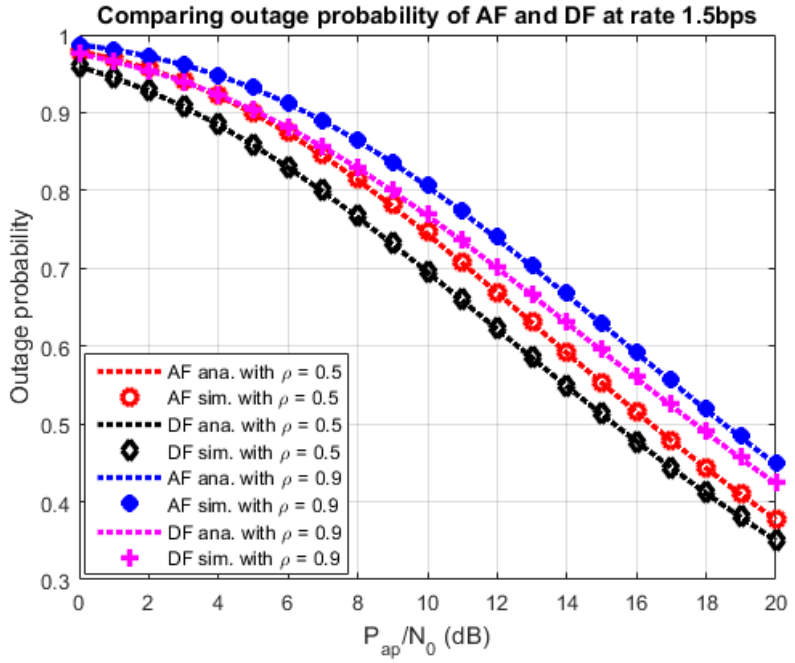

Figure 5.23. Outage probability of AF and DF protocols at rate 1.5 bps

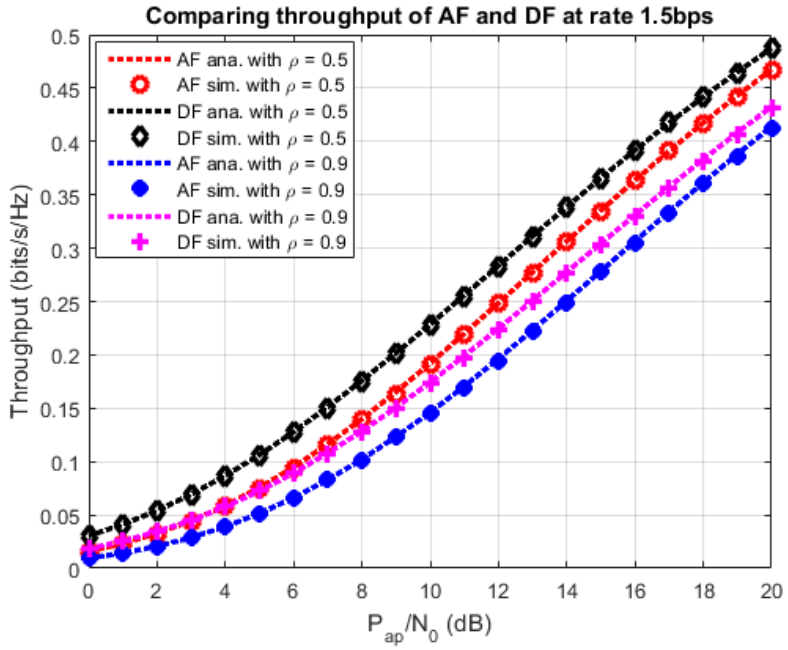

Figure 5.24. The throughput of AF and DF protocols at rate 1.5 bps

Finally, Figure 5.25 plots the optimal values of ρ versus Pap/N_0 for both AF and DF relaying protocols. It can be seen that the optimal ρ* value has a tendency to decrease when Pap/N_0 increases.

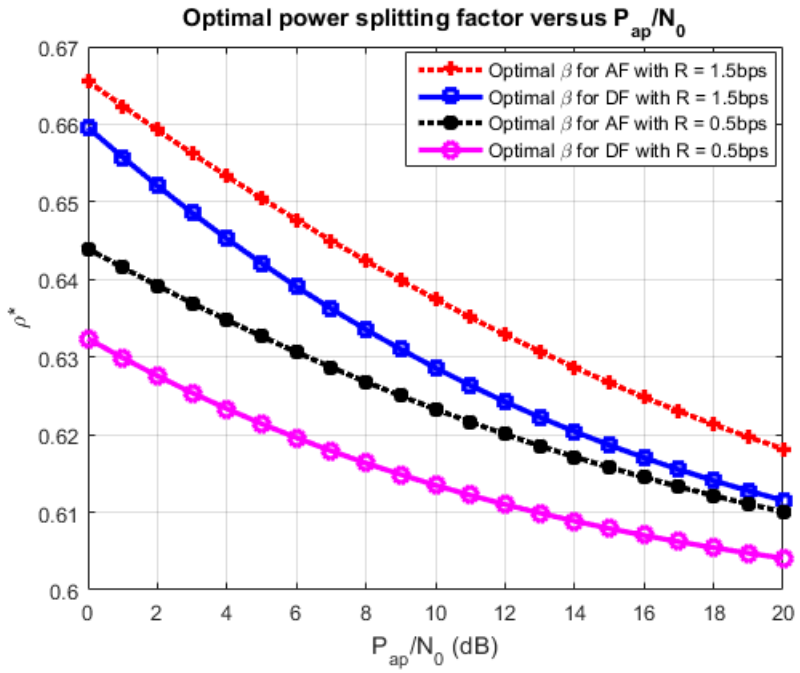

Figure 5.25. Optimal power-splitting factor versus Pap/N_0 for AF and DF protocol

5.5 Conclusion

In this chapter, the exact-form formulas of outage probability, as well as system throughput of a wireless power and information transferring system with a bidirectional relay under the Rayleigh fading condition, have been derived rigorously. This system is equipped with the energy-harvesting capability at the relay node. In particular, the time switching and power splitting–based energy-harvesting are applied. I consider both AF and DF relaying strategies at the intermediate node. It can be concluded from our analysis that there are two unique time switching and power-splitting factor that simultaneously maximizes the throughput and minimizes the outage probability. This optimal value can be found by numerical method. Monte Carlo simulations are also conducted to support our analysis. From the simulation results, it can be observed that the DF strategy is slightly better than its counterpart in the considered system. This is the first investigation on performance analysis of energy harvesting in a specific bidirectional wireless relay network, which can find application in wireless sensor networks. In addition, the randomness of the channel gain, which has not been studied in a similar model proposed by [18] is taken into account in this paper. While the motivation of this paper comes from the energy problem in wireless sensor networks, the analysis obtained in this work does not limit to wireless sensor networks themselves but can be applied for a wide range of wireless applications that employ the relay-node idea. Due to this reason, some specific issues related to sensor networks have not been considered in this chapter. For example, the energy required by sensor nodes when collecting data or making measurement should be taken into account. In that case, the energy source not only comes from the information source node but also from other available nodes. This harvested energy can be modelled as a randomly varying variable. That should be our further work in this topic. In addition, I can take into account other factors such as channel state information (CSI) error and hardware impairment.

6 PERFORMANCE ANALYSIS OF TIME SWITCHING FOR WIRELESS COMMUNICATIONS WITH FULL-DUPLEX RELAYING IN IMPERFECT CSI CONDITION

The second aim of this dissertation is to investigate the effect of channel state information (CSI) error on the performance of energy-harvesting-based relay networks [tan08, tan09, tan14]. While in chapters 2 and 5, the CSI is assumed to be known by the nodes involved in communication, this may not be obtained in reality. In this chapter, I take into account the channel estimation error when considering the performance analysis of energy harvesting strategy for Full-Duplex (FD) relay networks.

6.1 Introduction

The application of wireless information and power transfer to full-duplex relaying systems was first introduced in [16]. In that paper, the authors focused on a source-relay-destination dual-hop scenario where the relay is powered via RF energy harvesting and derived throughput performance analysis of the system. More interestingly, Zeng [17] proposed a new protocol for energy harvesting with full-duplex relaying, where part of the energy (loop energy) that is used for information transmission by the relay can be harvested and reused in addition to the dedicated energy sent by the source. However, all of the above analysis was based on the assumption that the channel state information (CSI) is perfectly available at the relay and the destinations.

Indeed, there have also been several results on performance analysis of relay networks with imperfect CSI. Recently, the exact integral and approximate closed-form expression for the outage probability of two-way full-duplex relaying networks with residual loop interference and imperfect CSI has been derived in [19], but energy harvesting has not been deployed in this paper. Reversely, Li et al. [20] did take account of the imperfect CSI condition in two-way AF relay systems with energy harvesting. Nonetheless, they only derived the maximum achievable sum rate, not the exact ergodic capacity of the system, and their results were limited at the half-duplex model.

As of the authors' knowledge, no work has considered the impact of channel estimation error on the performance of full-duplex relaying networks that apply the RF energy harvesting idea.

In this paper, we focus on the throughput performance of wireless information and power transfer with full-duplex relaying in the condition of imperfect CSI at both relay and destination. Using a similar setup as [16], we consider an FD relaying system equipped with two separate antennas, one for information transmission and one for information received.

Regarding the relaying and energy harvesting protocols, we focus on amplify-and-forward and time-switching relaying protocol. The optimal time-switching factor is found by the Golden section search algorithm. The most significant contribution of this paper is to measure the effect of channel estimation error on the performance of energy-harvested full-duplex relaying systems, both by mathematical analysis and simulation.

6.2 System model

In this chapter, I consider the effect of channel estimation error on the dual-hop full-duplex relaying system like Figure 4.8 with the energy harvesting protocol like in Figure 4.9. Regarding the channel model, I assume that the channel state information (CSI) is obtained with an error. The effect of CSI error on the performance of the model of interest is the main concentration of this paper. Let h and g denote the channels from the source to the relay and from the relay to the destination, respectively, and let f denote the loopback interference channel at the relay. I assume that all channels experience Rayleigh fading and keep constant during each transmission block (slow fading). Specifically, $|h|^2$ is an exponential random variable with mean $1/\lambda_h$,$|g|^2$ is exponentially distributed with mean $1/\lambda_g$, and $|\hat{f}|^2$ is exponentially distributed with mean $1/\lambda_r$, which is a key parameter related to the strength of the loopback interference. Due to imperfect channel estimation, the estimated channel gains obtained at the relay and the destination are expressed as

$$\begin{cases} h = \hat{h} + \Delta h \\ g = \hat{g} + \Delta g \\ f = \hat{f} + \Delta f \end{cases} \tag{6.1}$$

where $\Delta h, \Delta g,$ and Δf are the channel estimation error corresponding to *h, g,* and *f*, respectively. These estimation errors are all assumed to be Gaussian distributed with zero mean.

6.3 Amplify and forward

As mentioned above in section 4.3.1, during the energy harvesting phase, the second antenna of the relay can be exploited to enhance the energy capturing process. In [16], the authors confirm that at high SINR regime, there is no significant difference in performance when adding this extra antenna. Hence, we only consider the case that only the information receiving antenna is used to collect energy.

During the energy harvesting phase, the received signal at the relay node can be expressed as

$$y_R = hx_e + n_r \tag{6.2}$$

where h is the channel coefficient of the first antenna, x_e is the energy symbol with $E|x_e|^2 = P_s$, where $E[\mathrm{X}]$ denotes the expectation operation. n_r is the zero-mean additive white Gaussian noise (AWGN) with variance N_0. Hence, the energy harvested during this phase can be computed as

$$E_h = \eta P_s(\left|\hat{h}\right|^2 + \delta_{\Delta h}^2)\alpha T \tag{6.3}$$

$$P_r = \frac{\eta P_S(\left|\hat{h}\right|^2 + \delta_{\Delta h}^2)\alpha T}{(1-\alpha)T} = kP_S(\left|\hat{h}\right|^2 + \delta_{\Delta h}^2) \tag{6.4}$$

where η is a constant and denotes the energy conversion efficiency, k is defined as $k \triangleq \frac{\eta\alpha}{1-\alpha}$, and $\delta_{\Delta h}^2$ is the standard deviation of the channel estimation error Δh, which is a zero-mean Gaussian random variable as mentioned above.

Now, I consider the information transmission phase. Here, the received signal at the relay is given by

$$y_R = hx_s + fx_r + n_r \tag{6.5}$$

where x_s is the transmitted signal, which satisfies $E|x_s|^2 = P_s$, x_r is the loopback interference due to full-duplex relaying and satisfies $E|x_r|^2 = P_r$, f denotes the loopback interference channel, and n_r is the zero-mean AWGN with variance N_0. After applying interference cancellation methods to mitigate the loopback interference [41], the received signal at the relay is determined by

$$\begin{aligned} \hat{y}_R &= y_R - \hat{f}x_r \\ &= (\hat{h} + \Delta h)x_s + \Delta f x_r + n_r \end{aligned} \tag{6.6}$$

In this section, AF protocol is used, hence, the received signal at relay is amplified by a factor which is given by [41]

$$\beta^2 = \frac{P_R}{(|\hat{h}|^2 + \delta_{\Delta h}^2)P_s + \delta_{\Delta f}^2 P_R + N_0} \tag{6.7}$$

At the destination, the following signal is received:

$$\begin{aligned} y_d &= (\hat{g} + \Delta g)x_r + n_d \\ &= \hat{g}\beta\left\{(\hat{h} + \Delta h)x_s + \Delta f x_r + n_r\right\} + \Delta g\beta\left\{(\hat{h} + \Delta h)x_s + \Delta f x_r + n_r\right\} + n_d \end{aligned} \tag{6.8}$$

The end to end signal to interference noise ratio (SINR) can be expressed as

$$SINR = \frac{A}{B} \tag{6.9}$$

where

$$A = |\hat{g}|^2 |\hat{h}|^2 P_s P_r \tag{6.10}$$

$$B = P_s P_r \delta_{\Delta h}^2 |\hat{g}|^2 + P_r^2 |\hat{g}|^2 \delta_{\Delta f}^2 + |\hat{g}|^2 P_r N_0 + P_s P_r \delta_{\Delta g}^2 |\hat{h}|^2 + P_s P_r \delta_{\Delta g}^2 \delta_{\Delta h}^2 \tag{6.11}$$

$$+\delta_{\Delta g}^2 P_r^2 \delta_{\Delta f}^2 + P_r \delta_{\Delta g}^2 N_0 + P_s |\hat{h}|^2 N_0 + P_r \delta_{\Delta f}^2 N_0 + N_0^2 + P_s \delta_{\Delta h}^2 N_0$$

I divide both numerator and denominator of (6.9) by P_r and substitute (6.4) into (6.9). After doing some algebra, I obtain:

$$SINR = \frac{C}{D} \tag{6.12}$$

where

$$C = \left|\hat{g}\right|^2 \left|\hat{h}\right|^2 Q \tag{6.13}$$

$$D = Q\delta_{\Delta h}^2 \left|\hat{g}\right|^2 + kQ(\left|\hat{h}\right|^2 + \delta_{\Delta h}^2)\left|\hat{g}\right|^2 \delta_{\Delta f}^2 + \left|\hat{g}\right|^2 + Q\delta_{\Delta g}^2 \left|\hat{h}\right|^2 + Q\delta_{\Delta g}^2 \delta_{\Delta h}^2 + \delta_{\Delta g}^2 kQ(\left|\hat{h}\right|^2 + \delta_{\Delta h}^2)\delta_{\Delta f}^2$$
$$+\delta_{\Delta g}^2 + \frac{1}{k} + \delta_{\Delta f}^2 \tag{6.14}$$

and $Q = \frac{P_s}{N_0}$.

Assume that the source transmits at a constant rate R . Let $\gamma_0 = 2^R - 1$ be the lower threshold for SINR. Here, the average throughput can be computed as [16]:

$$R_{DL}(\alpha) = (1 - P_{out})R(1-\alpha) \tag{6.15}$$

where P_{out} is the outage probability. Hence, the optimal time-switching factor α^* could be obtained by solving the following optimization problem

$$\alpha^* = \arg\max_{\alpha} R_{DL}(\alpha) \tag{6.16}$$

One of the main contributions of this section is the analysis of the outage performance of the proposed system in the condition of imperfect CSI. My analytical result is stated in the following theorem.

Theorem 6.1 (Exact analysis)

The outage probability and the average throughput of the system can be expressed as

$$P_{out} = 1 - e^{\left(\frac{-\lambda_h b_2}{b_1} - \frac{\lambda_g a_1}{b_1}\right)} \times \sqrt{\frac{4V\lambda_h}{b_1}} K_1\left(\sqrt{\frac{4V\lambda_h}{b_1}}\right) \tag{6.17}$$

and

$$R_{DL}(\alpha) = R(1-\alpha) \times e^{\left(\frac{-\lambda_h b_2}{b_1} - \frac{\lambda_g a_1}{b_1}\right)} \times \sqrt{\frac{4V\lambda_h}{b_1}} K_1\left(\sqrt{\frac{4V\lambda_h}{b_1}}\right) \tag{6.18}$$

where $K_n(x)$ is the n[th] order modified Bessel function of the second kind and $V = \frac{\lambda_g\left(a_1 b_2 + a_2 b_1\right)}{b_1}$,

where a_1, a_2, b_1, b_2 are determined in the following equations

$$a_1 = \gamma_0(\delta_{\Delta g}^2 Q + \delta_{\Delta g}^2 \delta_{\Delta f}^2 kQ), \tag{6.19}$$

$$a_2 = \gamma_0(\delta_{\Delta g}^2 \delta_{\Delta f}^2 \delta_{\Delta h}^2 kQ + \delta_{\Delta g}^2 + \frac{1}{k} + \delta_{\Delta f}^2), \tag{6.20}$$

$$b_1 = Q - kQ\delta_{\Delta f}^2 \gamma_0 \tag{6.21}$$

$$b_2 = \gamma_0(Q\delta_{\Delta h}^2 + kQ\delta_{\Delta f}^2 \delta_{\Delta h}^2 + 1) \tag{6.22}$$

Proof.

The outage probability of our system is given by

$$P_{out} = Pr\{SINR \le (2^R - 1)\} \tag{6.23}$$

Let $x = \left|\hat{g}\right|^2$ and $y = \left|\hat{h}\right|^2$. The equation (6.23) can be rewritten as

$$P_{out} = P\left(x \le \frac{ya_1 + a_2}{yb_1 - b_2} \right) \tag{6.24}$$

where a_1, a_2, b_1, b_2 are given by equations (6.19)–(6.22).

Now, the outage probability can be computed as [12]

$$P_{out} = 1 - \lambda_h \int_{y=b2/b1}^{\infty} e^{-\left(\lambda_h y + \frac{\lambda_g [ya_1 + a_2]}{(yb_1 - b_2)}\right)} dy \quad . \tag{6.25}$$

Let $u = yb_1 - b_2$, then by changing the variable in (6.25), I obtain

$$P_{out} = 1 - \frac{\lambda_h e^{\left(\frac{-\lambda_h b_2}{b_1} - \frac{\lambda_g a_1}{b_1}\right)}}{b_1} \int_0^{\infty} e^{\left(-\frac{V}{u} - \frac{\lambda_h u}{b_1}\right)} du \tag{6.26}$$

After doing some reduction and apply the integral formula 3.324.1 in [46], I get the equation (6.17).

In (6.17) and (6.18), the outage probability and average system throughput are expressed in terms of the first order modified Bessel function of the second kind, which can be approximated to a simpler expression in high SNR regime. Hence, my next objective is to derive the asymptotic behaviour of the outage probability and average throughput of the proposed system when the transmitted power from the source to noise ratio goes to infinity.

Theorem 6.2 (Asymptotic analysis)

The outage probability P_{out} can be approximated by the following expression:

$$P_{out} = 1 - e^{-\gamma_0 b \delta^2} \sqrt{4\lambda_h \lambda_g \delta_{\Delta h}^2 \delta_{\Delta g}^2 I} \times K_1\left(\sqrt{4\lambda_h \lambda_g \delta_{\Delta h}^2 \delta_{\Delta g}^2 I}\right) \tag{6.27}$$

where b, δ^2, and I are given by $b = \frac{1 + k\delta_{\Delta f}^2}{1 - \gamma_0 k \delta_{\Delta f}^2}$, $\delta^2 = \lambda_h \delta_{\Delta h}^2 + \lambda_g \delta_{\Delta g}^2$, $I = \gamma_0^2 b^2 + \frac{\gamma_0 k \delta_{\Delta f}^2}{1 - \gamma_0 k \delta_{\Delta f}^2}$.

Proof.

The equation (6.17) can be rewritten as

$$P_{out} = 1 - e^{\left(\frac{-\lambda_h b_2}{b_1} - \frac{\lambda_g a_1}{b_1}\right)} \times \sqrt{\frac{4V\lambda_h}{b_1}} K_1\left(\sqrt{\frac{4V\lambda_h}{b_1}}\right) \tag{6.28}$$

As Q goes to infinity, the rational terms in (6.28) converge to the following quantities:

$$\lim_{Q \to \infty} \left(\frac{-\lambda_h b_2}{b_1} - \frac{\lambda_g a_1}{b_1}\right) = -\frac{\lambda_h \left(\gamma_0 \delta_{\Delta h}^2 + \gamma_0 k \delta_{\Delta h}^2 \delta_{\Delta f}^2\right)}{\left(1 - \gamma_0 k \delta_{\Delta f}^2\right)} - \frac{\lambda_g \left(\gamma_0 \delta_{\Delta g}^2 + \gamma_0 k \delta_{\Delta g}^2 \delta_{\Delta f}^2\right)}{\left(1 - \gamma_0 k \delta_{\Delta f}^2\right)}$$

$$= -\frac{\lambda_h \gamma_0 \delta_{\Delta h}^2 (1 + k\delta_{\Delta f}^2)}{\left(1 - \gamma_0 k \delta_{\Delta f}^2\right)} - \frac{\lambda_g \gamma_0 \delta_{\Delta g}^2 (1 + k\delta_{\Delta f}^2)}{\left(1 - \gamma_0 k \delta_{\Delta f}^2\right)} = -\gamma_0 b \delta^2$$

$$\lim_{Q\to\infty}\left(\frac{4V\lambda_h}{b_1}\right) = \lim_{Q\to\infty}\left(4\frac{\lambda_g\lambda_h\left[a_1b_2 + a_2b_1\right]}{b_1^2}\right) = \lim_{Q\to\infty} 4\lambda_g\lambda_h\left(\frac{a_1b_2}{b_1^2} + \frac{a_2}{b_1}\right)$$

$$= 4\lambda_g\lambda_h\left(\frac{\gamma_0(\delta_{\Delta g}^2 + \delta_{\Delta g}^2\delta_{\Delta f}^2 k)\gamma_0(\delta_{\Delta h}^2 + k\delta_{\Delta f}^2\delta_{\Delta h}^2)}{(1 - k\delta_{\Delta f}^2\gamma_0)^2} + \frac{\gamma_0\delta_{\Delta g}^2\delta_{\Delta f}^2\delta_{\Delta h}^2 k}{1 - k\delta_{\Delta f}^2\gamma_0}\right)$$

$$= 4\lambda_g\lambda_h\delta_{\Delta g}^2\delta_{\Delta h}^2\left(\gamma_0^2 b^2 + \frac{\gamma_0\delta_{\Delta f}^2 k}{1 - \gamma_0 k\delta_{\Delta f}^2}\right)$$

By the continuity of P_{out} with respect to Q, I obtain the desired results.

6.4 Decode and forward

In this section, the source message first decoded at the relay node. From the equation (6.5), the received signal-to-interference-and-noise-ratio (SINR) at the relay is given by

$$SINR_1 = \frac{\left(\left|\hat{h}\right|^2 + \delta_{\Delta h}^2\right)P_s}{\left(\left|\hat{h}\right|^2 + \delta_{\Delta h}^2\right)P_s + \left(\left|\hat{f}\right|^2 + \delta_{\Delta f}^2\right)P_r + N_0} \tag{6.29}$$

By dividing both numerator and denominator of (6.29) by $\left(\left|\hat{h}\right|^2 + \delta_{\Delta h}^2\right)P_s$, substituting (6.4) into (6.29) and using the fact that $N_0 << P_s$, I obtain:

$$SINR_1 = \frac{1}{k\left(\left|\hat{f}\right|^2 + \delta_{\Delta f}^2\right)} \tag{6.30}$$

From (6.8), the SINR at the destination can be expressed as

$$SINR_2 = \frac{P_r\left(\left|\hat{g}\right|^2 + \delta_{\Delta g}^2\right)}{N_0} = \frac{kP_s\left(\left|\hat{h}\right|^2 + \delta_{\Delta h}^2\right)\left(\left|\hat{g}\right|^2 + \delta_{\Delta g}^2\right)}{N_0} \tag{6.31}$$

For DF protocol, the outage probability can be given by

$$P_{out} = \Pr\left\{\min(SINR_1, SINR_2) < \gamma_0\right\} \tag{6.32}$$

Similar in previous section AF protocol, I can obtain the average throughput and find the optimal time-switching factor α^* from the equation (6.15) and (6.16).

Theorem 6.3

The outage probability can be expressed as

$$P_{out} = 1 - \left(1 - e^{-\frac{\lambda_r\left(1-\gamma_0 k\delta_{\Delta f}^2\right)}{\gamma_0 k}}\right)\left(e^{-\frac{a\lambda_g}{b}} + \lambda_g \int_0^{a/b} e^{-\left(y\lambda_g + \frac{\lambda_h[a-by]}{(cy+d)}\right)} dy\right) \tag{6.33}$$

where *a, b, c,* and *d* are defined as

$$a = \gamma N_0 - kP_s\delta_{\Delta h}^2\delta_{\Delta g}^2$$

$$b = kP_s\delta_{\Delta h}^2$$

$$c = kP_s$$

$$d = kP_s\delta_{\Delta g}^2$$

Proof.

The outage probability of our system is given by

$$P_{out} = \Pr\left\{\min\left(\frac{1}{k\left(\left|\hat{f}\right|^2 + \delta_{\Delta f}^2\right)}, \frac{kP_s\left(\left|\hat{h}\right|^2 + \delta_{\Delta h}^2\right)\left(\left|\hat{g}\right|^2 + \delta_{\Delta g}^2\right)}{N_0} < \gamma_0\right)\right\} \tag{6.34}$$

Let's $X = \left|\hat{h}\right|^2$, $Y = \left|\hat{g}\right|^2$ and $Z = \left|\hat{f}\right|^2$. The equation (6.34) can be rewritten as

$$P_{out} = 1 - \Pr\left\{\frac{1}{k(Z + \delta_{\Delta f}^2)} \geq \gamma_0\right\}\Pr\left\{\frac{kP_s(X + \delta_{\Delta h}^2)(Y + \delta_{\Delta g}^2)}{N_0} \geq \gamma_0\right\} \tag{6.35}$$

Now, I try to analyze each probability term in (6.35). The first term can be calculated by

$$\Pr\left\{\frac{1}{k(Z + \delta_{\Delta f}^2)} \geq \gamma_0\right\} = \Pr\left\{Z \leq \frac{1 - \gamma_0 k\delta_{\Delta f}^2}{\gamma_0 k}\right\} = 1 - e^{-\frac{\lambda_r\left(1-\gamma_0 k\delta_{\Delta f}^2\right)}{\gamma_0 k}}, \tag{6.36}$$

assuming that $1 - \gamma_0 k\delta_{\Delta f}^2 \geq 0$.

The second term is determined by

$$\Pr\left\{\frac{kP_s(X + \delta_{\Delta h}^2)(Y + \delta_{\Delta g}^2)}{N_0} \geq \gamma_0\right\} = \Pr\left\{X \geq \frac{\gamma_0 N_0 - kP_s\delta_{\Delta h}^2\delta_{\Delta g}^2 - kP_s\delta_{\Delta h}^2 Y}{kP_s Y + kP_s\delta_{\Delta g}^2}\right\} \tag{6.37}$$

Let's substitute a, b, c, d that are defined as above into (6.37), then apply some algebra to the second term above.

$$\begin{aligned}\Pr\left\{X \geq \frac{a-bY}{cY+d}\right\} &= \Pr\left\{X \geq \frac{a-bY}{cY+d} \middle| a-bY>0\right\}.\Pr\left(a-bY>0\right) \\ &+ \Pr\left\{X \geq \frac{a-bY}{cY+d} \middle| a-bY\leq 0\right\}.\Pr\left(a-bY\leq 0\right) \\ &= \lambda_g \int_0^{a/b} e^{-y\lambda_g} e^{-\frac{\lambda_h(a-by)}{(cy+d)}} dy + e^{-\frac{a\lambda_g}{b}}\end{aligned} \tag{6.38}$$

Finally, the Equation (6.33) can be obtained by substituting (6.36) and (6.38) to (6.35).

6.5 Optimal Time Switching Factor

The optimal value $\alpha*$ can be obtained by solving the equation $\frac{dP_{out}(\alpha)}{d\alpha}=0$. Given the outage expression in (6.17) and (6.33), this optimization problem does not admit a closed-form solution. However, the optimal $\alpha*$ can be efficiently solved via numerical calculation, as illustrated below.

Here, we can use the Golden section search algorithm to find the optimal factor $\alpha*$. This algorithm has been used in many global optimization problems in communications, for example, in [50]. The detailed algorithm, as well as the related theory, is described in [49].

6.6 Numerical Results and Discussion

In this section, numerical simulation is conducted to verify the analytical results developed in the previous section. I consider a network with one source, one relay, and one destination, where source-relay and relay-destination distances are both normalized to unit value. Other simulation parameters are listed in Table 6.1.

Table 6.1 Simulation parameters

Symbol	Name	Values
R	Source rate	3bps/Hz
γ_0	SINR threshold	7
η	Energy harvesting efficiency	0.8
$1/\lambda_h$	Mean of $\lvert h\rvert^2$	1
$1/\lambda_g$	Mean of $\lvert g\rvert^2$	1
P_s/N_0	Source-Power to Noise Ratio	0-50 dB

Figure 6.1 and Figure 6.2 shows the achievable rate and outage probability of the system versus the source-power to noise ratio P_s/N_0 in 2 cases: perfect CSI and imperfect CSI with all of the standard deviation of channel estimation errors are equal to $\delta_0 = 0.1$. The time-switching factor α is set to 0.3. It's can be observed that the simulation curve and the analytical curve almost overlap together.

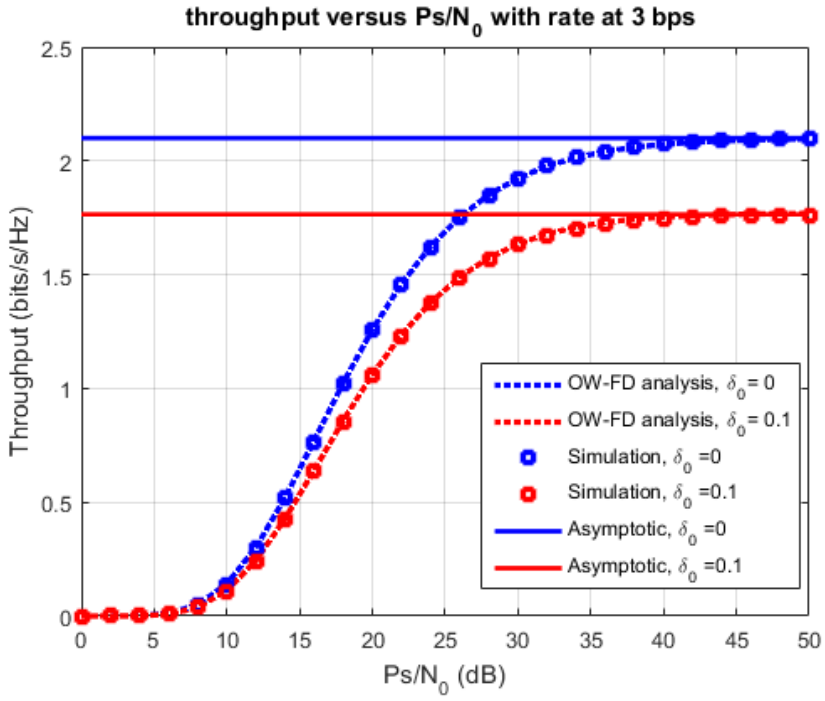

Figure 6.1 System throughput versus source-power to noise ratio for AF protocol

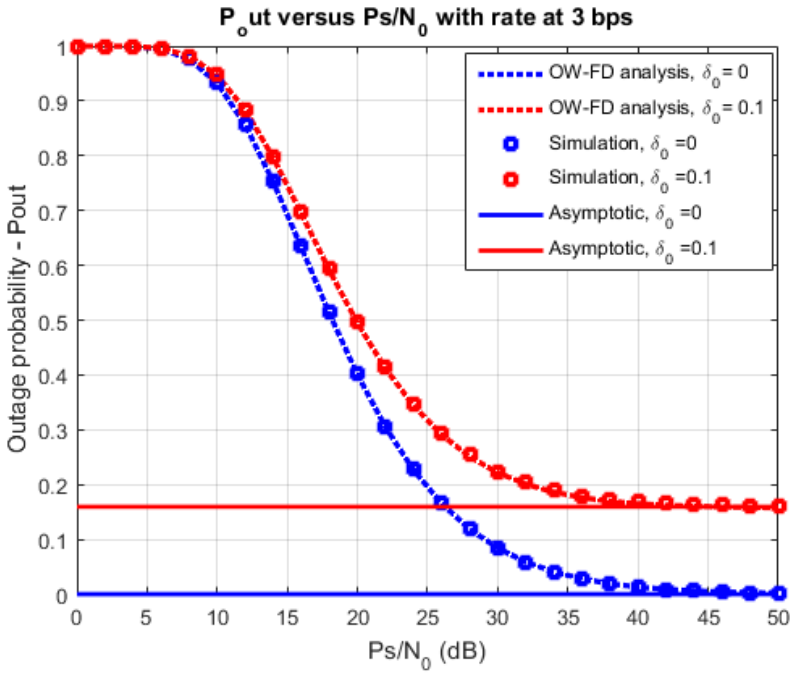

Figure 6.2 Outage probability versus source-power to noise ratio for AF protocol

This confirms our mathematical analysis in the previous section. I also notice that in the low SNR regime, the channel estimation error has little effect on system performance. However, when the transmit power goes large, the channel estimation error has an increasing impact on both achievable throughputs as well as outage probability. The asymptotic behaviour of the outage probability and system throughput when SINR goes to infinity is also illustrated in Figure 6.1 and Figure 6.2. The solid blue lines and red

lines in both figures indicate the asymptotic performance of the proposed system in cases of perfect and imperfect CSI, respectively.

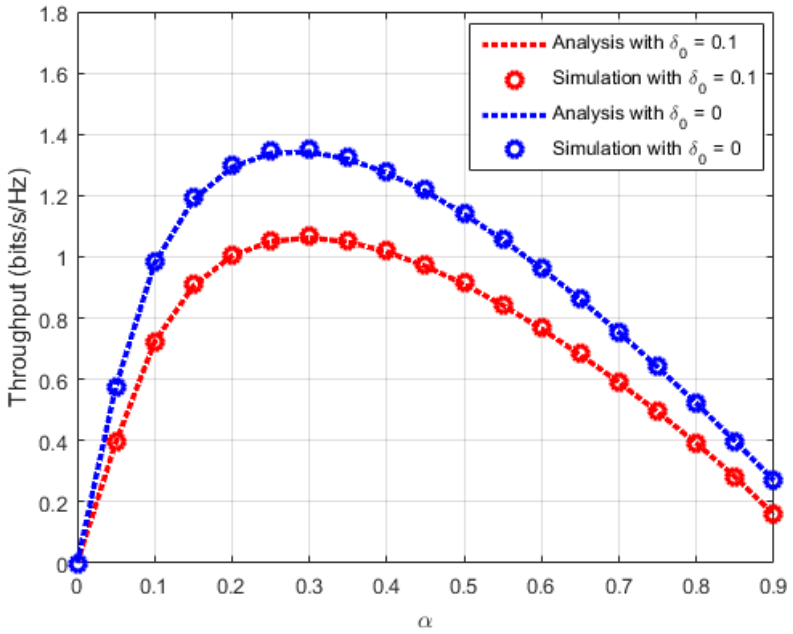

Figure 6.3. System throughput versus time switching factor for AF protocol

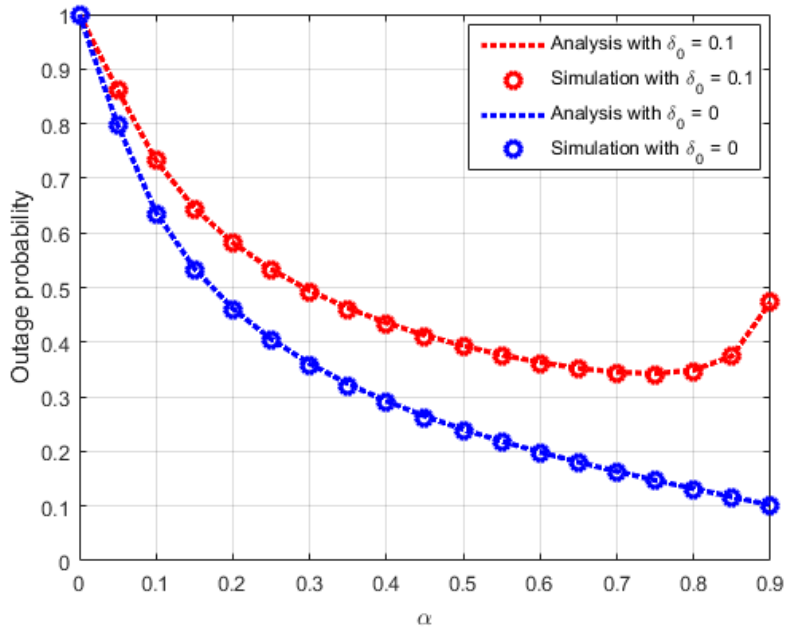

Figure 6.4. Outage probability versus time switching factor for AF protocol

The impact of time switching factor α on the instantaneous capacity is shown in Figure 6.3. Here, the source-power to noise ratio is set to 20dBW. Again, the analytical solutions are in exact agreement with the simulation results. There exists a unique time switching factor at which the system throughput is maximized. In practice, this optimal factor can be found iteratively using numerical methods. The outage

probability also depends on the time switching factor α, which is illustrated in Figure 6.4. Similar to the throughput performance, the outage probability can be minimized with an appropriate selection of α. However, the optimal α^* for outage performance is different from the optimal α^* for system throughput. The optimal time switching factor α^* can be found by using the Golden section search (GSS) algorithm as mentioned in Section 3.2. Figure 6.5 shows the values of optimal switching factor α^* according to different values of P_s while $\delta_{\Delta h} = \delta_{\Delta g} = \delta_{\Delta f} = 0.1$.

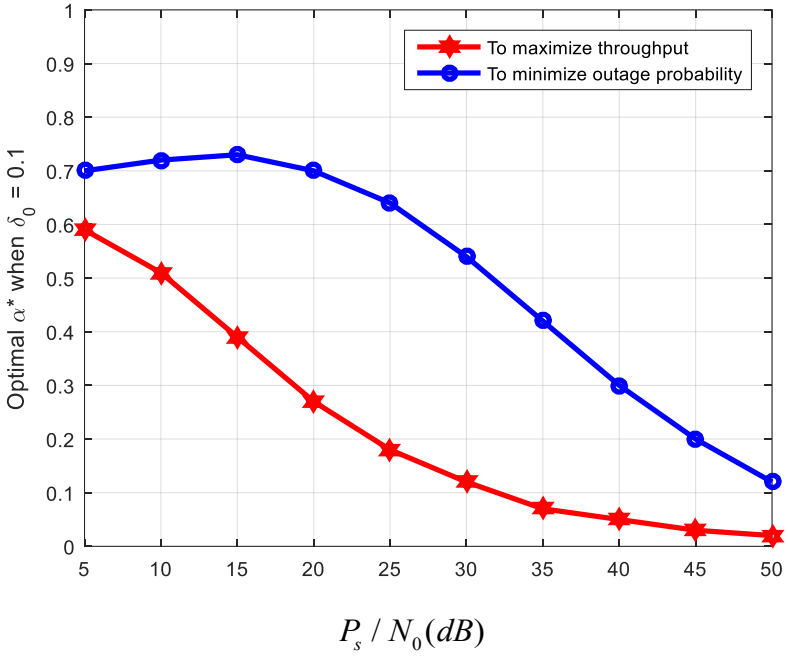

Figure 6.5. Optimal time switching for AF protocol

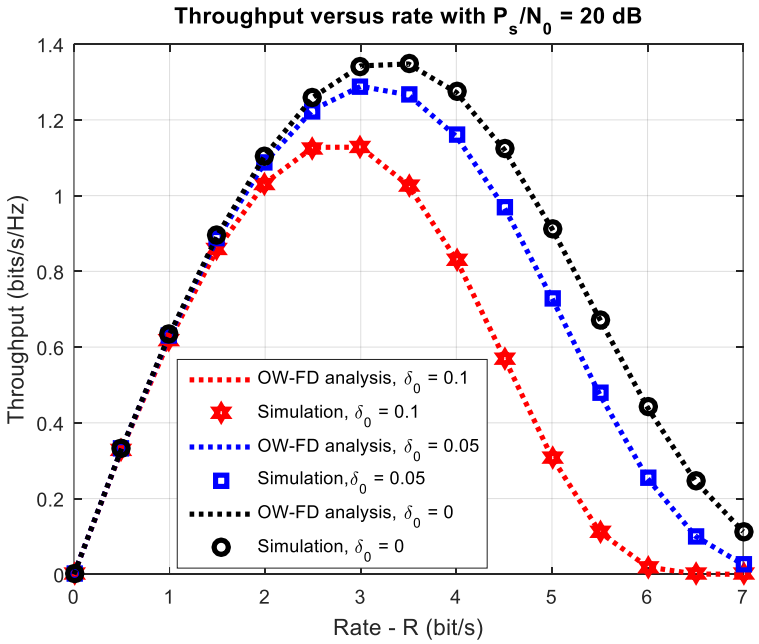

Figure 6.6 System throughput versus source transmitted rate for AF protocol

Figure 6.6 and Figure 6.7 examine the impact of transmission rate R_c on the throughput and outage probability of considered systems with $\alpha = 0.3$ and $P_s / N_0 = 20dB$. As in the case of perfect CSI [16], the throughput first increases with the transmission rate R and then decreases when R increases beyond the rate value of $3bps / Hz$. In other words, for a particular transmit power, there exists a unique transmission rate which yields maximum throughput. Regarding the outage probability, Figure 6.7 confirms that it increases when the transmission rate increases, i.e., there is a performance trade-off between the transmission rate and the outage probability of the system.

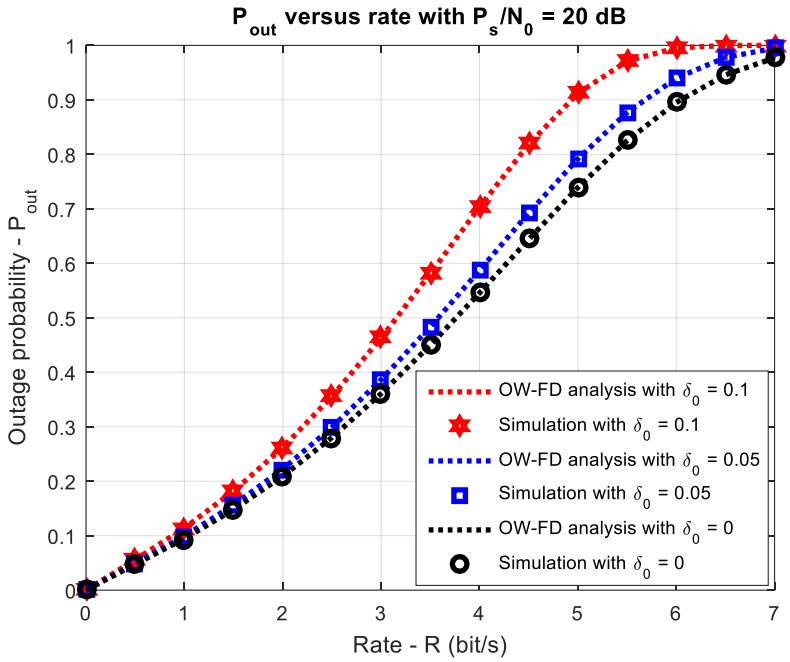

Figure 6.7. Outage probability versus source transmitted rate for AF protocol

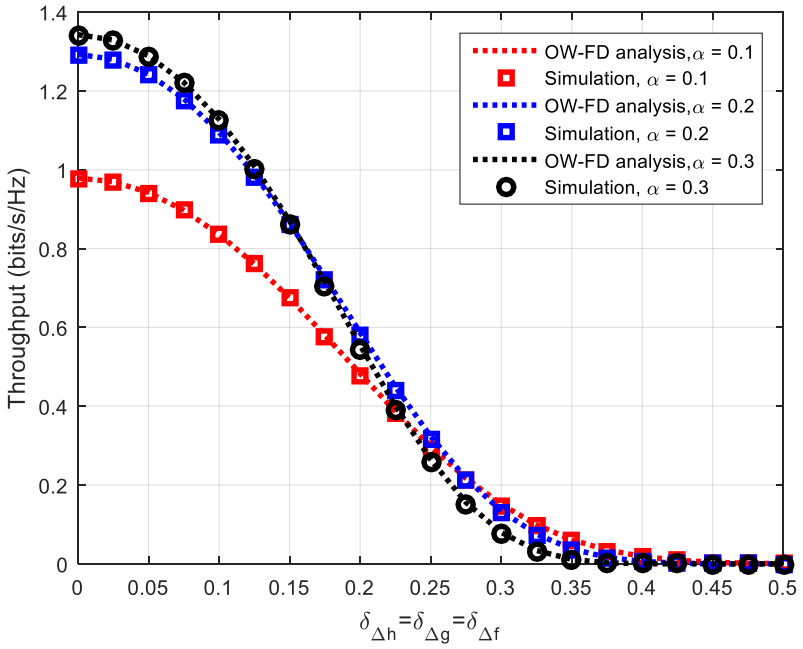

Figure 6.8. System throughput versus channel estimation error for AF protocol

Figure 6.8 and Figure 6.9 illustrate the impact of the channel estimation error on the throughput and outage probability of our system, respectively. Again, we set $P_s / N_0 = 20dB$ in this simulation. As we intuitively expected, the throughput decreases and the outage probability increases when the standard deviation of channel estimation error increases. In fact, the system performance degrades significantly after the error exceeds a certain threshold value (around 0.1 in this simulation scenario). From both figures, I can confirm that if we can keep the error bounded in some narrow interval, then the throughput and outage capacity is still close to ones in the case of perfect CSI.

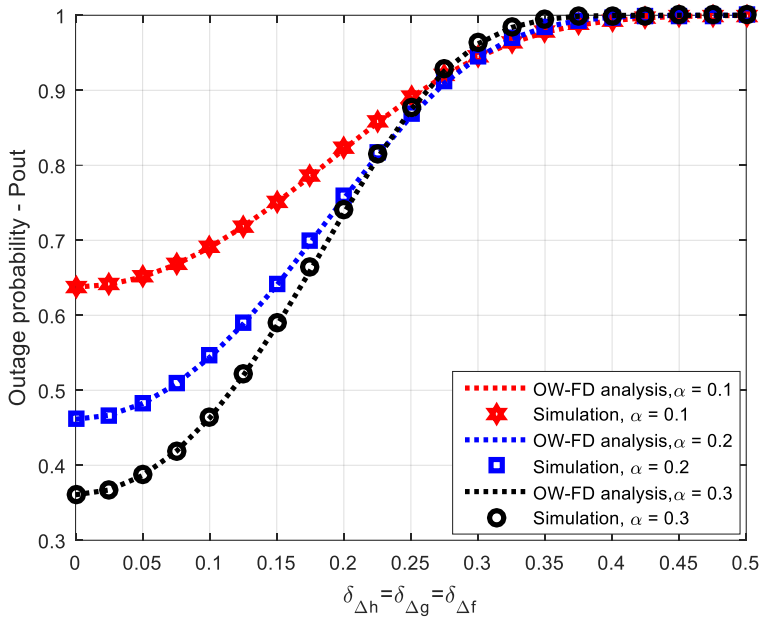

Figure 6.9. Outage probability versus channel estimation error for AF protocol

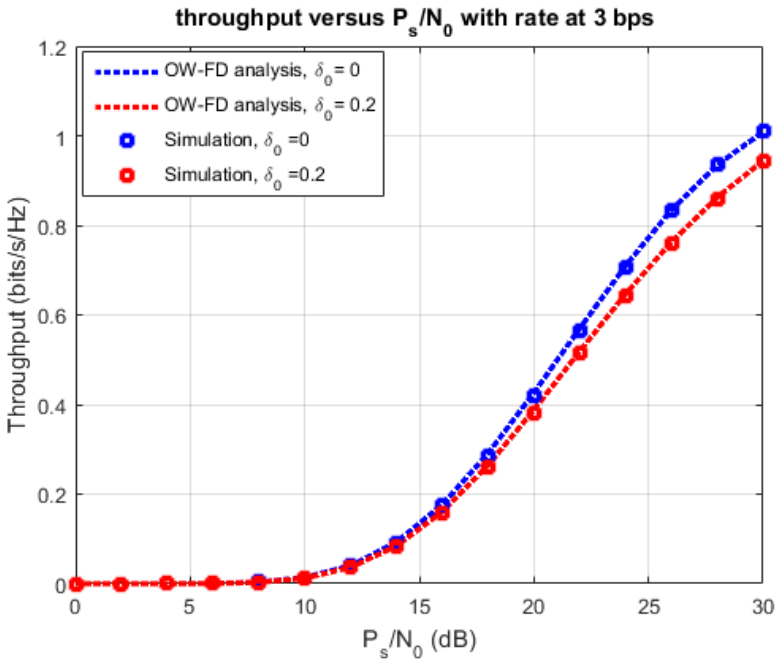

Figure 6.10. System throughput versus source-power to noise ratio for DF protocol

Figure 6.10 and 6.11 shows the system throughput and outage probability of the system versus the source-power to noise ratio Ps/N_0 in 2 cases: perfect CSI and imperfect CSI with all of the standard deviation of channel estimation errors are equal to $\delta_0 = 0.2$. The time-switching factor α is set to 0.3. It's can be observed that the simulation curve and the analytical curve overlap together. It can be observed from Figure 6.10 and 6.11 that the channel estimation error has little effect on system performance, especially in low SINR regime. When the transmit power increases, the channel estimation error has an increasing impact on both achievable throughput as well as outage probability, however, the gap is negligible if the variance of error is kept in some allowed limit.

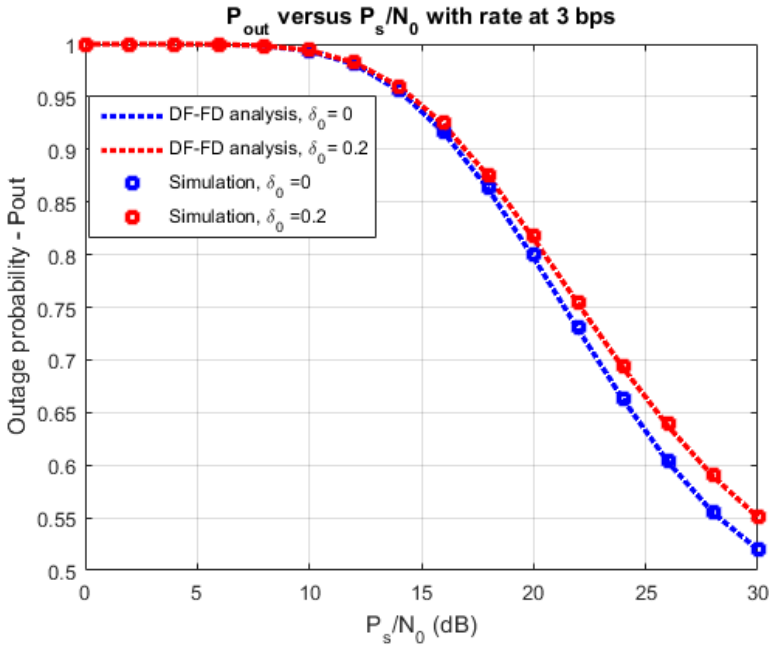

Figure 6.11. Outage probability versus source-power to noise ratio for DF protocol

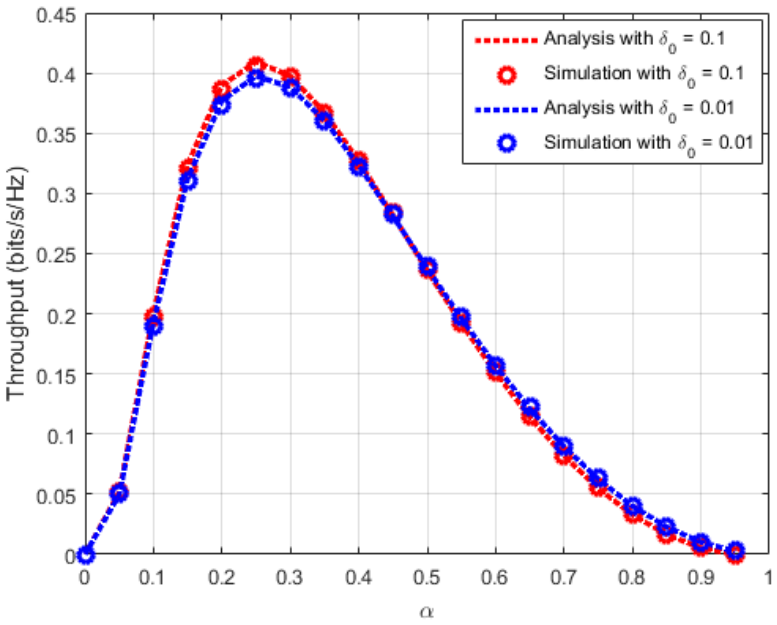

Figure 6.12. System throughput versus time switching factor for DF protocol

The impact of time switching factor α on the instantaneous capacity and outage probability is shown in Figure 6.12 and 6.13. Here, the source-power to noise ratio is set to 20 dB. Again, the analytical solutions are in exact agreement with the simulation results. There exists a unique time switching factor at which the system throughput is maximized. Again, there is not much difference in performance between the cases of $\delta_0 = 0.1$ and $\delta_0 = 0.01$.

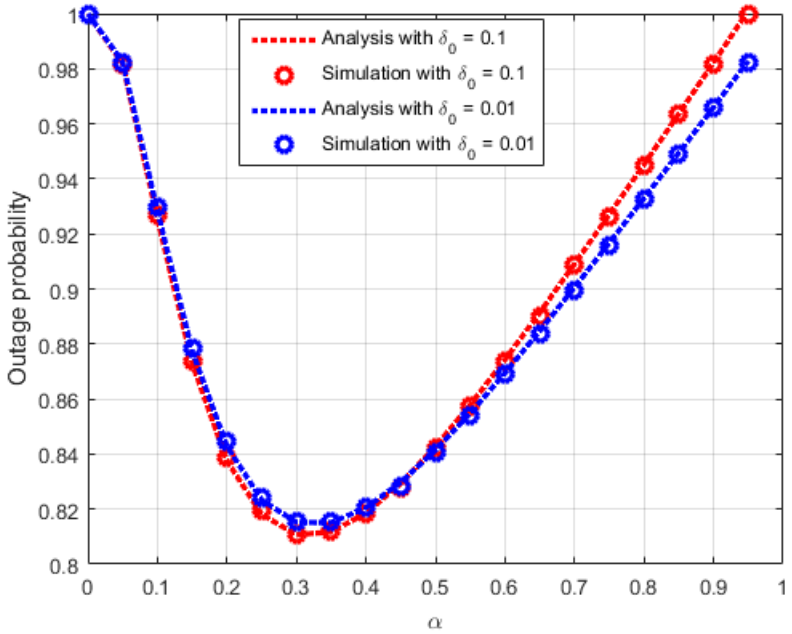

Figure 6.13. Outage probability versus time switching factor for DF protocol

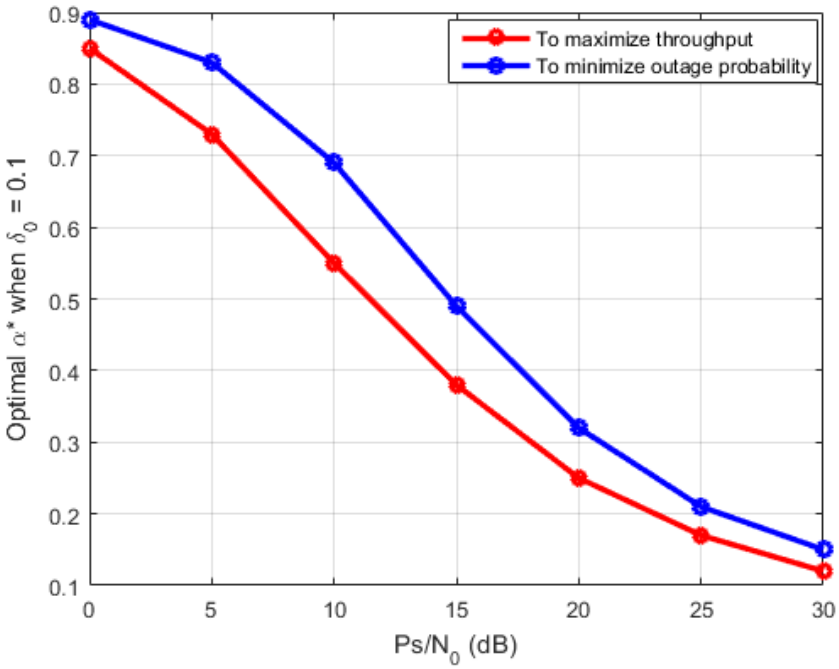

Figure 6.14. Optimal time-switching factor for DF protocol

The optimal time switching factor $\alpha*$ can be found by using the Golden section search (GSS) algorithm as mentioned in the previous section. Figure 6.14 shows the values of optimal switching factor $\alpha*$ according to different values of *Ps/N₀* while $\delta_{\Delta h} = \delta_{\Delta g} = \delta_{\Delta f} = 0.1$.

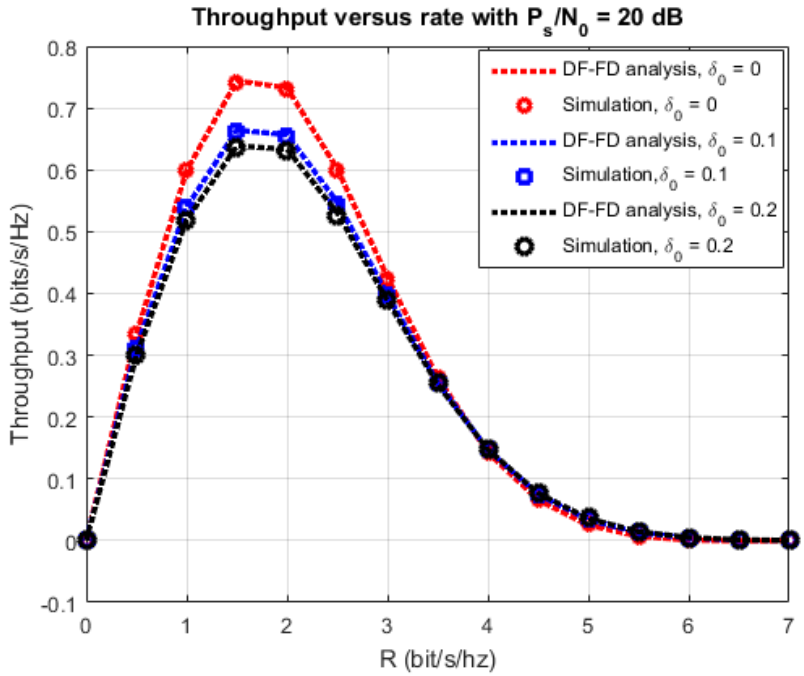

Figure 6.15. System throughput versus source transmitted rate for DF protocol

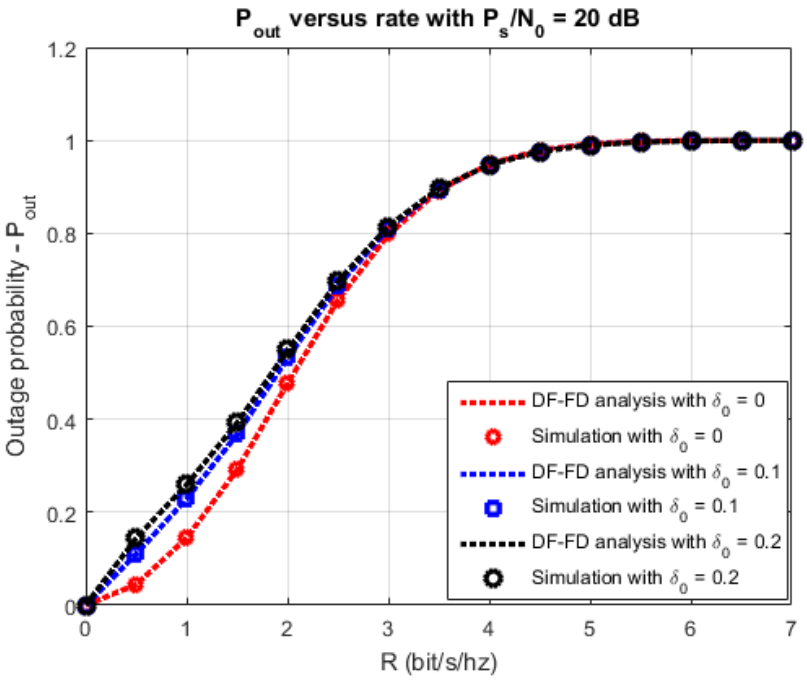

Figure 6.16. Outage probability versus source transmitted rate for DF protocol

Figure 6.15 and 6.16 illustrates the impact of transmission rate R on the throughput and outage probability of considered systems with α = 0.3 and Ps/N_0 = 20dB. The quality of the considered system is improved when the channel estimation error is reduced.

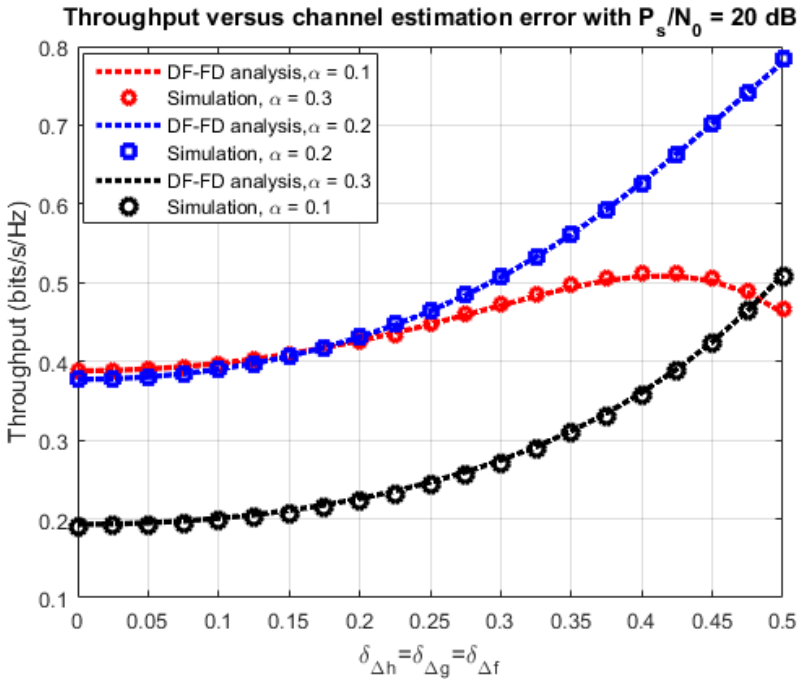

Figure 6.17. System throughput versus channel estimation error for DF protocol

Figure 6.17 and 6.18 illustrate the impact of the channel estimation error on the throughput and outage probability of our system, respectively. Again, I set Ps/N_0 = 20 dB in this simulation. As I intuitively expected, the throughput decreases and the outage probability increases when the standard deviation of channel estimation error increases.

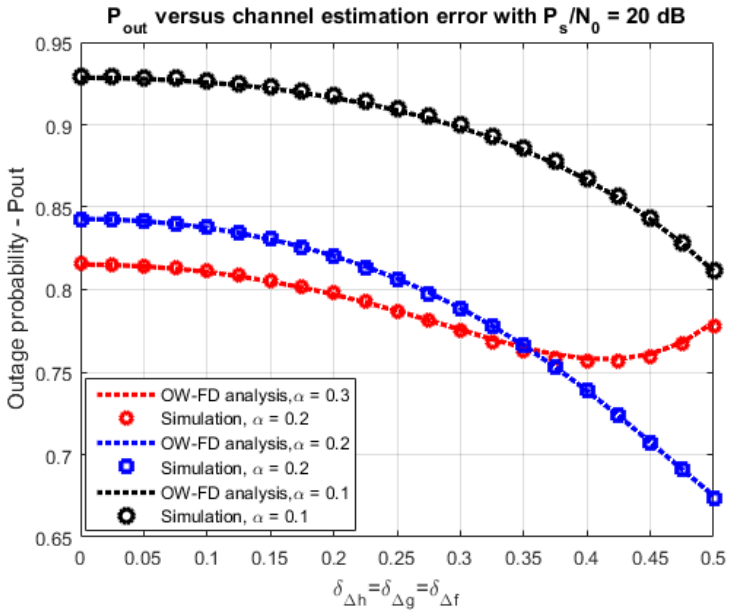

Figure 6.18. Outage probability versus channel estimation error for DF protocol

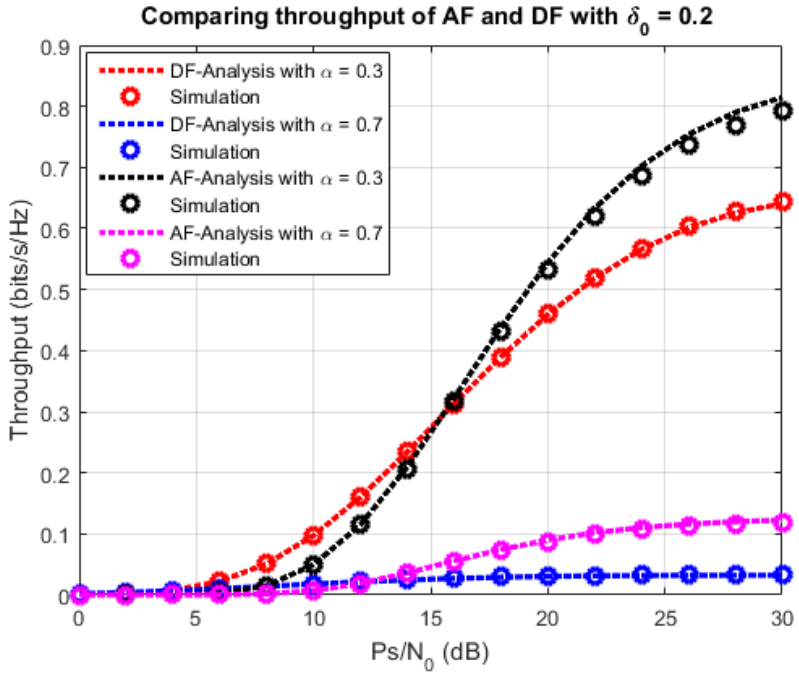

Figure 6.19. Throughput of AF and DF protocols when $\delta_{\Delta h} = \delta_{\Delta g} = \delta_{\Delta f} = 0.2$

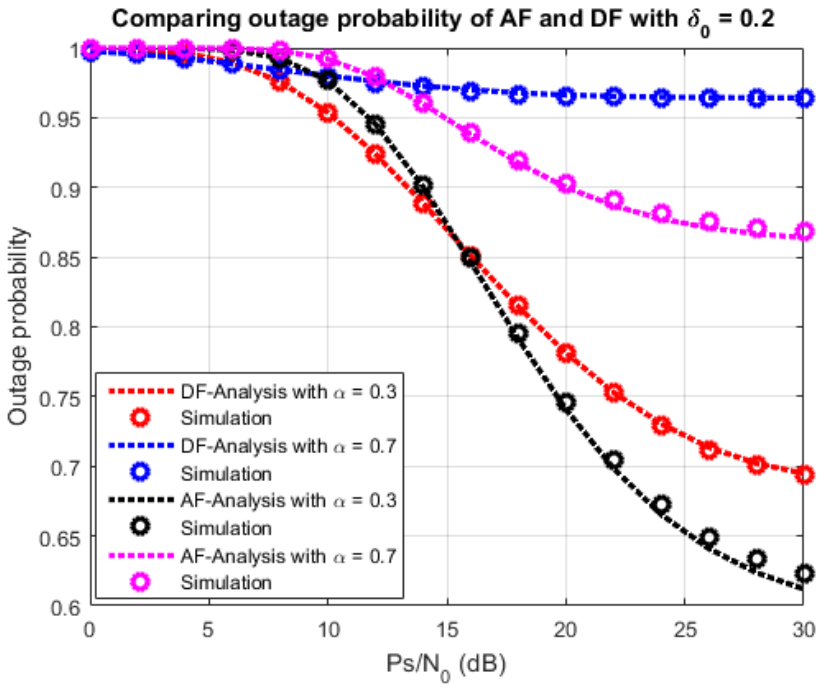

Figure 6.20. Outage probability of AF and DF protocols when $\delta_{\Delta h} = \delta_{\Delta g} = \delta_{\Delta f} = 0.2$

Figure 6.19 and 6.20 compare the performance of AF and DF protocols in the condition of imperfect CSI. In particular, the variance of channel estimation error is set to 0.2 in this simulation. The results show that as low P_s/N_0 regime, DF protocol is better than the AF protocol. However, as P_s/N_0 goes larger, the AF protocol becomes the dominant one.

6.7 Conclusion

In summary, I introduce the study of throughput and outage probability of various relay networks using RF energy harvesting, in which I focus on the impact of channel estimation error on the system performance in this chapter. Based on the assumption that the channel estimation error is zero-mean Gaussian distributed, I can derive the analytical formula for outage probability and throughput of the considered system as well as their asymptotic behaviour at high SINR regime, and validate these results by numerical analysis as well. It is expected from our initial research that the channel estimation error has little impact on the system performance at low SINR regime and more impact at high SINR regime. However, even at high SINR regime, the system performance can still be good if the channel estimation error is bounded in some interval, which is not impossible in practice with advanced channel estimation techniques.

7 PERFORMANCE ANALYSIS OF TIME SWITCHING BASED ENERGY HARVESTING UNDER IMPACT OF HARDWARE IMPAIRMENT

Another practical aspect that may have a severe impact on the performance of wireless relay networks is the hardware impairments at the source and the relay nodes. This problem has not been considered seriously in the previous studies of energy harvesting for relay networks. Therefore, our goal is to tackle this problem, specifically, I focus on the performance analysis of the energy harvesting models where hardware impairment is taken into account [tan04, tan06, tan10, tan13, tan15].

In this chapter, I provide the problem formulation to investigate the effect of hardware impairment on the performance of energy harvesting based relay networks in general and introduce some results that I have achieved so far for the cooperative relay networks as well as the cognitive radio networks.

7.1 Cooperative networks

7.1.1 Introduction

Common to all the works studying energy harvesting in relay networks is the assumption of perfect transceiver hardware at all nodes. However, in practice, the transceiver hardware is imperfect due to phase noise, I/Q imbalance and amplifier nonlinearities [21]. In [22], the authors have shown that hardware impairments limit the performance of dual-hop relaying systems, in terms of the capacity, throughput and symbol error rate (SER). The joint impact of hardware impairment and co-channel interference on the performance of relay networks was also mentioned in [23].

In this dissertation, we take account of the impact of hardware impairments at both source and relay nodes in the analysis of outage probability and throughput performance of wireless information and power transfer with half-duplex relaying. Regarding the relaying and energy harvesting protocols, we focus on decode-and-forward relaying and time-switching energy harvesting protocol. The effect of hardware impairments on system performance systems is evaluated both by mathematical analysis and simulation. The impact of other parameters such as power supply and time switching factor on system performance under hardware impairments is also investigated. Furthermore, the optimal time-switching factor to maximize system throughput is found by the numerical search algorithm.

7.1.2 System model

Let's consider a half-duplex system as an illustrative model for my dissertation. The system model and the TSR protocol is the same as in Figure 4.5 and 4.6. To focus on hardware impairment, we assume that the channel state information can be obtained perfectly. The channels from the source to the relay and from the relay to the destination are denoted as h and g, respectively. All channels are assumed as Rayleigh fading channels, which keep constant (slow fading).

During the energy harvesting phase, similar to section 4.2.1, the relay transmit power can be obtained:

$$P_r = \frac{E_h}{(1-\alpha)T/2} = \frac{2\eta P_s |h|^2 \alpha}{(1-\alpha)} = 2kP_s |h|^2 \quad (7.1)$$

where $k = \frac{\eta\alpha}{1-\alpha}$.

In the information transmission phase, due to hardware impairment, the received signal at the relay can be expressed as

$$y_r = h(x_s + \mu_s) + n_r \tag{7.2}$$

where x_s is the transmitted signal, which satisfies $E\left\{|x_s|^2\right\} = P_s$, μ_s denotes the distortion error caused by hardware impairment at the source node, which is modelled as a zero-mean Gaussian random variable with variance $P_s\sigma_1^2$, and n_r denotes the additive white Gaussian noise (AWGN) with variance N_0 at the relay node. During the second interval, the destination is receiving the forwarded signal from the relay. Here, I still assume that the link between source and destination is very weak, so the communication in this interval relies almost on the relay-destination link. Hence, the received signal at the destination node is given by

$$y_d = g(x_r + \mu_r) + n_d \tag{7.3}$$

where μ_r is the hardware noise at the relay, which is a zero-mean Gaussian random variable with variance $P_r\sigma_2^2$ and n_d is the noise at the destination, which is assumed to have the same power as n_r.

7.1.3 Amplify-and-forward

In this section, I consider the AF protocol. Hence the received signal at the relay is amplified by a factor β which is given by:

$$\beta = \frac{x_r}{y_r} = \sqrt{\frac{P_r}{|h|^2 P_s + |h|^2 P_s\sigma_1^2 + N_0}} \tag{7.4}$$

Substituting (7.2) and (7.4) into (7.3), I have:

$$\begin{aligned} y_d &= g\beta(hx_s + h\mu_s + n_r) + g\mu_r + n_d \\ &= \underbrace{g\beta h x_s}_{signal} + \underbrace{h\mu_s g\beta + g\beta n_r + g\mu_r + n_d}_{noise} \end{aligned} \tag{7.5}$$

Now, the end-to-end SNR at the destination node can be calculated by

$$SNR_{AF} = \frac{\mathrm{E}\left\{|signal|^2\right\}}{\mathrm{E}\left\{|noise|^2\right\}} = \frac{|g|^2 \beta^2 |h|^2 P_s}{|g|^2 \beta^2 |h|^2 P_s\sigma_1^2 + |g|^2 \beta^2 N_0 + |g|^2 P_r\sigma_2^2 + N_0} \tag{7.6}$$

Here, I assume that all transmitters have the same hardware structure, so that the impairments level are the same, i.e.., $\sigma_1 = \sigma_2 = \sigma$.

Theorem 7.1.

For the AF half-duplex relaying system with time-switching based energy harvesting that satisfies the condition $1-2\gamma_0\sigma^2-\gamma_0\sigma^4 \geq 0$ where $\gamma_0 = 2^R - 1$ is defined in the previous section. The outage probability of the system can be expressed as

$$\begin{aligned} P_{out} &= 1-\lambda_g e^{-\lambda_h \frac{a}{c}} \int_0^{\infty} e^{-y\lambda_g - \frac{b\lambda_h}{cy}} dy \\ &= 1-e^{-\lambda_h \frac{a}{c}} \sqrt{\frac{4b\lambda_g\lambda_h}{c}} K_1\left(\sqrt{\frac{4b\lambda_g\lambda_h}{c}}\right) \end{aligned} \tag{7.7}$$

where $K_n(x)$ is the n[th] order modified Bessel function of the second kind and

$$a = \gamma_0(1+\sigma^2) \tag{7.8}$$

$$b = \frac{\gamma_0(1+\sigma^2)+1}{2k\gamma_0} \tag{7.9}$$

$$c = Q(1-2\gamma_0\sigma^2-\gamma_0\sigma^4), Q = \frac{P_s}{N_0} \tag{7.10}$$

Proof. Let's denote $X = |h|^2$ and $Y = |g|^2$, then X and Y are exponential random variables with parameters $1/\lambda_h$ and $1/\lambda_g$, respectively. The equation (7.6) can be rewritten as

$$SNR_{AF} = \frac{XY\beta^2 P_s}{XY\beta^2 P_s\sigma^2 + Y\beta^2 N_0 + YP_r\sigma^2 + N_0} \tag{7.11}$$

Now, by substituting (7.1) and (7.4) into (7.6), and omitting the term $\frac{1}{2kQX}$ (because $1/Q$ is too small when comparing to 1 or to Q), I obtain:

$$SNR_{AF} = \frac{XYQ}{2XYQ\sigma^2 + Y + XYQ\sigma^4 + Y\sigma^2 + \frac{\sigma^2+1}{2k}} \tag{7.12}$$

With the condition that $1-2\gamma_0\sigma^2-\gamma_0\sigma^4 \geq 0$, the outage probability of my system is given by

$$P_{out}^{AF} = \Pr\left(SNR_{AF} \leq \gamma_0\right) = \Pr\left(X \leq \frac{aY+b}{cY}\right) \tag{7.13}$$

where a, b, c are defined by the equation (7.8) – (7.10). Now, the outage probability can be computed as

$$
\begin{aligned}
P_{out}^{AF} &= \iint\limits_{x\le\frac{ay+b}{cy}} f_{XY}(x,y)dxdy = \iint\limits_{x\le\frac{ay+b}{cy}} f_X(x)f_Y(y)dxdy \\
&= \int_0^\infty \lambda_g e^{-\lambda_g y}dy \int_0^{\frac{ay+b}{cy}} \lambda_h e^{-\lambda_h y}dx = \int_0^\infty \lambda_g e^{-\lambda_g y}\left[1-e^{-\lambda_h\frac{ay+b}{cy}}\right]dy \\
&= \int_0^\infty \lambda_g e^{-\lambda_g y}dy - \int_0^\infty \lambda_g e^{-\lambda_g y-\lambda_h\frac{a}{c}-\lambda_h\frac{b}{cy}}dy \\
&= 1-\lambda_g e^{-\lambda_h\frac{a}{c}}\int_0^\infty e^{-\lambda_g y-\lambda_h\frac{b}{cy}}dy
\end{aligned}
\tag{7.14}
$$

By applying the integral formula 3.324.1 in [46], I get the formula (7.7).

Remark 7.1. In this analysis, we assume that the variance of hardware impairment error is upper-bounded so that the quantity $1-2\gamma_0\sigma^2-\gamma_0\sigma^4 \ge 0$ is positive, otherwise, the outage probability would go to 1. This is reasonable in practice because we cannot increase the rate arbitrarily. For each required transmission rate, there is a corresponding constraint on hardware impairment error.

Theorem 7.2. Here, the average throughput can be computed in terms of the outage probability as [12]

$$R_{DL}^{AF}(\alpha) = (1-P_{out})R\frac{(1-\alpha)}{2} \tag{7.15}$$

Substituting (7.7) into (7.15), I have:

$$R_{DL}^{AF}(\alpha) = \frac{R}{2}(1-\alpha)e^{-\lambda_h\frac{a}{c}}\sqrt{\frac{4b\lambda_h\lambda_g}{c}}K_1\left(\sqrt{\frac{4b\lambda_h\lambda_g}{c}}\right) \tag{7.16}$$

7.1.4 Decode and forward

For the decode and forward protocol, I will consider the SNR at the relay node and destination node.

From the equation (7.2), the SNR at the relay node can be calculated by the following equation:

$$SNR_1 = \frac{P_s|h|^2}{P_s|h|^2\sigma_1^2+N_0} \tag{7.17}$$

From equation (7.3) and combine with the equation (7.1), the SNR at destination node can be obtained as

$$SNR_2 = \frac{P_r|g|^2}{P_r|g|^2\sigma_2^2+N_0} = \frac{2kP_s|h|^2|g|^2}{2kP_s|h|^2|g|^2\sigma_2^2+N_0} \tag{7.18}$$

Theorem 7.3.

For the DF half-duplex relaying system with time-switching based energy harvesting that satisfies the condition $\gamma_0\sigma^2 < 1$, the outage probability of the system can be expressed as

$$P_{out}^{DF} = \Pr\left\{SNR_{DF} = \min\left(SNR_1, SNR_2\right) \le \gamma_0\right\} \tag{7.19}$$

$$P_{out}^{DF} = 1 - e^{-\lambda_h x_0 - \frac{\lambda_g}{2k}} - \int_0^{1/2k} e^{-\lambda_g y - \frac{x_0\lambda_h}{2ky}} dy \tag{7.20}$$

where $x_0 = \dfrac{\gamma_0}{Q(1-\gamma_0\sigma^2)}, Q = \dfrac{P_s}{N_0}$.

Proof. Let's denote $X = |h|^2$ and $Y = |g|^2$. The equation (7.19) can be rewritten as

$$\begin{aligned} P_{out}^{DF} &= 1 - \Pr\left(\frac{QX}{QX\sigma^2 + 1} > \gamma_0, \frac{2kQXY}{2kQXY\sigma^2 + 1} > \gamma_0\right) \\ &= 1 - \Pr\left\{QX(1-\gamma_0\sigma^2) > \gamma_0, 2kQXY(1-\gamma_0\sigma^2) > \gamma_0\right\} \end{aligned} \tag{7.21}$$

In the following analysis, we assume that the hardware impairment is limited so that the condition is $\gamma_0\sigma^2 < 1$ satisfied. Now, the equation (7.21) can be rewritten as

$$P_{out}^{DF} = 1 - \Pr\left\{X > \frac{\gamma_0}{Q(1-\gamma_0\sigma^2)}, XY > \frac{\gamma_0}{2kQ(1-\gamma_0\sigma^2)}\right\} \tag{7.22}$$

By letting $x_0 = \dfrac{\gamma_0}{Q(1-\gamma_0\sigma^2)}$ and using the independence of random variables X and Y (which implies $f_{XY}(x,y) = f_X(x).f_Y(y)$, where $f_{XY}(.,.), f_X(.)$ and $f_Y(.)$ are the joint PDF of X and Y, the PDF of X and the PDF of Y, respectively), the above equation can be reduced to

$$\begin{aligned} P_{out}^{DF} &= 1 - \Pr\left(X > x_0, XY > \frac{x_0}{2k}\right) = 1 - \iint\limits_{S=\left\{x>x_0, xy>\frac{x_0}{2k}\right\}} f_X(x) f_Y(y) dxdy \\ &= 1 - \int_0^{y_0} f_Y(y)dy \int_{x_0/(2ky)}^{\infty} f_X(x)dx - \int_{y_0}^{\infty} f_Y(y)dy \int_{x_0}^{\infty} f_X(x)dx \\ &= 1 - e^{-x_0\lambda_h - \frac{\lambda_g}{2k}} - \lambda_g \int_0^{1/2k} e^{-y\lambda_g - \frac{x_0\lambda_h}{2ky}} dy \end{aligned} \tag{7.23}$$

Remark 7.2. In this analysis, we assume that the variance of hardware impairment error is upper-bounded so that the quantity $1-\gamma_0\sigma^2$ is positive. Otherwise, the outage probability would go to 1. This is reasonable in practice because we cannot increase the rate arbitrarily. For each required transmission rate, there is a corresponding constraint on hardware impairment error.

Theorem 7.4.

For the DF half-duplex relaying system with time-switching based energy harvesting, the average throughput of the system can be expressed as

$$R_{DL}^{DF}(\alpha)=\frac{R(1-\alpha)}{2}\left(e^{-\lambda_h x_0-\frac{\lambda_g}{2k}}+\lambda_g\int_0^{1/2k}e^{-y\lambda_g-\frac{x_0\lambda_h}{2ky}}dy\right) \tag{7.24}$$

7.1.5 Numerical Results and Discussion

In this section, I conduct a Monte Carlo simulation to verify the analysis developed in the previous section. For simplicity, in our simulation model, we assume that the source-relay and relay-destination distances are both normalized to unit value. Other simulation parameters are listed in Table 7.1.

Table 7.1. Simulation parameters

Symbol	Name	Values
R	Source rate	3bps/Hz
γ_0	SINR threshold	7
η	Energy harvesting efficiency	0.6
$1/\lambda_h$	Mean of $\|h\|^2$	0.5
$1/\lambda_g$	Mean of $\|g\|^2$	0.5
P_s/N_0	Source-Power to Noise Ratio	0-30 dB

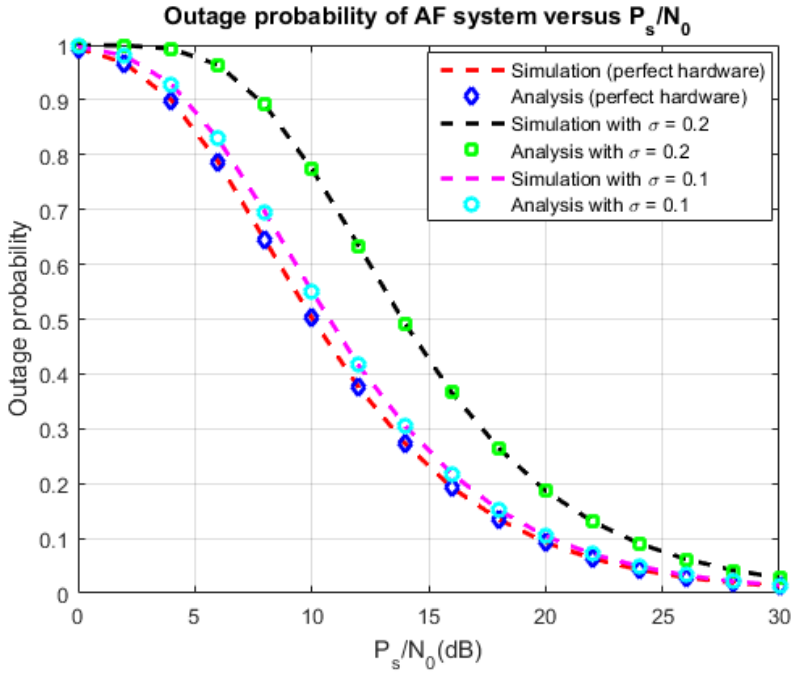

Figure 7.1. Outage probability versus source-power to noise ratio for AF protocol

Figure 7.1 and 7.2 shows the achievable throughput and outage probability of the system versus Ps/N_0 ratio with the variance of hardware impairment error set to be 0.1 and 0.2. The time-switching factor α is set to 0.5. It's can be observed that the simulation curve and the analytical curve almost overlap together. It could be recommended that at Ps/N_0 above 20dB, the hardware noise has less impact on the outage probability and the outage performance is acceptable for real applications. This confirms our mathematical analysis in the previous section.

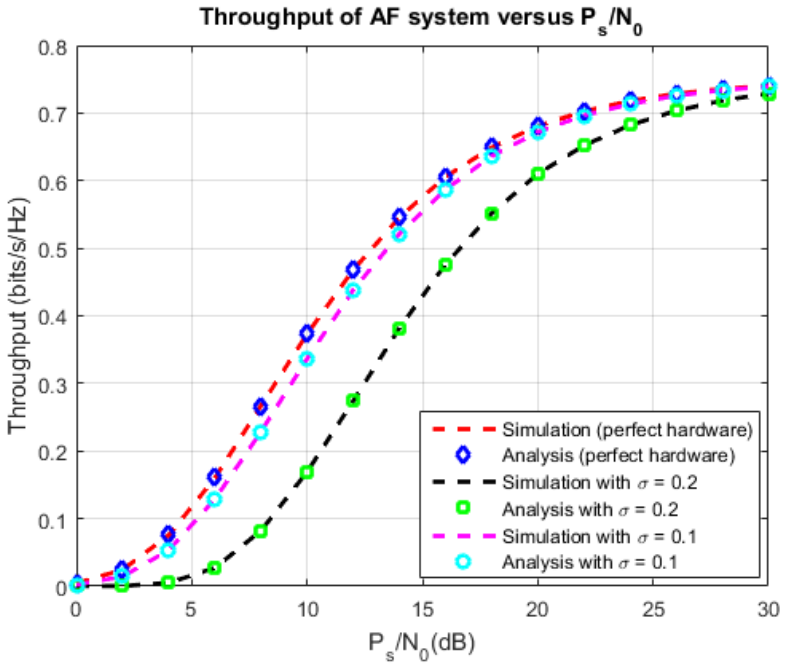

Figure 7.2. Throughput versus source-power to noise ratio for AF protocol

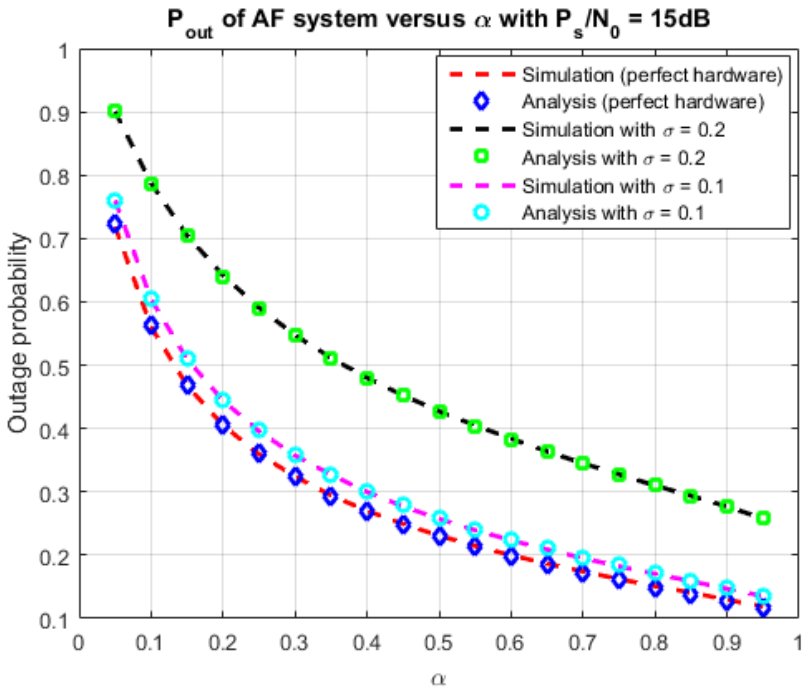

Figure 7.3. Outage probability versus time-switching factor for AF protocol

We can notice that in the low SNR regime, the hardware impairment error has a severe effect on system performance. However, when the transmit power goes large, the hardware impairment error has decreasing impact on both achievable throughput as well as outage probability. The impact of time switching factor on the instantaneous capacity is shown in Figure 7.3. In this experiment, Ps/N0 is set to 15 dB. Again, the analytical solutions are in exact agreement with the simulation results.

There exists a unique time switching factor at which the system throughput is maximized. In practice, this optimal factor can be found iteratively using numerical methods. The outage probability also depends on the time switching factor, which is illustrated in Figure 7.4.

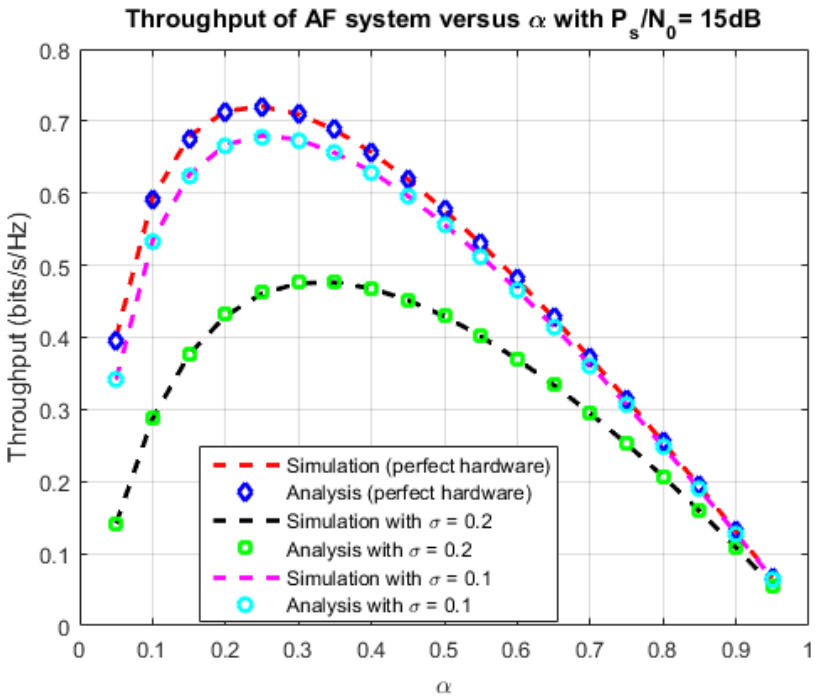

Figure 7.4. Throughput versus time-switching factor for AF protocol

Figures 7.5 and 7.6 illustrates the impact of hardware impairment level on the system performance with Ps/N_0 set to 15 dB. It can be observed that the performance is going down when the hardware impairment is more severe, as expected. Regarding the time-switching factor, we can see that the hardware impairment has a stronger impact when the time-switching factor is small. It can be explained as follows. For small time-switching factor, the available energy for transmission at the relay nodes is reduced so there is a higher risk for the signal to be undetectable because of the high level of impairment.

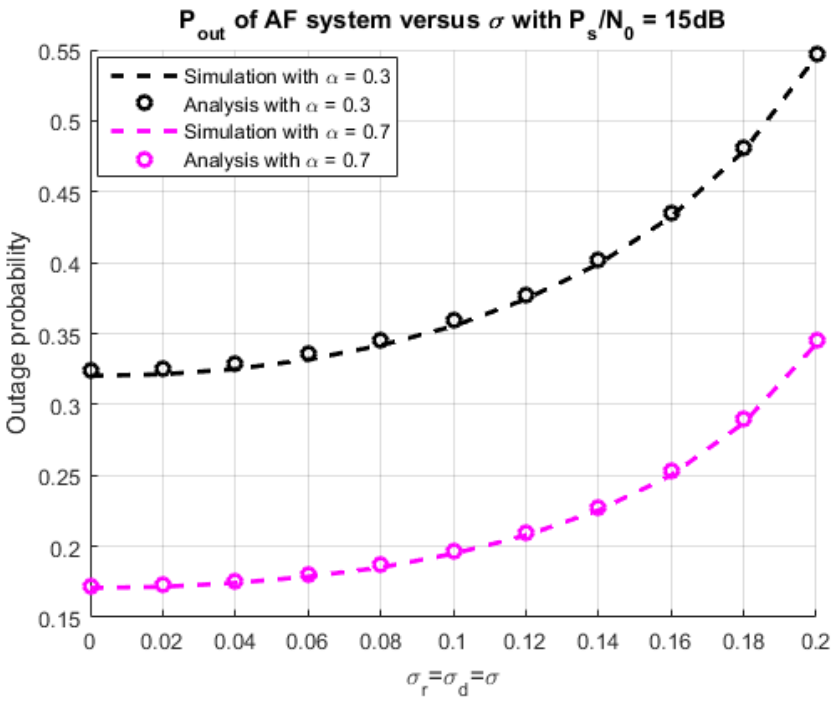

Figure 7.5. Outage probability versus level of hardware impairment for AF system

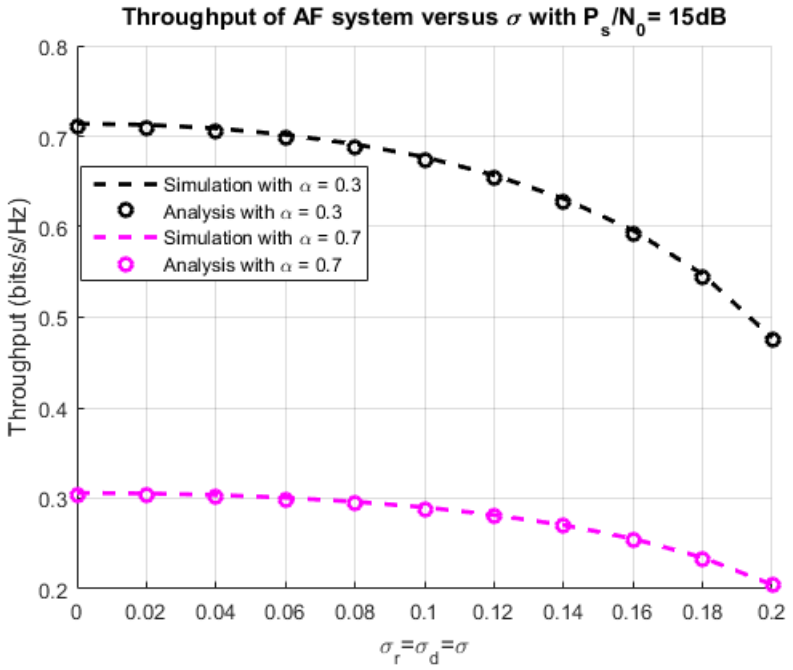

Figure 7.6. Throughput versus the level of hardware impairment for AF system

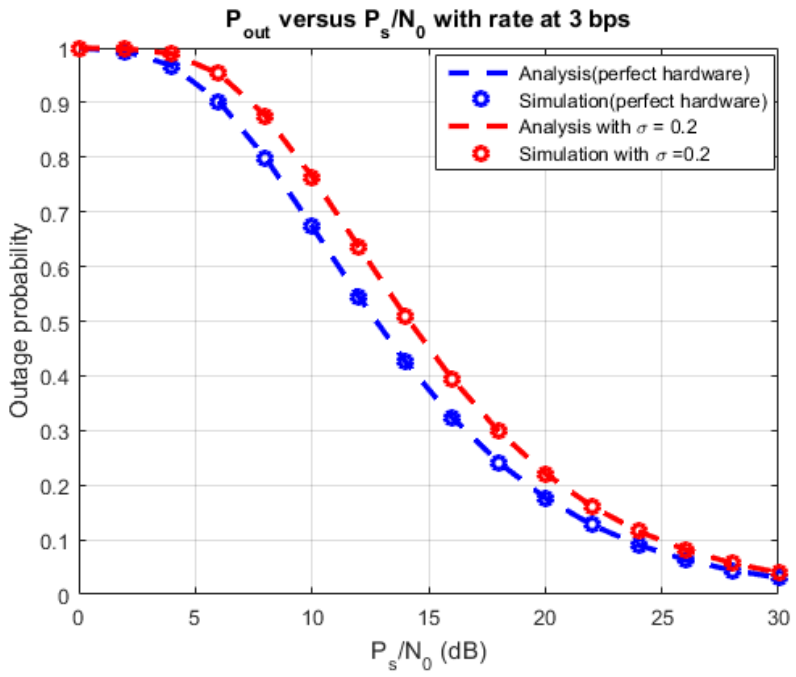

Figure 7.7. Outage probability versus source-power to noise ratio for DF protocol

Figures 7.7 and 7.8 shows the achievable throughput and outage probability of the system versus Ps/N_0 ratio with the variance of hardware impairment error set to be 0 (perfect hardware) and 0.2. The time-switching factor α is set to 0.5. It's can be observed that the simulation curve and the analytical curve almost overlap together.

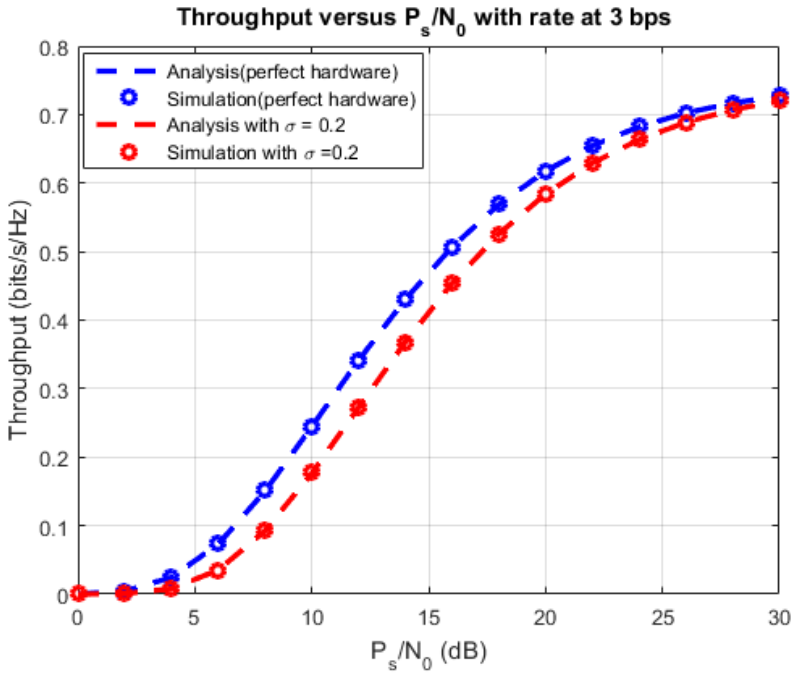

Figure 7.8. Throughput versus source-power to noise ratio for DF protocol

This confirms our mathematical analysis in the previous section. I can notice that in the low SNR regime, the hardware impairment error has a severe effect on system performance. However, when the transmit

power goes large, the hardware impairment error has a decreasing impact on both achievable throughput as well as outage probability. The impact of time switching factor on the instantaneous capacity is shown in Fig. 7.9. In this experiment, Ps/N0 is set to 20 dB. Again, the analytical solutions are in exact agreement with the simulation results. There exists a unique time switching factor at which the system throughput is maximized. In practice, this optimal factor can be found iteratively using numerical methods. The outage probability depends on the time switching factor, which is illustrated in Fig. 7.10.

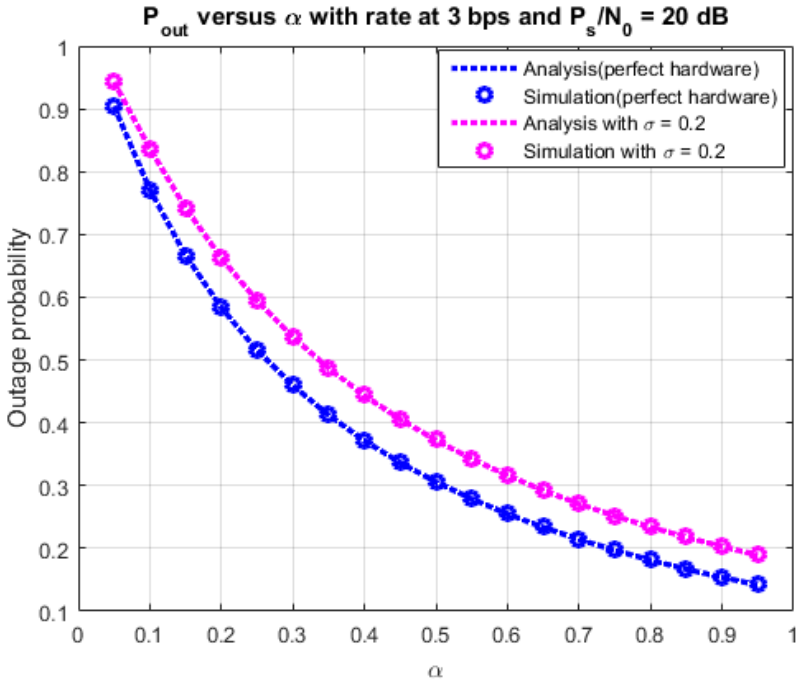

Figure 7.9. Outage probability versus time-switching factor for DF protocol

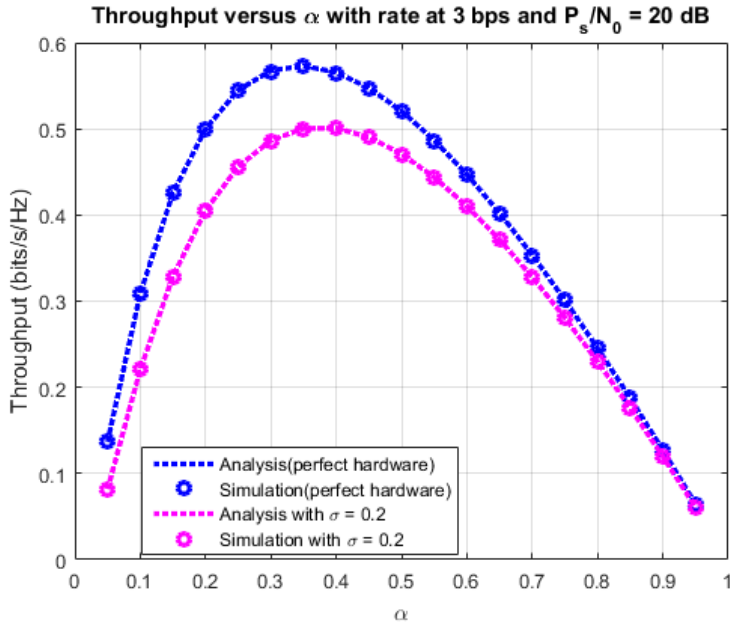

Figure 7.10. Throughput versus time-switching factor for DF protocol

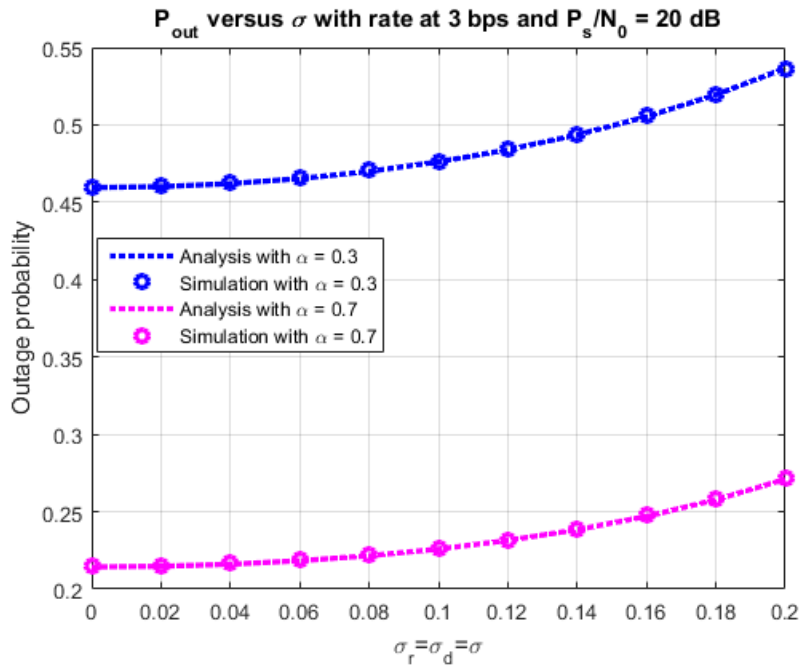

Figure 7.11. Outage probability versus the level of hardware impairment for DF system

The same results as in Figures 7.5 and 7.6 are obtained for the DF relaying system as illustrated in Figure 7.11 and Figure 7.12. The outage probability increases and the throughput decrease when the hardware impairment level goes up. In addition, the performance would be worse with a small time-switching factor.

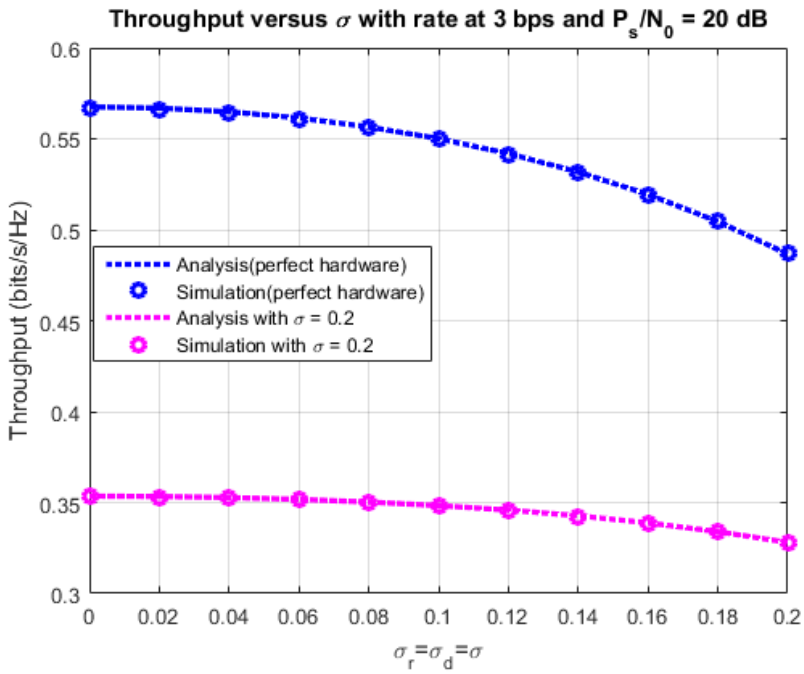

Figure 7.12. Throughput versus level of hardware impairment for DF system

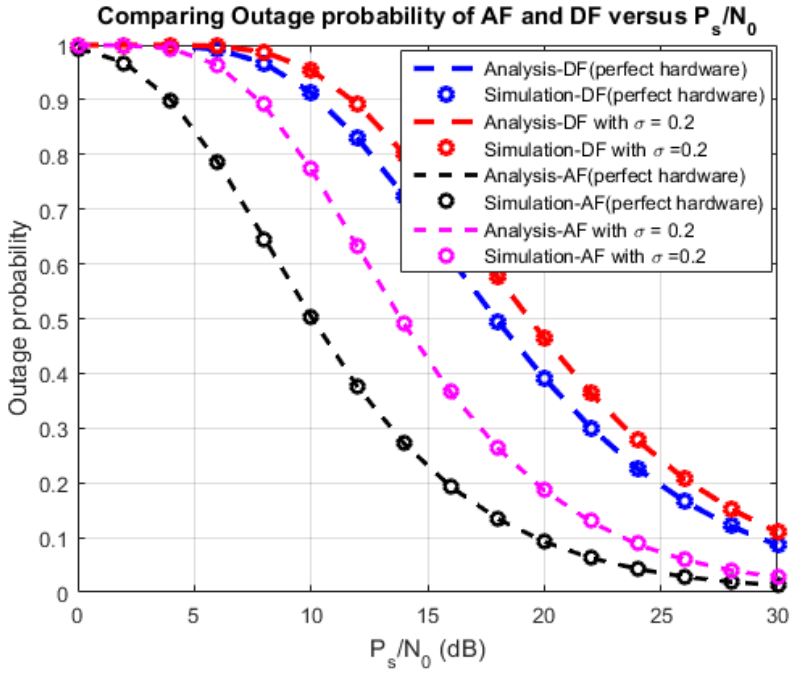

Figure 7.13. Comparing Throughput of AF and DF protocols

Figures 7.13 and 7.14 show a comparison between 2 relaying protocols: AF and DF. Here, the time-switching factor is set to $\alpha = 0.5$. We can observe that the AF protocol outperforms the DF protocol in both perfect hardware condition and hardware impairment condition.

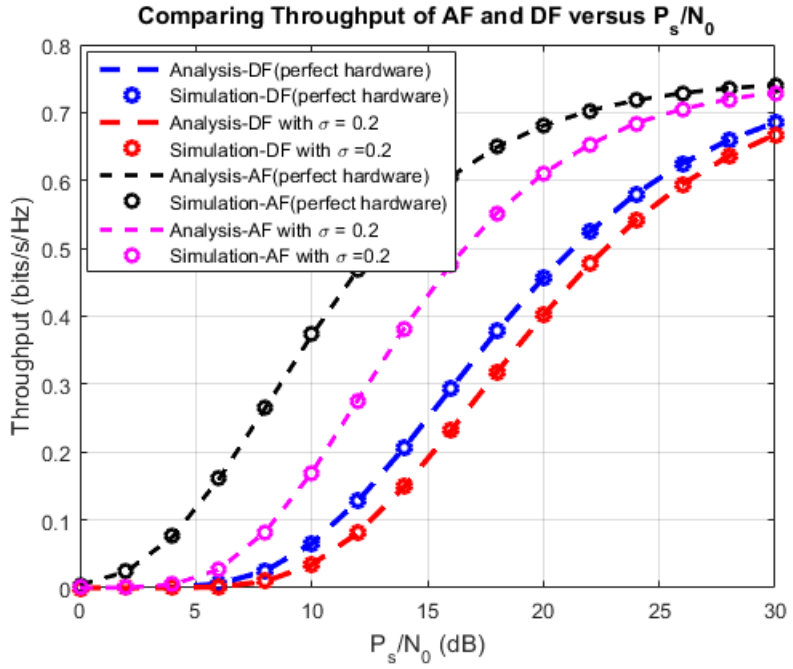

Figure 7.14. Comparing Outage probability of AF and DF protocols

7.2 Cognitive radio networks

7.2.1 Introduction

With the rapid increase of wireless devices and systems, spectrum scarcity becomes a critical issue due to the emergence of wireless services. To overcome this problem, Mitola [24] introduced cognitive radio (CR) concept, in which licensed users (primary users (PUs)) can share licensed bands to unlicensed users (secondary users (SUs)). The basic idea of the CR technique is that two wireless systems coexist and operate at the same spectrum resources. However, they have different priorities: PUs can use the licensed bands any time, while SUs can use the spectrum with lower priority [25]. In the conventional CR method [26], SUs must detect the presence/absence of PUs. If there are vacant bands detected, SUs can access them to transmit the secondary data. Recently, researchers have proposed two spectrum sharing methods in which SUs can use licensed bands without detecting PUs' operations. In the first method, named underlay CR [27,28], PUs and SUs can use the licensed bands at the same time, provided that the co-channel interference from the secondary transmission must be lower than a maximum threshold required by PUs. In the second method, named overlay CR [29-31], SUs can use licensed bands but they must help PUs enhance the quality of service (QoS). In particular, the secondary transmitters (STs) play a role as relays for the primary network and via this assistance, they can find opportunities to access the licensed bands.

So far, most of the published papers have assumed that transceiver hardware is perfect. However, in practice, the transceiver hardware of wireless devices is imperfect because it is affected by impairments such as amplifier-amplitude non-linearity, I/Q imbalance and phase noise [22]. Hence, the hardware impairments (HI) need to be taken into account when evaluating performances of wireless relay networks. In [51], outage probability (OP) of two-way relay networks with the hardware noises at relay was investigated. The authors in [23] proposed and evaluated the outage performance of proactive relay selection protocols in co-channel interference networks. In [52], the authors investigated the joint impact of the imperfect hardware and the wireless power transfer on the outage performance of two-way underlay CR. The results in [22], [51] and [23] have presented that the presence of HI degrades the system performances over fading channels.

In practical wireless networks, users are usually in motion, which requires extra energy in addition to energy used for signal transmission. Moreover, CR secondary users also consume energy for spectrum sensing process. Therefore, it is very imperative that energy efficiency must be considered for secondary users in CR networks. To the best of our knowledge, there are several reports related to cooperative CR models using the EH technique. In particular, in [32], the ST is deployed with a rechargeable battery which can harvest energy from the environment. The authors in [33] proposed optimal spectrum access for EH-based CR networks, where the ST at the beginning of each time slot needs to determine whether to remain idle so as to conserve energy, or to execute spectrum sensing to acquire knowledge of the current spectrum occupancy state. In [53,54], the authors studied the performance of the secondary networks operating on underlay mode. Published works [34,35] evaluated the performances of both primary and secondary networks in overlay CR environment, where a single EH-based ST uses the AF or DF technique to forward the combined signals to both primary receiver (PR) and secondary receiver (SR). The authors in [36] proposed a cooperative spectrum access protocol in which the SU can harvest

the energy from the primary signals and then assists the primary data transmission using Alamouti technique. Li et al. [55] also proposed a spectrum sharing method based on competitive price game model.

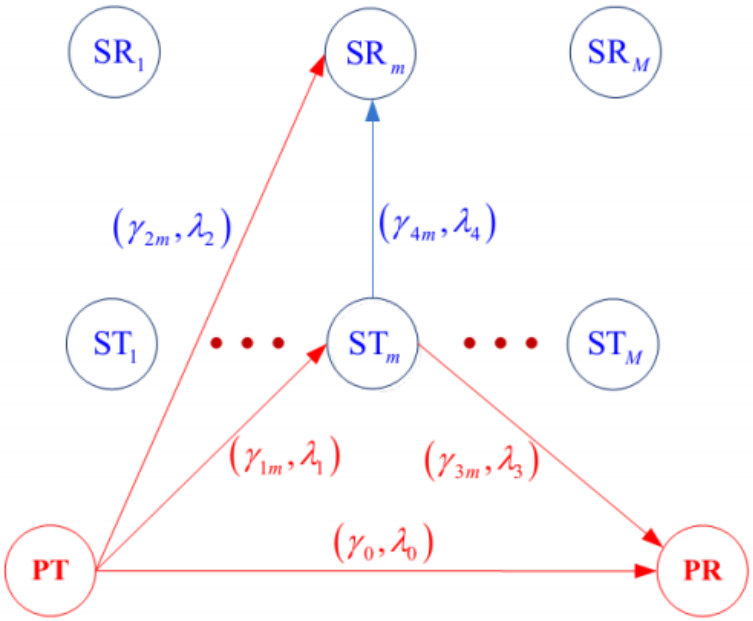

Figure 7.15. The cognitive radio network system

In this paper, we propose a new cooperative spectrum sharing relaying protocols, where the best EH-based ST is chosen to assist the data transmission between the nodes PT and PR. We also propose incremental relaying cooperation [2] in which the PR only requires help from STs when the communication between the PT and PR is not successful. Different from the schemes proposed in [34], [35], [36], the proposed scheme includes multiple ST-SR pairs and only the best ST is selected for the cooperation. Moreover, the impact of hardware impairments on the outage performance of the primary and secondary networks is also investigated. For performance evaluation, we derive exact and lower-bound closed-form expressions of outage probability for both networks over the Rayleigh fading channel. We then perform Monte-Carlo simulations to verify the theoretical derivations.

7.2.2 System model

In figure 7.15, I present the system model of the proposed scheme, where the primary network includes one primary transmitter- primary receiver (PT-PR) pair, while there are M secondary transmitter-secondary receiver (ST-SR) pairs in the secondary network. The PT attempts to transmit its data to the PR with the help of STs, i.e., STm (m=1,2,…,M). Via cooperation, the STm can access the licensed band to transmit its data to the SRm. Assume that all of the terminals are equipped with a single antenna and operate on half-duplex mode. I also assume that the STs (SRs) are close together and form a cluster, and hence, the distances from the PT to STs (SR) are assumed to be the same [56]. Let me denote d_0, d_1, d_2, d_3 and d_4 as the distance of the PT-PR, PT-STm, PT-SRm, STm-PR and STm-SRm links, respectively. I also denote $h_{PT,PR}, h_{PT,STm}, h_{PT,SRm}, h_{STm,PR}$ *and* $h_{STm,SRm}$ as channel coefficients of the PT-PR, PT-STm, PT-SRm, STm-PR and STm-SRm links, respectively. I assume that all of the links are modelled to be block and flat Rayleigh fading channels, which remain constant during an interval T and

change independently over different intervals. As mentioned in [56], channel gains $\gamma_0, \gamma_{1m}, \gamma_{2m}, \gamma_{3m}$ *and* γ_{4m} ($\gamma_0 = \left|h_{PT,PR}\right|^2, \gamma_{1m} = \left|h_{PT,STm}\right|^2, \gamma_{2m} = \left|h_{PT,SRm}\right|^2, \gamma_{3m} = \left|h_{STm,PR}\right|^2$ and $\gamma_{4m} = \left|h_{STm,SRm}\right|^2$) are exponential random variables (RVs) with parameters $\lambda_0, \lambda_1, \lambda_2, \lambda_3$ *and* λ_4, respectively [56]. Moreover, to take path-loss into account, the parameters can be expressed as a function of the distance and the path-loss exponent by [56]: $\lambda_0 = d_0^{\chi}, \lambda_1 = d_1^{\chi}, \lambda_2 = d_2^{\chi}, \lambda_3 = d_3^{\chi}$ and $\lambda_4 = d_4^{\chi}$, respectively, where χ is the path-loss coefficient. We assume that the STs are limited-energy terminals which must harvest energy from the RF signals generated by the PT. It is also assumed that the nodes STs and SRs have enough energy for processing the control messages in set-up phases [54] as well as for decoding the received data. The operation of the proposed protocol is split into three sub-blocks. Similar to the time switching scheme in [54], a duration of αT is used for the STs to harvest the energy from the PT, a duration of (1 − α) T/2 for the STs and the PR to receive the data from the PT, and a duration of (1 − α) T/2 is employed to forward the data from the selected ST to the PR and the intended SR. Then, the energy that the STm can harvest is given as [54, eq. (13)]:

$$E_m = \eta \alpha T P_{\gamma_{1m}} \tag{7.25}$$

where $\eta (0 < \eta \le 1)$ is the energy conversion efficiency that depends on the internal inverter circuit in the STs, and P is the transmit power of the PT. Hence, the transmit power of the STm over time (1 − α) T/2 can be obtained by [54, eq. (14)]:

$$P_m = \frac{E_m}{(1-\alpha)T/2} = \frac{2\eta\alpha P_{\gamma_{1m}}}{1-\alpha} = \mu P_{\gamma_{1m}} \tag{7.26}$$

where $\mu = \dfrac{2\eta\alpha}{1-\alpha}$,

At the next sub-block, the PT transmits its data to the PR, which is also received by the STm and SRm. Under the imperfect hardware, the received signal at the node X, X∈ {STm; SRm; PR}, can be given as

$$y_X = \sqrt{P} h_{PT,X} \left(x_P + \eta_{t,PT} \right) + \eta_{r,X} + n_X \tag{7.27}$$

where x_P is the primary signal transmitted by the PT, n_X is the additive white Gaussian noise (AWGN), $\eta_{t,PT}$ and $\eta_{r,X}$ are the noises caused by the hardware impairments at the transmitter PT and the receiver X, respectively. Similar to [57], n_X , $\eta_{t,PT}$ and $\eta_{r,X}$ are modelled as zero-mean Gaussian noises with the variance of N_0, κ_{PT}^t *and* $\kappa_X^r P \left|h_{PT,X}\right|^2$, respectively, where κ_{PT}^t *and* κ_X^r indicate the level of hardware impairments at the nodes PT and X. From (7.27), the achievable data rate between the nodes PT and PR can be calculated by

$$C_0 = \frac{(1-\alpha)T}{2}\log_2\left\{1+\frac{P\left|h_{PT,PR}\right|^2}{\left(\kappa_{PT}^t+\kappa_{PR}^r\right)P\left|h_{PT,PR}\right|^2+N_0}\right\} = \frac{(1-\alpha)T}{2}\log_2\left(1+\frac{\psi\gamma_0}{\kappa_{PT,PR}\psi\gamma_0+1}\right) \tag{7.28}$$

where $\psi = P/N_0$ is the average transmit signal-to-noise ratio (SNR), $\kappa_{PT,PR} = \kappa_{PT}^t + \kappa_{PR}^r$ is a total hardware impairment level. Similarly, we can obtain the instantaneous channel capacity of the PT − STm and PT − SRm links, respectively as

$$C_{1m} = \frac{(1-\alpha)T}{2}\log_2\left(1+\frac{\psi\gamma_{1m}}{\kappa_{PT,STm}\psi\gamma_{1m}+1}\right), \quad C_{2m} = \frac{(1-\alpha)T}{2}\log_2\left(1+\frac{\psi\gamma_{2m}}{\kappa_{PT,SRm}\psi\gamma_{2m}+1}\right) \tag{7.29}$$

where $\kappa_{PT,STm} = \kappa_{PT}^t + \kappa_{STm}^r \; and \; \kappa_{PT,SRm} = \kappa_{PT}^t + \kappa_{SRm}^r$.

At the end of the second sub-block, the PR attempts to decode the received signal. If this node can decode the source signal successfully, it informs the decoding status by generating an ACK message. In this case, the STs and SRs remove the primary signal from their buffers and use the third sub-block to transmit the secondary data. Because the transmission between the PT and the PR is successful, the primary network allows the secondary users to use the third sub-block to transmit their signals.

To optimize the performance of the secondary network, we propose a strategy to select the best ST-SR pair. At first, let us consider the signal received at the SRm due to the transmission of the STm:

$$y_{SRm} = \sqrt{P_m}h_{STm,SRm}\left(z_m+\eta_{t,STm}\right)+\eta_{r,SRm}+n_{Rm} \tag{7.30}$$

where z_m is the signal transmitted by the STm and $\eta_{t,STm}$ is the noise caused by the hardware impairments at the STm which can be modelled as zero-mean Gaussian noise with variance of κ_{STm}^t.

From (7.26) and (7.30), the instantaneous channel capacity of the STm − SRm link can be given as

$$C_{4m} = \frac{(1-\alpha)T}{2}\log_2\left(1+\frac{\mu\psi\gamma_{1m}\gamma_{4m}}{\kappa_{STm,SRm}\mu\psi\gamma_{1m}\gamma_{4m}+1}\right) \tag{7.31}$$

where $\kappa_{STm,SRm} = \kappa_{STm}^t + \kappa_{SRm}^r$.

From (7.31), the best ST-SR pair can be selected by the following method:

$$ST_a - SR_a : \gamma_{1a}\gamma_{4a} = \max_{m=1,2,\ldots,M}\left(\gamma_{1m}\gamma_{4m}\right) \tag{7.32}$$

Equation (7.32) implies that the ST-SR pair which provides the highest channel gain of the ST-SR links is selected for the communication at the third sub-block. Next, let me consider the event that the decoding status at the PR is unsuccessful. In this case, it sends back a NACK message to request a

retransmission from one of the STs. We denote W_{SR} as a set of the SRs that can decode the primary signal successfully. Without loss of generality, I can assume that $W_{SR} = \{SR_1, SR_2, ..., SR_{N_R}\}$, where $N_R (0 \le N_R \le M)$ is the cardinality of W_{SR}. Similarly, each SR will feedback the ACK (or NACK) message to indicate the successful (or unsuccessful) decoding status. Because when the SR decodes the primary signals correctly, it can remove the primary signal component from the signals received from the ST [30, 31].

If there is at least one SR decoding the primary signal correctly $(N_R \ge 1)$, from the successful STs, i.e, $ST_1, ST_2, ..., ST_{N_R}$, I propose a method to select the ST for the cooperation at the next sub-block as follows:

$$ST_b : P_b = \max_{j=1,2,...,N_R} \left(P_j\right) or\, \gamma_{1b} = \max_{j=1,2,...,N_R} \left(\gamma_{1j}\right) \tag{7.33}$$

where the ST providing the maximum harvested energy (or the highest channel gain between the PT and STs) is selected as the best candidate. If the node ST_b can decode the primary signal x_P successfully, it combines linearly x_P and its own signal z_b, follows the strategy given in [31] as:

$$x_c = \sqrt{\beta P_b} x_P + \sqrt{(1-\beta) P_b} z_b \tag{7.34}$$

where $\beta P_b \; and \; (1-\beta) P_b$ are the fractions of the total transmit power P_b, which are allocated to the signals x_P and z_b, respectively. Then, the ST_b broadcasts the combined signal x_c, and the received signals at the PR and SR_b can be given, respectively by

$$\begin{aligned} y_{PR} &= \sqrt{\beta P_b} h_{ST_b,PR} \left(x_P + \eta_{t,ST_b,1}\right) + \sqrt{(1-\beta) P_b} h_{ST_b,PR} \left(z_b + \eta_{t,ST_b,2}\right) + \eta_{r,PR} + n_{PR} \\ y_{SR_b} &= \sqrt{\beta P_b} h_{ST_b,SR_b} \left(x_P + \eta_{t,ST_b,3}\right) + \sqrt{(1-\beta) P_b} h_{ST_b,SR_b} \left(z_b + \eta_{t,ST_b,4}\right) + \eta_{r,SR_b} + n_{SR_b} \end{aligned} \tag{7.35}$$

It is noted from (7.35) that the variances of the hardware impairments $\eta_{t,ST_b,u}, \eta_{r,PR} \; and \; \eta_{r,SR_b}$ are $\kappa^t_{ST_b}, \kappa^r_{PR} P_b \left|h_{ST_b,PR}\right|^2$ and $\kappa^r_{SR_b} P_b \left|h_{ST_b,SR_b}\right|^2$, respectively, where u=1,2,3,4. Moreover, because the SR_b obtained the signal x_P before, it can remove the interference component $\sqrt{\beta P_b} h_{ST_b,SR_b} x_P$ from the received signal. After cancelling the interference, the signal y_{SR_b} can be rewritten by

$$y^*_{SR_b} = \sqrt{(1-\beta) P_b} h_{ST_b,SR_b} \left(z_b + \eta_{t,ST_b,4}\right) + \sqrt{\beta P_b} h_{ST_b,SR_b} \eta_{t,ST_b,3} + \eta_{r,SR_b} + n_{SR_b} \tag{7.36}$$

Combining (7.26), (7.35) and (7.36), I respectively obtain the achievable capacity for the ST_b – PR and ST_b – SR_b links as

$$C_{3b} = \frac{(1-\alpha)T}{2}\log_2\left\{1+\frac{\beta\mu\psi\gamma_{1b}\gamma_{3b}}{\left(1-\beta+\kappa_{ST_b,PR}\right)\mu\psi\gamma_{1b}\gamma_{3b}+1}\right\},$$
$$C_{4b} = \frac{(1-\alpha)T}{2}\log_2\left\{1+\frac{\left(1-\beta\right)\mu\psi\gamma_{1b}\gamma_{4b}}{\kappa_{ST_b,SR_b}\mu\psi\gamma_{1b}\gamma_{4b}+1}\right\} \quad (7.37)$$

where $\kappa_{ST_b,PR} = \kappa^t_{ST_b} + \kappa^r_{PR}$ *and* $\kappa_{ST_b,SR_b} = \kappa^t_{ST_b} + \kappa^r_{SR_b}$.

Next, I consider the case where there is no SR receiving the primary signal successfully, i.e., $N_R = 0$. In this case, one of the STs has to use the total harvested energy to serve the PR. Let W_{ST} as a set of STs that can decode the primary signal successfully. Without loss of generality, I can assume that $W_{ST} = \{ST_1, ST_2, ..., ST_{N_T}\}$ where $N_T (0 \le N_T \le M)$ is the cardinality of W_{ST} . It is obvious that if $N_T = 0$, the system cannot select any STs for the retransmission, and hence the primary signal is dropped. In this case, the PT would start a new transmission without sharing the licensed band to the secondary network because the STs cannot help the PR retransmit the data. Otherwise, the best ST is chosen by the following selection strategy:

$$ST_c : \gamma_{3c} = \max_{j=1,2,...,N_T}\left(\gamma_{3j}\right) \quad (7.38)$$

where the successful ST having the highest channel gain between itself and the PR is selected as the best relay. Then, the received signal at the PR can be given by

$$y_{PR} = \sqrt{P_c}h_{ST_c,PR}\left(x_P + \eta_{t,ST_c}\right) + \eta_{r,PR} + n_{PR} \quad (7.39)$$

Finally, the instantaneous data rate of the STc-PR link can be formulated by

$$C_{3c} = \frac{(1-\alpha)T}{2}\log_2\left(1+\frac{\mu\psi\gamma_{1c}\gamma_{3c}}{\kappa_{ST_c,PR}\mu\psi\gamma_{1c}\gamma_{3c}+1}\right) \quad (7.40)$$

where $\kappa_{ST_c,PR} = \kappa^t_{ST_c} + \kappa^r_{PR}$.

7.2.3 Performance Evaluation

For ease of analysis, we assume that the total hardware impairment levels are the same, i.e., $\kappa_{Y,Z} = \kappa$, for all $\{Y,Z\} \in \{PT, PR, STm, SRm\}$. When the hardware impairment levels are different, with the same manner I also obtain exact and asymptotic expressions of outage probability for both networks.

Mathematical Preliminaries

Firstly, it is well-known that cumulative density function (CDF) and probability density function (PDF) of an exponential RV Y with parameter λ_Y can be given, respectively as

$$F_Y(y) = 1 - e^{-\lambda_Y y}, f_Y(y) = \lambda_Y e^{-\lambda_Y y} \quad (7.41)$$

Next, let me consider a RV Y_{max}, i.e., $Y_{\max} = \max_{i=1,2,...,K}(Y_i)$, where K is a positive integer and Y_i is an exponential RV whose parameter is λ_Y. Hence, the CDF of Y_{max} can be given as (see in [59, eq.(7)])

$$F_{Y_{\max}}(y) = \sum_{m=0}^{K}(-1)^m C_K^m e^{-m\lambda_Y y} \tag{7.42}$$

where $C_K^m = \dfrac{K!}{m!(K-m)!}$

Then, the corresponding PDF can be obtained by

$$f_{Y_{\max}}(y) = \sum_{m=0}^{K-1}(-1)^m C_{K-1}^m K\lambda_Y e^{-(m+1)\lambda_Y y} \tag{7.43}$$

We now consider a RVs $Z*$ that is product of two exponential RVs Z_1 and Z_2 ($Z*=Z_1Z_2$), whose parameters are Ω_1 and Ω_2, respectively. The CDF of $Y*$ can be formulated by

$$F_{Z_*}(z) = \Pr(Z_1 Z_2 < z) = \int_0^{+\infty} f_{Z_1}(t) F_{Z_2}(z/t)dt \tag{7.44}$$

Using the CDF and PDF obtained in (7.41) for (7.44), and then applying [46, eq. (3.324.1)] for the corresponding integral, I obtain:

$$F_{Z_*}(z) = 1 - \sqrt{4\Omega_1\Omega_2 z}K_1\left(\sqrt{4\Omega_1\Omega_2 z}\right) \tag{7.45}$$

where $K_1(.)$ is the modified Bessel function of the second kind [46].

Outage Probability Analysis

Outage probability is defined by the probability that the achievable rate at a receiver is below a target rate, i.e., R_{th}. Moreover, the receiver can be assumed to correctly decode received signals if the data rate is higher than Rth. At first, notations used in this sub-section can be listed as follows:

$$\begin{aligned} &\theta = 2^{\frac{2R_{th}}{(1-\alpha)T}} - 1, \rho_0 = \frac{\theta}{(1-\kappa\theta)\psi}, \\ &\rho_1 = \frac{\theta}{[\beta-(1-\beta+\kappa)\theta]\psi}, \rho_2 = \frac{\theta}{(1-\beta-\kappa\theta)\psi} \end{aligned} \tag{7.46}$$

Now, the outage probability of the primary network can be formulated by

$$P_{out}^{PR} = \Pr\left(C_0 < R_{th}\right)\Pr\left(N_R = 0\right)\times\left\{\Pr\left(N_T = 0\right) + \sum_{u=1}^{M} C_M^u \Pr\begin{bmatrix} N_T = u-1 \\ C_{1c} \geq R_{th} \\ C_{3c} < R_{th} \end{bmatrix}\right\}$$
$$+ \Pr\left(C_0 < R_{th}\right)\sum_{m=1}^{M} C_M^m \Pr\left(N_R = m\right)\Pr\left(C_{1b} < R_{th}\right) \quad (7.47)$$
$$+ \Pr\left(C_0 < R_{th}\right)\sum_{m=1}^{M} C_M^m \Pr\left(N_R = m\right)\Pr\begin{bmatrix} C_{1b} \geq R_{th} \\ C_{3b} < R_{th} \end{bmatrix}$$

In (7.47), $\Pr\left(N_T = x\right) and \Pr\left(N_R = y\right)$ are probabilities that the number of successful SRs and STs equals x and y, respectively.

Theorem 7.5.

The outage probability P_{out}^{PR} can be calculated by

$$P_{out}^{PR} = \begin{cases} OP_1^{PR}, if\ \theta < \beta/(1-\beta+\kappa) \\ OP_2^{PR}, if\ \beta/(1-\beta+\kappa) \leq \theta < 1/\kappa \\ 1 \quad\quad , if\ \theta \geq 1/\kappa \end{cases} \quad (7.48)$$

where $OP_1^{PR} and\ OP_2^{PR}$ are given by (7.49) and (7.50).

$$OP_1^{PR} = (1-e^{-\lambda_0\rho_0})(1-e^{-\lambda_2\rho_0})^M(1-e^{-\lambda_1\rho_0})^M$$
$$+(1-e^{-\lambda_0\rho_0})(1-e^{-\lambda_2\rho_0})^M\sum_{u=1}^{M} C_M^u(1-e^{-\lambda_1\rho_0})^{M-u}e^{-(u-1)\lambda_1\rho_0}\sum_{v=0}^{u}(-1)^v C_u^v\int_{\rho_0}^{\infty}\lambda_1 e^{-\lambda_1 x}e^{-\frac{v\lambda_3\rho_0}{\mu x}}dx$$
$$+(1-e^{-\lambda_0\rho_0})\sum_{m=1}^{M} C_M^m(1-e^{-\lambda_2\rho_0})^{M-m}e^{-m\lambda_2\rho_0}(1-e^{-\lambda_1\rho_0})^m \quad (7.49)$$
$$+(1-e^{-\lambda_0\rho_0})\sum_{m=1}^{M} C_M^m(1-e^{-\lambda_2\rho_0})^{M-m}e^{-m\lambda_2\rho_0}\sum_{t=0}^{m-1}(-1)^t C_{m-1}^t m\lambda_1\left[\frac{e^{-(t+1)\lambda_1\rho_0}}{(t+1)\lambda_1} - \int_{\rho_0}^{\infty} e^{-(t+1)\lambda_1 x}e^{-\frac{\lambda_3\rho_1}{\mu x}}dx\right]$$

$$OP_2^{PR} = (1-e^{-\lambda_0\rho_0})(1-e^{-\lambda_2\rho_0})^M(1-e^{-\lambda_1\rho_0})^M$$
$$+(1-e^{-\lambda_0\rho_0})(1-e^{-\lambda_2\rho_0})^M\sum_{u=1}^{M} C_M^u(1-e^{-\lambda_1\rho_0})^{M-u}e^{-(u-1)\lambda_1\rho_0}\sum_{v=0}^{u}(-1)^v C_u^v\int_{\rho_0}^{\infty}\lambda_1 e^{-\lambda_1 x}e^{-\frac{v\lambda_3\rho_0}{\mu x}}dx \quad (7.50)$$
$$+(1-e^{-\lambda_0\rho_0})\sum_{m=1}^{M} C_M^m(1-e^{-\lambda_2\rho_0})^{M-m}e^{-m\lambda_2\rho_0}$$

Proof. At first, I calculate OP_1^{PR} in (7.49). Under the condition $\theta < \beta/(1-\beta+\kappa)$, the probability

$\Pr(C_0 < R_{th}), \Pr(C_{1b} < R_{th}), \Pr(N_R = 0), \Pr(N_T = 0)\, and\, \Pr(N_R = m)$ can be computed, respectively as

$$\begin{aligned}
&\Pr(C_0 < R_{th}) = 1 - e^{-\lambda_0 \rho_0}, \\
&\Pr(C_{1b} < R_{th}) = \left(1 - e^{-\lambda_1 \rho_0}\right)^m, \\
&\Pr(N_R = 0) = \left(1 - e^{-\lambda_2 \rho_0}\right)^M, \\
&\Pr(N_T = 0) = \left(1 - e^{-\lambda_1 \rho_0}\right)^M, \\
&\Pr(N_R = m) = \left(1 - e^{-\lambda_2 \rho_0}\right)^{M-m} e^{-m\lambda_1 \rho_0}
\end{aligned} \tag{7.51}$$

Next, considering the probability $\Pr\left[\begin{cases} N_T = u-1 \\ C_{1c} \geq R_{th} \\ C_{3c} < R_{th} \end{cases}\right]$ which can be given by

$$\begin{aligned}
\Pr(N_T = u-1, C_{1c} \geq R_{th}, C_{3c} < R_{th}) &= \left(1 - e^{-\lambda_1 \rho_0}\right)^{M-u} e^{-(u-1)\lambda_1 \rho_0} \Pr(\gamma_{1c} \geq \rho_0, \mu\gamma_{1c}\gamma_{3c} < \rho_0) \\
&= \left(1 - e^{-\lambda_1 \rho_0}\right)^{M-u} e^{-(u-1)\lambda_1 \rho_0} \int_{\rho_0}^{\infty} f_{\gamma_{1c}}(x) F_{\gamma_{3c}}\left(\frac{\rho_0}{\mu x}\right) dx
\end{aligned} \tag{7.52}$$

By using (7.41) for the PDF $f_{\gamma_{1c}}(x)$ and (7.42) for the CDF $F_{\gamma_{3c}}(\rho_0 / \mu x)$, I obtain (7.53) by

$$\begin{aligned}
&\Pr(N_T = u-1, C_{1c} \geq R_{th}, C_{3c} < R_{th}) \\
&= \left(1 - e^{-\lambda_1 \rho_0}\right)^{M-u} e^{-(u-1)\lambda_1 \rho_0} \times \sum_{v=0}^{u} (-1)^v C_u^v \int_{\rho_0}^{\infty} \lambda_1 e^{-\lambda_1 x} e^{-\frac{v\lambda_3 \rho_0}{\mu x}} dx
\end{aligned} \tag{7.53}$$

Next, I can formulate the probability $\Pr\left[\begin{cases} C_{1b} \geq R_{th} \\ C_{3b} < R_{th} \end{cases}\right]$ as

$$\Pr(C_{1b} \geq R_{th}, C_{3b} < R_{th}) = \Pr(\gamma_{1b} \geq \rho_0, \mu\gamma_{1b}\gamma_{3b} < \rho_1) = \int_{\rho_0}^{+\infty} f_{\gamma_{1b}}(x) F_{\gamma_{3b}}\left(\frac{\rho_1}{\mu x}\right) dx \tag{7.54}$$

Combining (7.41), (7.43) and (7.54), and after some manipulations, I arrive at

$$\Pr(C_{1b} \geq R_{th}, C_{3b} < R_{th}) = \sum_{t=0}^{m-1} (-1)^t C_{m-1}^t m\lambda_1 \times \left[\frac{e^{-(t+1)\lambda_1 \rho_0}}{(t+1)\lambda_1} - \int_{\rho_0}^{+\infty} e^{-(t+1)\lambda_1 x} e^{-\frac{\lambda_3 \rho_1}{\mu x}} dx \right] \tag{7.55}$$

Then, substituting (7.51), (7.53) and (7.55) into (7.47), I obtain OP_1^{PR} as expressed in (7.49).

Next, when $\beta / (1 - \beta + \kappa) \leq \theta < 1/\kappa$, it is obvious that

$$\Pr(C_{1b} \geq R_{th}, C_{3b} < R_{th}) = \Pr(C_{1b} \geq R_{th}) = 1 - \left(1 - e^{-\lambda_1 \rho_0}\right)^m \tag{7.56}$$

Combining (7.51), (7.53), (7.56) and (7.47), the probability OP_2^{PR} can be obtained as in (7.50).

Finally, when $\theta \geq 1/\kappa$, I can observe that the primary network is always in outage, i.e., $P_{out}^{PR} = 1$.

Theorem 7.6.

At high SNR values, i.e., $\psi = P/N_0 \to +\infty$, the outage probability P_{out}^{PR} can be approximated by closed-form expressions as follows:

$$P_{out}^{PR} \overset{\psi \to +\infty}{\approx} \begin{cases} OP_1^{PR,\infty}, if\ \theta < \beta/(1-\beta+\kappa) \\ OP_2^{PR,\infty}, if\ \beta/(1-\beta+\kappa) \leq \theta < 1/\kappa \end{cases} \tag{7.57}$$

where, $OP_1^{PR,\infty}$ *and* $OP_2^{PR,\infty}$ are calculated as in (7.58) and (7.59).

$$\begin{aligned} OP_1^{PR,\infty} &= (1-e^{-\lambda_0\rho_0})(1-e^{-\lambda_2\rho_0})^M(1-e^{-\lambda_1\rho_0})^M \\ &+(1-e^{-\lambda_0\rho_0})(1-e^{-\lambda_2\rho_0})^M \sum_{u=1}^{M} C_M^u (1-e^{-\lambda_1\rho_0})^{M-u} e^{-(u-1)\lambda_1\rho_0} \\ &\times\left(e^{-\lambda_1\rho_0} + \sum_{v=1}^{u}(-1)^v C_u^v \sqrt{\frac{4v\lambda_1\lambda_3\rho_0}{\mu}} K_1\left(\sqrt{\frac{4v\lambda_1\lambda_3\rho_0}{\mu}}\right)\right) \\ &+(1-e^{-\lambda_0\rho_0})\sum_{m=1}^{M} C_M^m (1-e^{-\lambda_2\rho_0})^{M-m} e^{-m\lambda_2\rho_0}(1-e^{-\lambda_1\rho_0})^m \\ &+(1-e^{-\lambda_0\rho_0})\sum_{m=1}^{M} C_M^m (1-e^{-\lambda_2\rho_0})^{M-m} e^{-m\lambda_2\rho_0} \\ &\times\sum_{t=0}^{m-1}(-1)^t C_{m-1}^t m\left(\frac{e^{-(t+1)\lambda_1\rho_0}}{t+1} - \sqrt{\frac{4\lambda_1\lambda_3\rho_1}{\mu(1+t)}} K_1\left(\sqrt{\frac{4(1+t)\lambda_1\lambda_3\rho_1}{\mu}}\right)\right) \end{aligned} \tag{7.58}$$

$$\begin{aligned} OP_2^{PR,\infty} &= (1-e^{-\lambda_0\rho_0})(1-e^{-\lambda_2\rho_0})^M(1-e^{-\lambda_1\rho_0})^M + (1-e^{-\lambda_0\rho_0})(1-e^{-\lambda_2\rho_0})^M \\ &\times\sum_{u=1}^{M} C_M^u (1-e^{-\lambda_1\rho_0})^{M-u} e^{-(u-1)\lambda_1\rho_0} \times\left(e^{-\lambda_1\rho_0} + \sum_{v=1}^{u}(-1)^v C_u^v \sqrt{\frac{4v\lambda_1\lambda_3\rho_0}{\mu}} K_1\left(\sqrt{\frac{4v\lambda_1\lambda_3\rho_0}{\mu}}\right)\right) \\ &+(1-e^{-\lambda_0\rho_0})\sum_{m=1}^{M} C_M^m (1-e^{-\lambda_2\rho_0})^{M-m} e^{-m\lambda_2\rho_0} \end{aligned} \tag{7.59}$$

Proof. At the high ψ regimes, I obtain the following approximation:

$$\int_{\rho_0}^{+\infty} e^{-ax} e^{-\frac{b}{x}} \overset{\psi \to +\infty}{\approx} \int_{0}^{+\infty} e^{-ax} e^{-\frac{b}{x}} dx \overset{\psi \to +\infty}{\approx} \sqrt{\frac{4b}{a}} K_1\left(\sqrt{\frac{4b}{a}}\right) \tag{7.60}$$

where a and b are positive real numbers.

Then, using (7.60) for the corresponding integrals in (7.49) and (7.50), I respectively obtain (7.58) and (7.59).

Similarly, the outage probability of the secondary network can be formulated by the following formula:

$$\begin{aligned} P_{out}^{SR} &= \Pr\left(C_0 \geq R_{th}\right)\Pr\left(C_{4a} < R_{th}\right) + \Pr\left(C_0 < R_{th}\right)\Pr\left(N_R = 0\right) \\ &+ \Pr\left(C_0 < R_{th}\right)\sum_{m=1}^{M} C_M^m \Pr\left(N_R = m\right)\Pr\left(C_{1b} < R_{th}\right) \\ &+ \Pr\left(C_0 < R_{th}\right)\sum_{m=1}^{M} C_M^m \Pr\left(N_R = m\right)\Pr\left(C_{1b} \geq R_{th}, C_{4b} < R_{th}\right) \end{aligned} \tag{7.61}$$

Theorem 7.7.

The exact outage probability of the secondary network can be computed by

$$P_{out}^{SR} = \begin{cases} OP_1^{SR}, if\, \theta < (1-\beta) < \kappa \\ OP_2^{SR}, if\, (1-\beta)/\kappa \leq \theta < 1/\kappa \\ 1 \quad\quad , if\, \theta \geq 1/\kappa \end{cases} \tag{7.62}$$

where OP_1^{SR} *and* OP_2^{SR} can be found from (7.63) and (7.64):

$$\begin{aligned} OP_1^{SR} &= e^{-\lambda_0\rho_0}\left(1 - \sqrt{\frac{4\lambda_1\lambda_4\rho_0}{\mu}}K_1\left(\sqrt{\frac{4\lambda_1\lambda_4\rho_0}{\mu}}\right)\right)^M + (1-e^{-\lambda_0\rho_0})(1-e^{-\lambda_2\rho_0})^M \\ &+ (1-e^{-\lambda_0\rho_0})\sum_{m=1}^{M} C_M^m (1-e^{-\lambda_2\rho_0})^{M-m} e^{-m\lambda_2\rho_0}(1-e^{-\lambda_1\rho_0})^m \\ &+ (1-e^{-\lambda_0\rho_0})\sum_{m=1}^{M} C_M^m (1-e^{-\lambda_2\rho_0})^{M-m} e^{-m\lambda_2\rho_0}\sum_{t=0}^{m-1}(-1)^t C_{m-1}^t m\lambda_1\left[\frac{e^{-(t+1)\lambda_1\rho_0}}{(t+1)\lambda_1} - \int_{\rho_0}^{\infty} e^{-(t+1)\lambda_1 x} e^{-\frac{\lambda_4\rho_2}{\mu x}} dx\right] \end{aligned} \tag{7.63}$$

$$OP_2^{SR} = e^{-\lambda_0\rho_0}\left(1 - \sqrt{\frac{4\lambda_1\lambda_4\rho_0}{\mu}}K_1\left(\sqrt{\frac{4\lambda_1\lambda_4\rho_0}{\mu}}\right)\right)^M + 1 - e^{-\lambda_0\rho_0} \tag{7.64}$$

Proof. At first, I consider the first case: $\theta < (1-\beta)/\kappa$. In this case, by using (7.45), I obtain:

$$\Pr\left(C_{4a} \leq R_{th}\right) = \Pr\left(\gamma_{1a}\gamma_{4a} \leq \frac{\rho_0}{\mu}\right) = \left\{1 - \sqrt{\frac{4\lambda_1\lambda_4\rho_0}{\mu}}K_1\left(\sqrt{\frac{4\lambda_1\lambda_4\rho_0}{\mu}}\right)\right\}^M \tag{7.65}$$

Similar to (7.55), I have:

$$\begin{aligned} \Pr\left(C_{1b} \geq R_{th}, C_{4b} < R_{th}\right) &= \sum_{t=0}^{m-1}(-1)^t C_{m-1}^t m\lambda_1 \\ &\times\left[\frac{e^{-(t+1)\lambda_1\rho_0}}{(t+1)\lambda_1} - \int_{\rho_0}^{+\infty} e^{-(t+1)\lambda_1 x} e^{-\frac{\lambda_4\rho_2}{\mu x}} dx\right] \end{aligned} \tag{7.66}$$

Substituting $\Pr\left(C_0 \geq R_{th}\right) = e^{-\lambda_0 \rho_0}$, (7.51), (7.65) and (7.66) into (7.62), the outage probability OP_1^{SR} can be obtained by (7.63).

Let's consider the second case where $(1-\beta)/\kappa \leq \theta < 1/\kappa$, similar to (7.56), I can obtain OP_2^{SR} as given by (7.64).

Theorem 7.8.

The outage probability OP_1^{SR} can be approximated at the high ψ region as

$$\begin{aligned} OP_1^{SR,\infty} \overset{\psi \to +\infty}{\approx} OP_{SR}^{1,\infty} &= e^{-\lambda_0 \rho_0}\left(1 - \sqrt{\frac{4\lambda_1\lambda_4\rho_0}{\mu}} K_1\left(\sqrt{\frac{4\lambda_1\lambda_4\rho_0}{\mu}}\right)\right)^M + (1-e^{-\lambda_0\rho_0})(1-e^{-\lambda_2\rho_0})^M \\ &+ (1-e^{-\lambda_0\rho_0})\sum_{m=1}^{M} C_M^m (1-e^{-\lambda_2\rho_0})^{M-m} e^{-m\lambda_2\rho_0}(1-e^{-\lambda_1\rho_0})^m \\ &+ (1-e^{-\lambda_0\rho_0})\sum_{m=1}^{M} C_M^m (1-e^{-\lambda_2\rho_0})^{M-m} e^{-m\lambda_2\rho_0} \sum_{t=0}^{m-1} (-1)^t C_{m-1}^t m \\ &\times \left(\frac{e^{-(t+1)\lambda_1\rho_0}}{t+1} - \sqrt{\frac{4\lambda_1\lambda_4\rho_2}{\mu(t+1)}} K_1\left(\sqrt{\frac{4(t+1)\lambda_1\lambda_4\rho_2}{\mu}}\right)\right) \end{aligned} \tag{7.67}$$

Proof. Similar to the proof of Proposition 2.

For performance comparison, we introduce the direct transmission (DT) protocol, in which the PT communicates with the PR without the help of the STs. In this protocol, the data rate of the PT-PR link is given by

$$C_{PT-PR}^{DT} = \log_2\left(1 + \frac{\psi\gamma_0}{\kappa\psi\gamma_0 + 1}\right) \tag{7.68}$$

The outage probability of DT protocol can be expressed by

$$P_{out}^{DT} = \Pr\left(C_{PT-PR}^{DT} \leq R_{th}\right) = \begin{cases} 1 & ,if\ \vartheta \geq 1/\kappa \\ 1 - e^{-\frac{\lambda_0 \vartheta}{1-\kappa\vartheta}} & ,if\ \vartheta < 1/\kappa \end{cases} \tag{7.69}$$

7.2.4 Numerical Results and Discussion

In this section, I present Monte Carlo simulations to verify the derivations in Section 7.2.3. For the simulation environment, I consider two-dimensional X-Y networks in which PT, PR, STs, SRs are respectively placed at (0,0), (1,0), $(x_{ST}, 0)$ and $(x_{ST}, 0.25)$, respectively, where $0 < x_{ST} < 1$. In all of the simulations, the time block is normalized by 1 (T = 1) and the path loss exponent is fixed by 4 $(\chi = 4)$.

In Figure 7.16 and 7.17, I present the outage probability of the primary and secondary networks as a function of ψ (dB). The parameters of these figures are fixed by $R_{th}=1, x_{ST}=0.5, \kappa=0.01,$ $\alpha=0.1, \beta=0.95, \eta=0.5$ and $M \in \{1,2,3,6\}$. From Figure 7.16, I can see that the outage performance of the primary network significantly enhances, as compared with the DT protocol. Moreover, it can be observed that the outage probability decreases with the increasing the number of the ST-SR pairs.

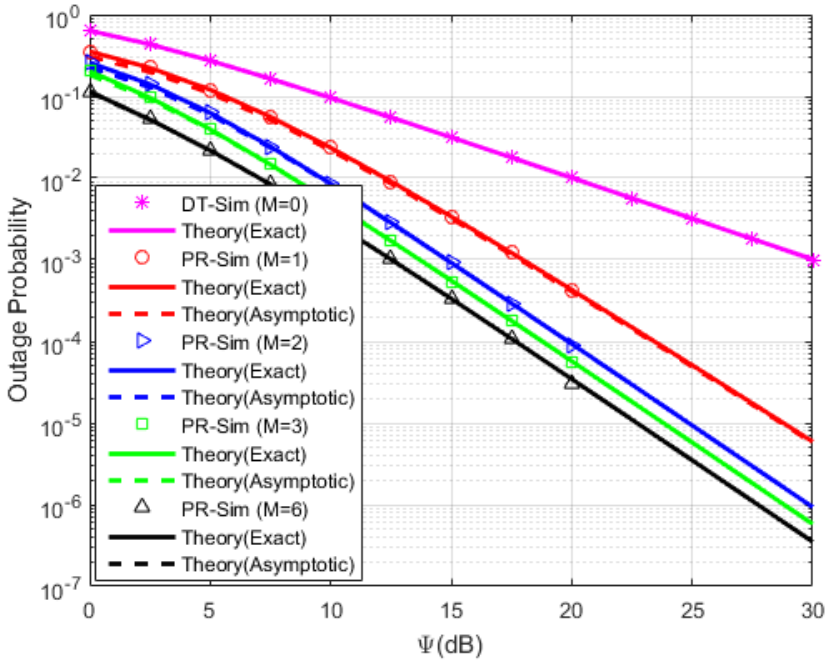

Figure 7.16 Outage probability of the primary network as a function of the transmit SNR (Ψ) in dB

As observed in Figure 7.17, the outage performance of the secondary network is also better with high M values. It is worth noting from Figure 7.16, 7.17 that the simulation results match very well with the exact theoretical results and the approximate theoretical results rapidly converge to the exact ones.

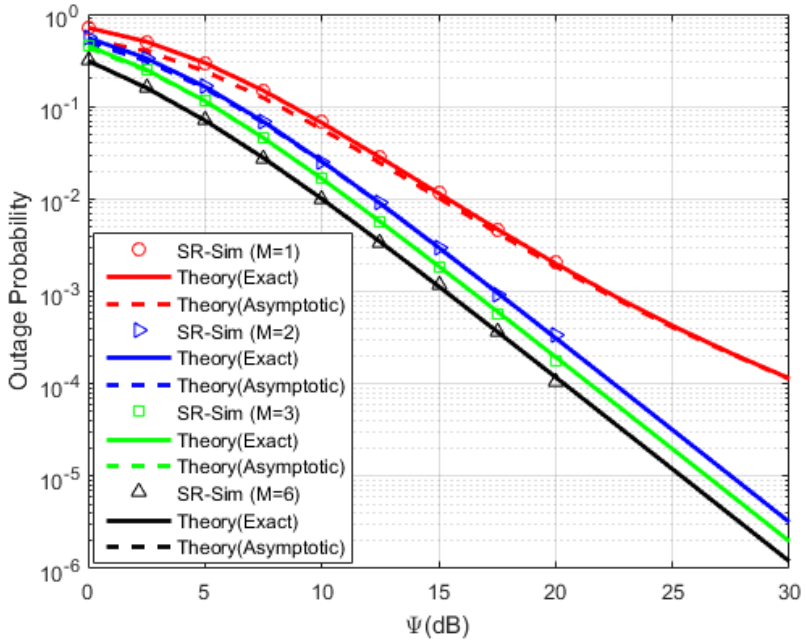

Figure 7.17. Outage probability of the secondary network as a function of the transmit SNR (Ψ) in dB

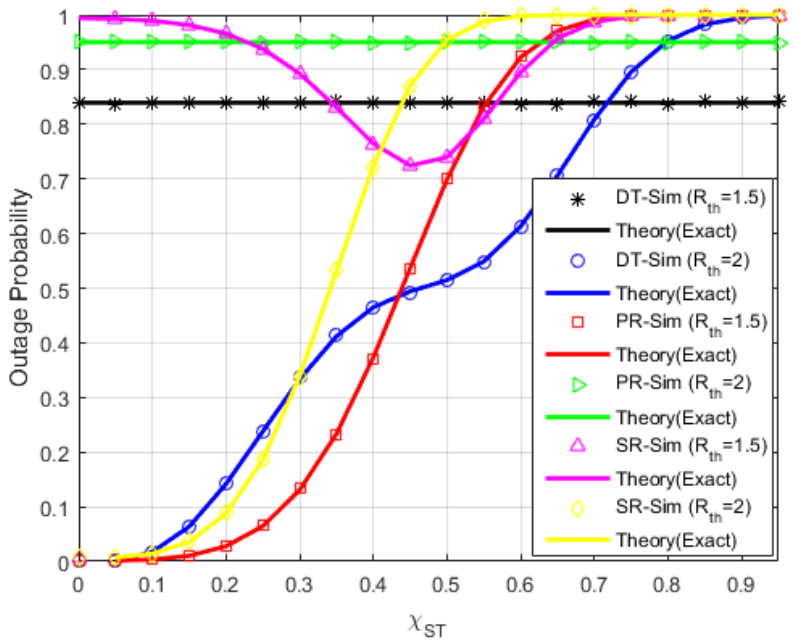

Figure 7.18. Outage probability of the primary and secondary networks as a function of x_{ST}

Figure 7.18 illustrates the outage performance of both networks as a function of the coordinate x_{ST} when $R_{th} \in \{1.5, 2\}, \kappa = 0, \alpha = 0.1, \beta = 0.95, \eta = 0.5, M = 2$ and $\psi = 0$ dB. We can observe from Figure 7.18 that the outage probability rapidly increases with the increasing of Rth. It is also seen that the

outage performance of the secondary network in the proposed protocol decreases when the value of x_{ST} increases. It is due to the fact that the link distances, i.e., PT-ST and PT-SR, increase when x_{ST} increases, which reduces the probability that the nodes ST and SR can decode the primary data successfully (or decreases the probability that STs can access the licensed bands as well as the probability that SRs can remove the interference component from the primary data). Moreover, the position of the nodes ST also impacts on the performance of the primary network in the proposed scheme. In particular, when Rth = 1.5, the outage probability increases when the value of x_{ST} changes from 0.05 to 0.95. More interesting, with Rth = 2, there exists an optimal value for x_{ST} at which the outage probability of the primary network is lowest. In most of the values of x_{ST} and Rth, the primary network in our scheme outperforms that in the DT protocol. This figure also presents that by placing the nodes ST at appropriate positions, the proposed method will provide high-performance gain, as compared with the DT one. Again, the simulation and analytical results are in good agreement, which validates the correction of our derivations.

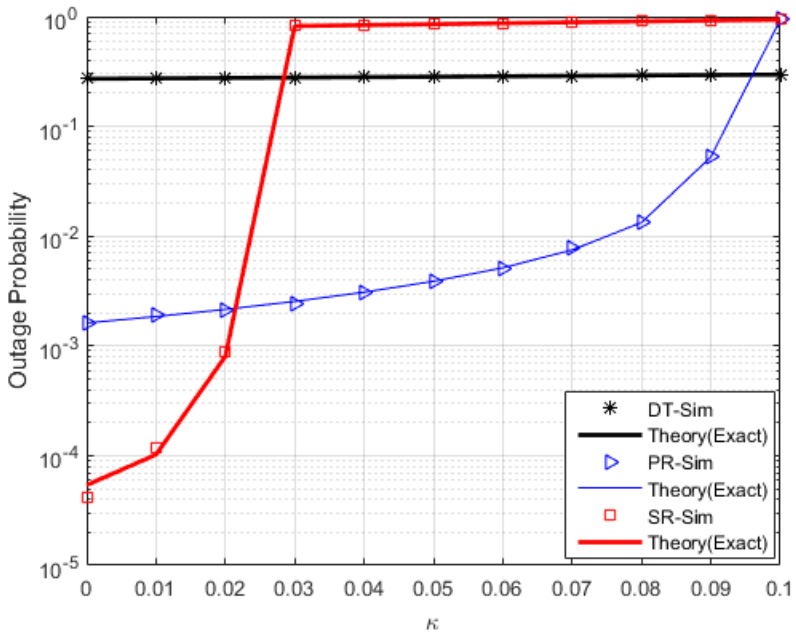

Figure 7.19. Outage probability of the primary and secondary networks as a function of κ

In Figure 5, I investigate the impact of the hardware impairments on the performance of both networks. In this simulation, I assign the values to the parameters as follows: $R_{th} = 1, x_{ST} = 0.15, \alpha = 0.2, \beta = 0.9,$

$\eta = 0.75, M = 3 and \psi = 5dB$ .I can see that the outage probability of the considered protocols increases with the increase of the value κ . Moreover, the outage performance of the DT protocol only changes slightly, while that of the proposed scenario significantly degrades.

Figure 7.20 shows the impact of the fraction of time used for the energy harvesting time slot (α) on the outage performance with $R_{th} = 1.5, x_{ST} = 0.1, \kappa = 0, \beta = 0.95, \eta = 1, M = 3 and \psi = 0dB$. As seen from this figure, the performance of the primary and secondary networks varies with the change of the α. However, it can be observed that there exists the optimal value α∗ so that the performance of the primary and secondary networks is best.

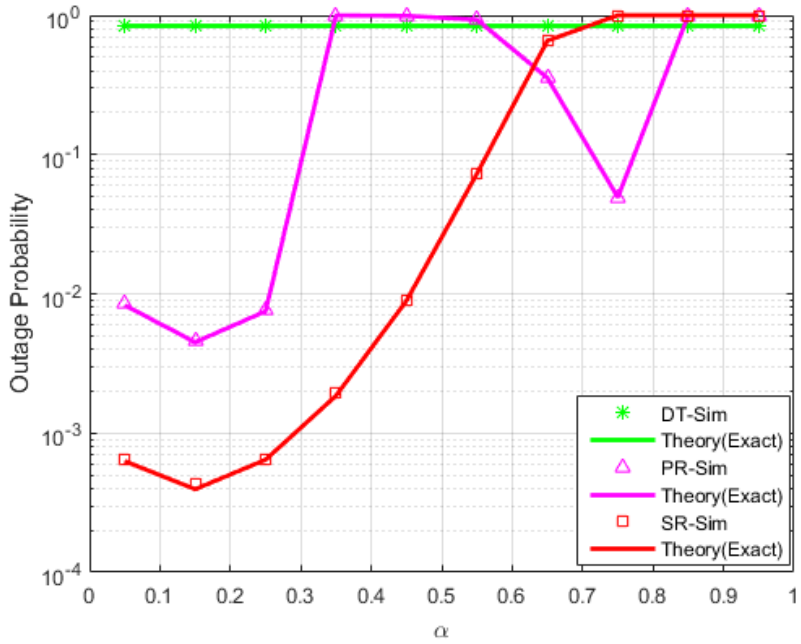

Figure 7.20. Outage probability of the primary and secondary networks as a function of α

In Figure 7.21, I investigate the impact of the fraction of the transmit power allocated to the primary signal (β) on the system performance. The simulation parameters of this figure are $R_{th} = 1.5, x_{ST} = 0.25, \kappa = 0.01, \eta = 0.25, M = 2 and \psi = 5 dB.$ I can see that the performance of the primary (secondary) network is better (worse) with high (low) β values. In this figure, the outage probability of the primary network (secondary) network almost equals 1 when β is less (higher) than 0.93 (0.91).

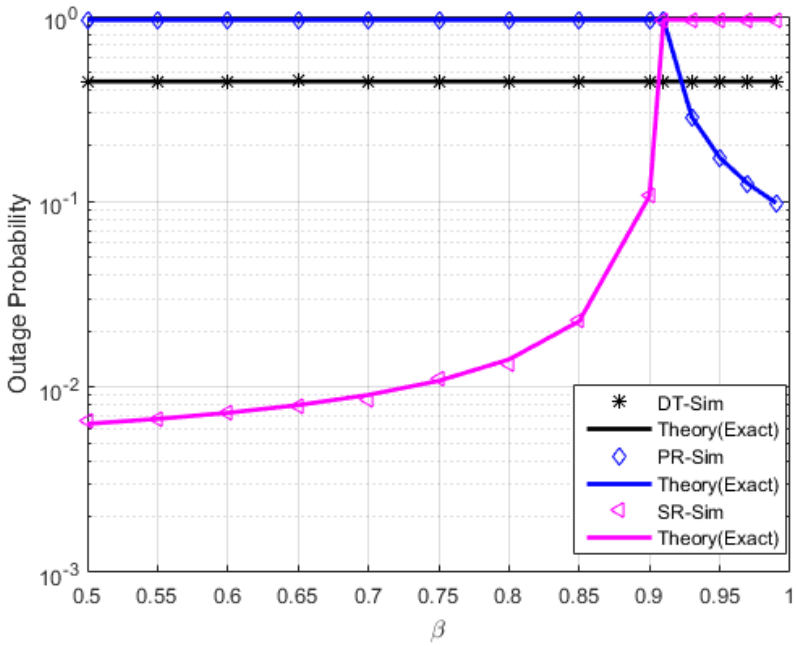

Figure 7.21 Outage probability of the primary and secondary networks as a function of β

7.3 Conclusion

In summary, this section concentrates on the impact of hardware impairments on the system performance of the energy-harvesting-based relaying schemes. In our model, the hardware impairments at both source and relay nodes are modelled as Gaussian random variables. I derive the analytical formula for outage probability and system throughput and verify these results by Monte Carlo simulation. From the numerical results, it can be observed that the hardware impairments have a severe impact on the system performance at low SINR regime. However, at high SINR regime, the system can still achieve good performance if the impairments are bounded, which is, in fact, probable in practice. Moreover, in the cognitive radio network, I proposed an overlay spectrum access protocol to enhance the performance of the primary and secondary networks. The main contribution is to derive exact and lower-bound closed-form expressions of the outage probability, which were verified by computer simulations. The proposed system can be optimized by appropriately designing the fraction of time block used for the energy harvesting process and the fraction of the transmit power allocated to the primary signal. The two models serve as illustrative examples for our analysis works on hardware impairment. Further results on relay selection for EH-based networks have also been published in [tan01]. Another performance analysis for half-duplex bidirectional sensor networks under hardware impairments was introduced in my recent published work [tan04, tan06].

8 CONCLUSION

The core of this dissertation is the rigorous exploration on the concept of energy harvesting and apply this concept to various models of wireless relay networks (from the conventional models to novel models), where relay nodes harvest energy from the source and use this energy to help forward the information message from the source nodes to the destination nodes. This Ph.D. dissertation has introduced the framework for the design, analysis, and simulation of energy harvesting schemes in wireless relay networks.

Specifically, in my dissertation I defined three main aims:

1. The first aim is to provide the basic analysis of outage probability and average throughput of various energy harvesting relay network models [tan03, tan11, tan12]. Chapter 5 describes the methods and results to achieve this goal.

In order to carry out this framework, in this dissertation, the closed-form or at least integral-form formulas of outage probability and average throughput should be derived for every single energy harvesting based relay network model that has been proposed in this dissertation. Besides the basic relaying model such as half-duplex and full-duplex relaying, some advanced relaying models has been proposed to serve specific applications, for example, the bidirectional relaying schemes for wireless sensor networks or the relaying system for cognitive radio networks.

2. Secondly, I provide the mathematical analysis and simulation results to evaluate the effect of channel state information error on the performance of energy-harvesting-based relay networks [tan08, tan09, tan14]. This content is explained in details in chapter 6.

In fact, the effect of channel state information error on system performance is a vital goal of this project. By taking into account the channel estimation error, I investigate the robustness of the proposed energy harvesting to evaluate the possibility for practical implementation of our proposed algorithms. The results of this studying are the closed-form formulas for performance indicators including outage probability and throughput, as well as the numerical results to support the analysis.

3. Finally, I provide the mathematical analysis and simulation results to evaluate the effect of hardware impairment on the performance of energy-harvesting-based relay networks [tan04, tan06, tan10, tan13, tan15]. Chapter 7 introduces the solutions and results to complete this goal.

To fulfil this aim, during this dissertation work, the impact of the hardware noise on some potential energy harvesting schemes is carefully investigated both by analysis and numerical simulation. A performance evaluation as well as the recommendation for practical implementation of energy harvesting approach should be provided in our project.

As final words, I conclude that our main contribution is to provide a thorough analysis of energy harvesting solution for wireless relay networks from multiple perspectives: theoretical framework, practical consideration, the variety of the strategies to serve for different applications, as well as the variety of the channel conditions to be studied. Furthermore, this work can also be extended with more relaying schemes in the future, and with different channel conditions, like Ricean [tan03, tan04, tan05, tan06, tan07] or Nakagami-m channels. Another future direction is to go deeper to the hardware implementation of the proposed algorithm, which is out of the scope of my dissertation.

REFERENCES

1. A. Sendonaris, E. Erkip, and B. Aazhang, "User cooperation diversity Part I: System description," IEEE Transactions on Communications, vol.51, no.11, p. 1927–1938, Nov. 2003.

2. J. N. Laneman, D. N. C. Tse, and G. W. Wornell, "Cooperative diversity in wireless networks: Efficient protocols and outage behavior," *IEEE Trans. Inf. Theory*, vol. 50, no. 12, pp. 3062–3080, Dec. 2004.

3. K.Singh, A.Gupta, T.Ratnarajah," Energy Efficient Resource Allocation for Multiuser Relay Networks," *IEEE Trans. Commun*., vol.16, no.2, p. 1218 – 1235, Feb. 2017.

4. G.Brante, I.Stupia, R.Demo Souza, L.Vandendorpe," Outage Probability and Energy Efficiency of Cooperative MIMO with Antenna Selection," *IEEE Transactions on Communications*, vol.12, no.11, p. 5896 – 5907, Nov.2013.

5. Ulukus, S., Yener, A ., Erkip, E ., Simeone, O., Zorzi, M., Grover, P., Huang, K.: "Energy harvesting wireless communications: a review of recent advances" *IEEE Journal on Selected Areas in Communications*, Vol.33, no.3, p.360–381, 2015.

6. Bi, S., Ho, C.K., Zhang, R.: "Recent advances in joint wireless energy and information transfer" *IEEE Information Theory Workshop (ITW)*, p. 341–345, November 2014.

7. K. Wu, D. Choudhury and H. Matsumoto, "Wireless power transmission, technology, and applications," *IEEE Proc.* , vol. 101, no. 6, p. 1271-1275, Jun. 2013.

8. Suzhi Bi, Chin Keong Ho, and Rui Zhang, "Recent advances in joint wireless energy and information transfer," *Proc. Of Information Theory Workshop (ITW)*, 2014 IEEE, p.341-345, 2014.

9. Lav R. Varshney, "Transporting information and energy simultaneously," *Proc. Of IEEE International Symposium on Information Theory*, 2008. ISIT 2008, pp. 1612-1616, 2008.

10. Pulkit Grover and Anant Sahai, "Shannon meets Tesla: Wireless information and power transfer," Proc. of 2010 IEEE International Symposium on Information Theory Proceedings (ISIT), p.2363-2367, 2010.

11. Rui Zhang and Chin Keong Ho, "MIMO broadcasting for simultaneous wireless information and power transfer," *IEEE Transactions on Wireless Communications*, vol. 12, no.5, p.1989-2001, 2013.

12. A. A. Nasir, X. Zhou, S. Durrani, and R. A. Kennedy, "Relaying protocols for wireless energy harvesting and information processing," *IEEE Transactions on Wireless Communications*, vol. 12, no. 7, p.3622-3636, 2013.

13. A. A. Nasir, X. Zhou, S. Durrani, and R. A. Kennedy, "Throughput and ergodic capacity of wireless energy harvesting based DF relaying network," *Proc. of 2014 IEEE International Conference on Communications (ICC)*, p. 4066–4071, 2014.

14. Zhiguo Ding, Samir M. Perlaza, Inaki Esnaola, and H. Vincent Poor, "Power allocation strategies in energy harvesting wireless cooperative networks," *Proc. of IEEE Transactions on Wireless Communications*, vol. 13, no. 2, p. 846-860, 2014.

15. Zhiguo Ding, I. Krikidis, B. Sharif, and H. V. Poor, "Wireless information and power transfer in cooperative networks with spatially random relays," *IEEE Transactions on Wireless Communications*, vol. 13, no. 7, p. 4440-4453, 2014.

16. Caijun Zhong, Himal A. Suraweera, Gan Zheng, Ioannis Krikidis, and Zhaoyang Zhang, "Wireless information and power transfer with full duplex relaying," *IEEE Transactions on Communications*, vol. 62, no. 10, pp. 3447-3461, 2014.

17. Yong Zeng and Rui Zhang, "Full-duplex wireless-powered relay with self-energy recycling," *IEEE Wireless Communications Letters*, vol. 4, no. 2, p. 201-204, 2015.

18. Zeng, Y., Chen, H., and Zhang, R. "Bidirectional Wireless Information and Power Transfer With a Helping Relay," *IEEE Communications Letters*, May 2016, vol. 20, no. 5, p. 862–865.

19. Dongwook Choi and Jae Hong Lee, "Outage probability of two-way full-duplex relaying with imperfect channel state information," *IEEE Communications Letters*, vol.18, no.6, p.933-936, 2014.

20. Dandan Li D., Chao Shen, and Zhengding Qiu, "Sum rate maximization and energy harvesting for two-way AF relay systems with imperfect CSI," *Proc. of2013 IEEE International Conference on Acoustics, Speech and Signal Processing (ICASSP)*, pp.4958-4962, 2013.

21. Schenk, T.: RF Imperfections in High-Rate Wireless Systems: "Impact and Digital Compensation" Springer, The Netherlands, 2008.

22. Bjornson, E., Matthaiou, M., Debbah, M.: "A new look at dual-hop relaying: performance limits with hardware impairments" *IEEE Transactions on Communications*, Vol.61, no.11, p. 4512–4525, 2013.

23. Duy, T.T., Duong, T.Q., Da Costa, D.B., Bao, V.N.Q., Elkashlan, M.: "Proactive relay selection with joint impact of hardware impairment and co-channel interference" *IEEE Transactions on Communications, Vol.* 63, no.5, p. 1594–1606, 2015.

24. Mitola, J. and Maquire, G. Q. J. "Cognitive radio: making software radios more personal," *IEEE Personal Communications*, August 1999, vol. 6, no. 4, p. 13-18.

25. Haykin, S. "Cognitive radio: brain-empowered wireless communications," *IEEE Journal on Selected Areas in Communications*, February 2005, vol. 23, no. 2, p. 201–220.

26. Huang, X. L., Hu, F.,Wu, J.,et al." Intelligent cooperative spectrum sensing via hierarchical Dirichlet process in cognitive radio networks," *IEEE Journal on Selected Areas in Communications*, October 2014,vol. 33, no. 5, p. 771–787.

27. Duy, T.T. and Kong, H.Y. “Performance Analysis of Incremental Amplify-and-Forward Relaying Protocols with Nth Best Partial Relay Selection under Interference Constraint,” *Wireless Personal Communications*, August 2013, vol. 71, no. 4, p. 2741–2757.

28. Duy, T.T. and Kong, H.Y. “Adaptive Cooperative Decode-and-Forward Transmission with Power Allocation under Interference Constraint,” *Wireless Personal Communications*, January2014, vol.74, no.2, p. 401–414.

29. Simeone,O.,Stanojev, I.,Savazzi, et al.“Spectrum leasing to cooperating secondary ad hoc networks,” *IEEE Journal on Selected Areas in Communications*, January 2008, vol. 26, no. 1, p. 203–213.

30. Han, Y., Pandharipande, A., and Ting, S.H. “Cooperative decode-and-forward relaying for secondary spectrum access,” *IEEE Transactions on Wireless Communications*, October 2009, vol.8, no.10, p. 4945-4950.

31. Duy, T.T. and Kong, H.Y. “Performance Analysis of Two-Way Hybrid Decode-and-Amplify Relaying Scheme with Relay Selection for Secondary Spectrum Access,” *Wireless Personal Communications*, March 2013, vol. 69, no. 2, p. 857-878.

32. Gao, X., Xu, W., Li, S., and Lin, J. “An online energy allocation strategy for energy harvesting cognitive radio systems,” *Proceedings of the 8th International Conference on Wireless Communications and Signal Processing (WCSP2013),* Hangzhou (China), October2013, p. 1-5.

33. Park, S. and Hong, D. “Optimal spectrum access for energy harvesting cognitive radio networks,” *IEEE Transactions on Wireless Communications*, December 2013, vol. 12, no. 12, p. 6166–6179.

34. Wang, Z., Chen, Z., Luo, L., et al. “Outage analysis of cognitive relay networks with energy harvesting and information transfer,” *Proceedings of 2014 IEEE International Conference on Communications (ICC2014)*, Sydney (Australia), June 2014, p. 4348–4353.

35. Son, P.N., Har, D., and Kong, H.Y. “Joint power allocation or energy harvesting and power superposition coding in cooperative spectrum sharing,” *Computing Research Repository*. [Online] Cited 2015.

36. Zhai, C., Liu, J., and Zheng, L. “Relay based spectrum sharing with secondary users powered by wireless energy harvesting,” *IEEE Transactions on Communications*, May 2016, vol. 64, no. 5, p. 1875–1887.

37. N. Shinohara, “ Power without wires,” *IEEE Microwave Mag*. ,vol.12,no.7, pp. 564–573, Dec. 2011.

38. Perera, T.D.P.; Jayakody, D.N.K.; Sharma, S.K.; Chatzinotas, S.; Li, J. “Simultaneous Wireless Information and Power Transfer (SWIPT): Recent Advances and Future Challenges,” *IEEE Communications Surveys and Tutorials* ,2018, 20, p.264–302.

39. Zewde, Tewodros Aklilu."Wireless Information and Power Transfer in Communication Networks: Performance Analysis and Optimal Resource Allocation," Syracuse University, ProQuest Dissertations Publishing, 2017. 10619564.

40. H. Ju and R . Z hang, " Throughput maximization in wireless powered communication networks," *IEEE Transactions on Wireless Communications*,vol. 13,no. 1, pp. 418–428, Jan. 2014.

41. Taneli Riihonen, Stefan Werner, and Risto Wichman, "Hybrid full-duplex/half-duplex relaying with transmit power adaptation," *IEEE Transactions on Wireless Communications*, vol. 10, no. 9, p. 3074-3085, 2011.

42. Zhang, Y., Pflug, H., Visser, H. J., and Dolmans, G. "Wirelessly powered energy autonomous sensor networks", 2014 IEEE Wireless Communications and Networking Conference (WCNC), 2014, p. 2444–2449.

43. Xu, J., Zhong, Z., Ai, B. Wireless powered sensor networks: Col-laborative energy beamforming considering sensing and circuit power consumption.IEEE Wireless Communications Letters, 2016, vol. 5, no. 4, p. 344–347. DOI: 10.1109/LWC.2016.2558503.

44. Gurakan, B., Ozel, O., Yang, J., and Ulukus, S.," Energy Cooperation in Energy Harvesting Communications", *IEEE Transactions on Communications*, December 2013, vol. 61, no. 12, p. 4884–4898.

45. Nguyen, T. N., Do, DT.., Tran, P. T., and Voznak, M. "Time Switching for Wireless Communications with Full-Duplex Relaying in Imperfect CSI Condition." *KSII Transactions on Internet and Information Systems*, September 2016, vol. 10, no. 9, p. 4223–4239.

46. Zwillinger, D., Moll, V., Gradshteyn, I., and Ryzhik, I. 8 - Special Functions. In *Table of Integrals, Series, and Products*. Eighth Edition. Boston: Academic Press, 2015, p. 867 – 1013.

47. Chaudhry, M. A. and Zubair, S. M., "Extended incomplete gamma functions with applications", *Journal of Mathematical Analysis and Applications*, 2002, vol. 274, no. 2, p. 725 – 745.

48. Bi, S., Zeng, Y., and Zhang, R. "Wireless powered communication networks: an overview", IEEE Wireless Communications, April 2016, vol. 23, no. 2, p. 10–18.

49. Chong, E. K. P. and Zak, S. H., "An introduction to optimization", Vol. 76. 4th ed. John Wiley & Sons, 2013. ISBN: 978–1–118–27901–4.

50. Trung. Q. Duong, Tran Trung Duy, Michail Matthaiou, and Theodoros Tsiftsis, "Cognitive cooperative networks in dual-hop asymmetric fading channels", in 2013 IEEE Global Communications Conference (GLOBECOM), pp. 955-961, 2013.

51. Matthaiou, M. and Papadogiannis, A. Two-way relaying under the presence of relay transceiver hardware impairments. IEEE Communications Letters, June 2013, vol. 17, no. 6, p. 1136–1139. DOI: 10.1109/LCOMM.2013.042313.130191.

52. Nguyen, D.K., Matthaiou, M., Duong, T.Q., et al. RF en-ergy harvesting two-way cognitive DF relaying with transceiver im-pairments. InProceedings of the 2015 IEEE Conference on Communication Workshop (ICCW2015), London (England), June 2015, p. 1970–1975. DOI: 10.1109/ICCW.2015.7247469.

53. Mousavifar, S., Liu, Y., Leung, C., et al. Wireless energy harvesting and spectrum sharing in cognitive radio. InProceed-ings of the 80th IEEE Vehicular Technology Conference (VTC Fall), Vancouver (Canada), September 2014, p. 1-5. DOI: 10.1109/VTC-Fall.2014.6966232.

54. SON, P.N. and KONG, H.Y. "Exact outage analysis of energy harvesting underlay cooperative cognitive Networks". IEICE Transactions on Communications, 2015, vol. E98-B, no. 4, p. 661–672.

55. Li, Y.B., Yang, R., Lin, Y., and Ye, F. The spectrum sharing in cognitive radio networks based on competitive price game.Radio-engineering, September 2012, vol. 21, no. 3, p. 802–808.

56. DUY, T.T. and KONG, H.Y. "Performance Analysis of Incremental Amplify-and-Forward Relaying Protocols with Nth Best Partial Relay Selection under Interference Constraint". Wireless Personal Communications, August 2013, vol. 71, no. 4, p. 2741–2757.

57. Duy, T. T., Duong, T. Q., Da Costa, D., et al. "Proactive relay selection with joint impact of hardware impairment and co-channel interference". IEEE Transactions on Communications, May 2015, vol. 63, no. 5, p. 1594–1606.

58. X. Zhou, R. Zhang, and C. K. Ho, "Wireless information and power transfer: Architecture design and rate-energy tradeoff", *IEEE Transactions on Communications*, November 2013, Vol.61, no.11, p. 4754 – 4767.

59. DUY, T.T. and KONG, H. "Secrecy performance analysis of multihop transmission protocols in cluster networks". Wireless Personal Communications, June 2015, vol. 82, no. 4, p. 2505–2518.

CANDIDATE'S RESEARCH OUTPUTS CITED IN THE DISSERTATION

[tan01] Tan N.Nguyen, T.H.Q.Minh, Phuong T. Tran, Miroslav Voznak, T.T.Duy, Thanh-Long Nguyen and Phu Tran Tin,"Performance Enhancement for Energy Harvesting Based Two-Way Relay Protocols in Wireless Ad-hoc Networks with Partial and Full Relay Selection Methods", *Ad-hoc networks, Vol.84, pp. 178-187, Mar.2019.* (IF 3.151)

[tan02] Tan N. Nguyen, T.H.Q.Minh, Thanh-Long Nguyen, Duy-Hung Ha and Miroslav Voznak," Multi-Source Power Splitting Energy Harvesting Relaying Network In Half-Duplex System Over Block Rayleigh Fading Channel: System Performance Analysis", *Electronics, Vol.8, No.1, Art.no.67, Jan 2019.* (IF 2.11)

[tan03] Tan N.Nguyen, Phu Tran Tin , Duy Hung Ha, Miroslav Voznak, Phuong T. Tran, Minh Tran and Thanh-Long Nguyen,"Hybrid TSR–PSR Alternate Energy Harvesting Relay Network over Rician Fading Channels: Outage Probability and SER Analysis", *Sensors, Vol.18, No.11, Art. no. 3839, Nov. 2018.* (IF 2.475)

[tan04] Tan N.Nguyen,T.H.Q.Minh, Phuong T.Tran and Miroslav Voznak," Energy Harvesting over Rician Fading Channel: A Performance Analysis for Half-Duplex Bidirectional Sensor Networks under Hardware Impairments", *Sensors, Vol.18, No.6, Art. no. 1781, Jun.2018.* (IF 2.475)

[tan05] Tan N. Nguyen, T.H.Q.Minh, Duy-Hung Ha, Thanh-Long Nguyen and Miroslav Voznak," Energy harvesting based two-way full-duplex relaying network over Rician fading environment: performance analysis", *Proceedings of the Estonian Academy of Sciences, Vol.68, No.1, pp. 111-123, Feb.2019.* (IF 0.843)

[tan06] Tan N.Nguyen, Phuong T.Tran, T.H.Q.Minh and Miroslav Voznak," Two-Way Half Duplex Decode and Forward Relaying Network with Hardware Impairment over Rician Fading Channel: System Performance Analysis", *Elektronika Ir Elektrotechnika, Vol.24, No.2, pp.74-78, 2018.* (IF 1.088)

[tan07] Tan N.Nguyen, T.H.Q.Minh, Phuong T.Tran and Miroslav Voznak,"Adaptive Energy Harvesting Relaying Protocol for Two-Way Half Duplex System Network over Rician Fading Channels", *Wireless Communications and Mobile Computing, Vol.2018, 10 pages, Apr.2018.* (IF 0.869)

[tan08] Tan N.Nguyen, Dinh-Thuan Do, Phuong T.Tran and Miroslav Voznak,"Time Switching for Wireless Communications with Full-Duplex Relaying in Imperfect CSI Condition", *KSII Transactions on Internets and Information Systems,Vol.10, No.9, pp.4223-4239, Sep.2016.* (0.452)

[tan09] Tan N.Nguyen, Minh Tran, Phuong T. Tran, Phu Tran Tin, Thanh-Long Nguyen, Duy-Hung Ha and Miroslav Voznak,"On the Performance of Power Splitting Energy Harvested Wireless Full-Duplex Relaying Network with Imperfect CSI over Dissimilar Channels ", *Security and Communication Networks, Vol.2018, 11 pages, Art.no.6036087.* (IF 0.904)

[tan10] Tan N.Nguyen, Tran Trung Duy, Gia-Thien Luu, Phuong T.Tran and Miroslav Voznak ,"Energy Harvesting-based Spectrum Access With Incremental Cooperation, Relay Selection and Hardware Noises", *RadioEngineering*, *Vol 26, No. 1, pp. 240-250, Apr. 2017.* (IF 1.048)

[tan11] Tan N.Nguyen, Phuong T.Tran, Hoang-Sy Nguyen, Dinh-Thuan Do and Miroslav Voznak,"On the Performance of a Wireless Powered Communication System Using a Helping Relay ", *RadioEngineering*, *Vol 26, No.3, pp. 860-868, Sep. 2017*.(IF 1.048)

[tan12] Tan N.Nguyen, Phuong T.Tran and Miroslav Voznak," Power-splitting-based energy harvesting protocol for wireless powered communication networks with a bidirectional relay", *International Journal of Communication Systems, Vol.31, No.13, Article No. e3721 Sep.2018*.(IF 1.717)

[tan13] Tan N.Nguyen, Phuong T.Tran, Huong-Giang Hoang, Hoang-Sy Nguyen, and Miroslav Voznak," On the Performance of Decode-and-Forward Half-Duplex Relaying with Time Switching Based Energy Harvesting in the Condition of Hardware Impairment", *The International Conference on Advances in Information and Communication Technology*, *Vol.538, pp.421-430, Nov.2016.*

[tan14] Tan N.Nguyen, Phuong T.Tran, Hoang-Sy Nguyen, Thu-Quyen T.Nguyen and Miroslav Voznak," On the Performance of Energy Harvesting for Decode-and-Forward Full-Duplex Relay Networks in Imperfect CSI Condition", *The 3rd International Conference on Advanced Engineering-Theory and Applications (AETA2016),Vol.415, pp.838-849, Dec.2016.*

[tan15] Tan N.Nguyen, Phuong T.Tran, Miroslav Voznak and Ladislav Behan,"Performance of Time Switching Based Energy Harvesting for Amplify-and-Forward Half-Duplex Relaying with Hardware Impairment," *2017 27th International Conference Radioelektronika, art. no. 7936646, Apr. 2017.*

OVERVIEW OF CANDIDATES RESULTS AND ACTIVITIES

Overview of publication activities

I provide the following list indexed results in relevant scientific databases, in order to document my research activities within the entire period of my doctoral study:

- ORCID: orcid.org/0000-0002-2286-6652, Scopus Author ID: 57184694000
- records in **Scopus**: 27 (6 conference papers, 21 articles in journals)
- records in **Web of Science**: 28 (6 conference papers, 22 articles in journal)
- h-index according to ISI/WoS: 5 (46 citations)
- h-index according to Scopus: 4 (50 citations)

Project memberships and participations

- In 2015-2018, a member of WiCOM group in TDTU, *Wireless Communications Research Group*, head of group: prof. Vozňák.
- In 2017, Specific research, SGS FEI VSB-TU Ostrava, *project SP2017/82 Networks and Security, Modelling, Simulation, Knowledge Retrieval and Communication Technologies for Smart Cities*, project coordinator: prof. Vozňák.
- In 2018, Specific research, SGS FEI VSB-TU Ostrava, *project SP2018/170 Network and Communication Technologies for Smart Cities*, project coordinator: Dr. Řezáč.
- In 2018, The Czech Ministry of Education, Youth and Sports, *project Large Infrastructures for Research, Experimental Development and Innovations, project No. LM2015070*, project coordinator: doc. Vondrák.

Other results with wider relation to the topic of dissertation achieved during the PhD study and indexed on WoS or SCOPUS

1. **Tan N.Nguyen**, Tran Trung Duy, Phuong T. Tran and Miroslav Voznak,"Performance Evaluation of User Selection Protocols in Random Networks with Energy Harvesting and Hardware Impairments", *Advances in Electrical and Electronic Engineering, Vol.14, No.4, pp.372-377, Dec.2016.* (ESCI)
2. Phu Tran Tin, Tran H.Q.Minh, **Tan N.Nguyen** and Miroslav Voznak,"System Performance Analysis of Half-Duplex Relay Network over Rician fading channel", *Telkomnika, Vol.16, No.1, pp.189-199, Feb.2018.* (SCOPUS).
3. **Tan N. Nguyen**, P.T.Tin, Phuong T.Tran, T.H.Q.Minh and Miroslav Voznak,"Power-Splitting Protocol in Power Beacon-assisted Energy Harvesting Full-Duplex Relaying Networks: Performance Analysis", *2018 11th IFIP Wireless and Mobile Networking Conference* (WMNC).

4. Hoang-Sy Nguyen, Anh-Hoa Thi Bui, **Nhat-Tan Nguyen** and Miroslav Voznak,"Opportunistic Multiple Relay Selection Schemes in both Full-Duplex and Half-Duplex Operation for Decode-and-Forward Cooperative Networks", *The International Conference on Advances in Information and Communication Technology, Vol.538, pp.431-441, Nov.2016.*

Other results achieved during the PhD study and indexed on WoS or SCOPUS

1. Phu Tran Tin, N.H.K. Nhan, Minh Tran, T.T.Trang, **Tan N.Nguyen** and Miroslav Voznak,"Co-Doping Red-Emitting Sr2si5n8:Eu2+ Into Yellow-Emitting Phosphor-Packaging For Enhancing The Optical Properties Of The 8500 K Remote-Phosphor Packaging Wleds", *Digest Journal of Nanomaterials and Biostructures*, *Vol.13, No.4, pp.1027-1034, Nov.2018.* (SCIE)
2. Phu Tran Tin, N.H.K.Nhan, T.H.Q.Minh, Miroslav Voznak, **Tan N.Nguyen** and Tran Thanh Trang, "Sr2Si5N8:Eu2+ phosphor: a novel recommendation for improving the lighting performance of the 7000 K remote-packaging white LEDs ", *Proceedings of the Estonian Academy of Sciences, Vol.67, No.4, pp. 337-341, Sep.2018.* (SCIE)
3. N.H.K.Nhan, T.H.Q.Minh, **Tan N.Nguyen**, Miroslav Voznak and V. V. Huynh,"Effect Of The Green-Emitting Caf2:Ce3+,Tb3+ Phosphor Particles' Size On Color Rendering Index And Color Quality Scale Of The In-Cup Packaging Multichip White Leds", *Digest Journal of Nanomaterials and Biostructures*, *Vol.13, No.2, pp.345-351, May.2018.* (SCIE)
4. N.H.K.Nhan, T.H.Q.Minh,V. V. Huynh, Phuong T.Tran, **Tan N.Nguyen** and Miroslav Voznak , "Improving optical performance of multi-chip white LEDs by bi-layers remote-packaging phosphors", *Journal of Optoelectronics and Advanced Materials*, *Vol.20, No.3-4, pp.93-97, Apr.2018.* (SCIE)
5. N.H.K.Nhan, T.H.Q.Minh, **Tan N.Nguyen** and Miroslav Voznak,"Bi-layers Red-emitting Sr2Si5N8: Eu 2+ Phosphor and Yellow-emitting YAG: Ce Phosphor: A New Approach for Improving the Color Rendering Index of the Remote Phosphor Packaging WLEDs",*Current Optics and Photonics, Vol.1,No. 6,pp. 613-617,Dec. 2017.* (SCIE)
6. N.H.K.Nhan, T.H.Q.Minh, **Tan N.Nguyen** and Miroslav Voznak,,"Red-emitting ca2si5n8eu2+ phosphor: a new recommendation for improving color uniformity and color quality scale of the conformal packaging multi-chip white leds", *Journal of Ovonic Research* , *Vol 13, No.6, pp. 325-331, Nov. 2017*. (SCIE)
7. N.H.K.Nhan, T.H.Q.Minh, **Tan N.Nguyen** and Miroslav Voznak,"Co-Doping Green-Emitting Caf2:Ce3+, Tb3+ and Yellow Emitting Phosphor Particles for Improving the Cct Deviation and Luminous Efficacy of the In-cup Phosphor Packaging Wleds", *Digest Journal of Nanomaterials and Biostructures*, *Vol 12, No.3, pp.891-898,Aug.2017.* (SCIE)
8. **Tan N.Nguyen**, Phuong T. Tran and Miroslav Voznak,"A Novel Compressed Sensing Approach to Speech Signal Compression", *The 2rd International Conference on Advanced Engineering-Theory and Applications (AETA2015), Vol.371, pp.75-85, Dec.2015.*